Peripheral Functionalization of Hexa-*peri*-hexabenzocoronene through Ir-catalyzed C-H Borylation

イリジウム触媒による直接ホウ素化を経由した ヘキサベンゾコロネンの周辺官能基化

Ryuichi YAMAGUCHI

山口龍一

Department of Applied Chemistry, Graduate School of Engineering
Nagoya University

2014

Table of Contents

Chapter 1.

General Introduction

Contents

1-1. Polycyclic aromatic hydrocarbons (PAHs)

Polycyclic aromatic hydrocarbons (PAHs) are recognized as one of key materials in the field of structural organic chemistry. Their electronic and self-assembling properties also offer us opportunities for novel device fabrications.[1] PAHs such as pyrene, phenanthrene, perylene, hexa-*peri*-hexabenzocoronene (HBC), triphenylene, and coronene can be regarded as two-dimensional graphite segments (Figure 1-1).[2]

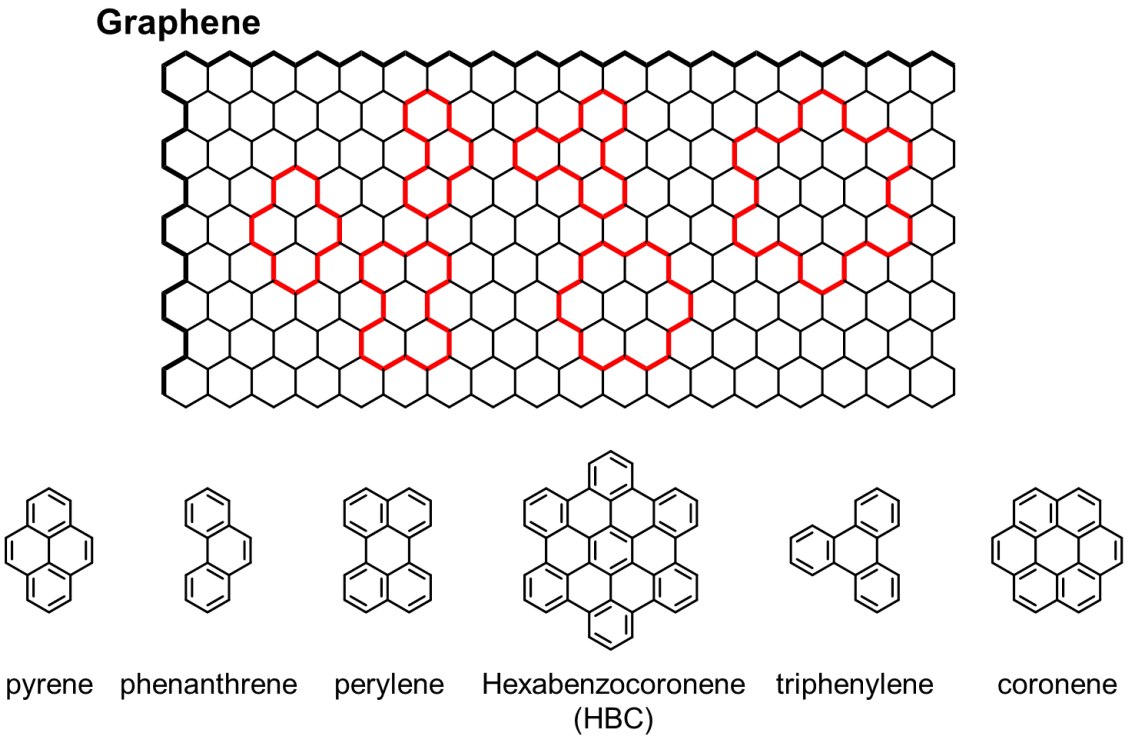

Figure 1-1. Polycyclic aromatic hydrocarbons.

These molecules have been studied as a next generation of carbon materials for such as supramolecules, liquid crystals, and materials for electronics.[3] In addition, these molecules have been investigated as a model of graphene,[4] to reveal aromaticity and edge properties of PAHs.[5] In recent years, biradical characters of PAHs have been actively studied.[6,7]

The author considers that there are three stages in the study of PAHs (Figure 1-2). The first stage is a development of the synthetic methods of the core skeleton of PAHs. The second stage is the development of functionalization methods and introduction of substituents to PAHs core. The final stage is control of the aggregated state by accumulation of single molecules. In particular, re-

searches on the introduction of substituents (*Stage-2*) are important to control the state of aggregation and improve the solubility of PAHs flamework.[8] In this study, the author aimed to establish a new functionalization concept, which is different from the conventional methods in *stage-2* of PAHs.

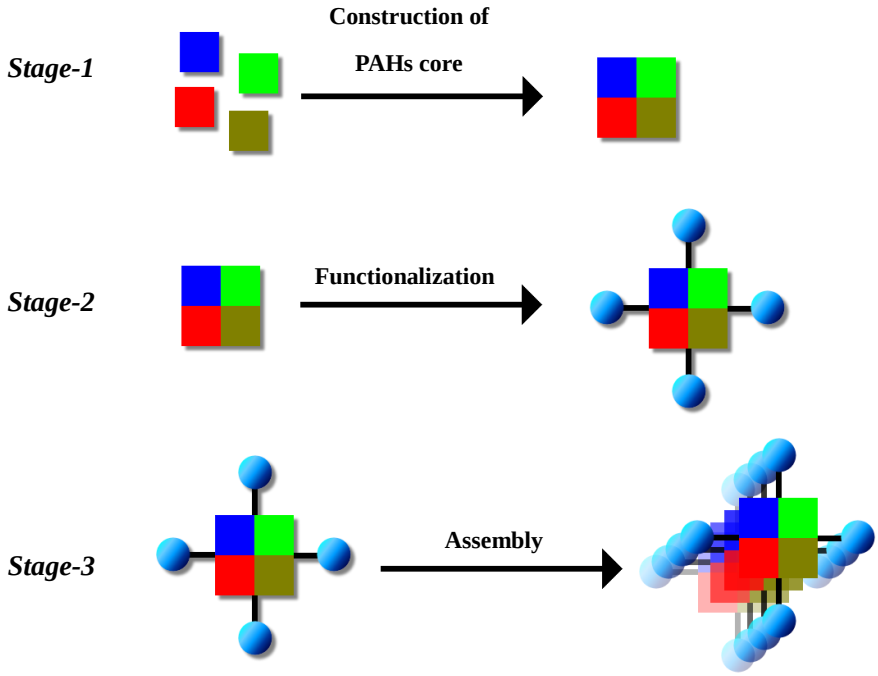

Figure 1-2. Stages in the study and application of PAHs.

1-2. Hexa-*peri*-hexabenzocoronene (HBC)

HBC is one of typical PAHs, which consists of 42 carbon atoms.[9] HBC and its derivatives have received much attention due to their high stability and facile self-assembling behaviors (Figure 1-3).

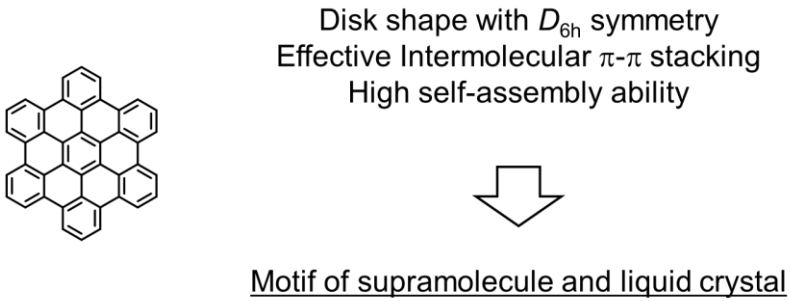

Figure 1-3. Hexa-*peri*-hexabenzocoronene (HBC).

The first synthesis of HBC was done by Clar and coworkers.[10] The UV-vis absorption spectrum of HBC in dichloromethane exhibits three typical absorption bands named as α-, β-, and

p-bands, respectively (Figure 1-4).[11] The α-band is the lowest energy absorption band, which usually has low intensity owing to its forbidden nature of the $S_0 \rightarrow S_1$ transition.

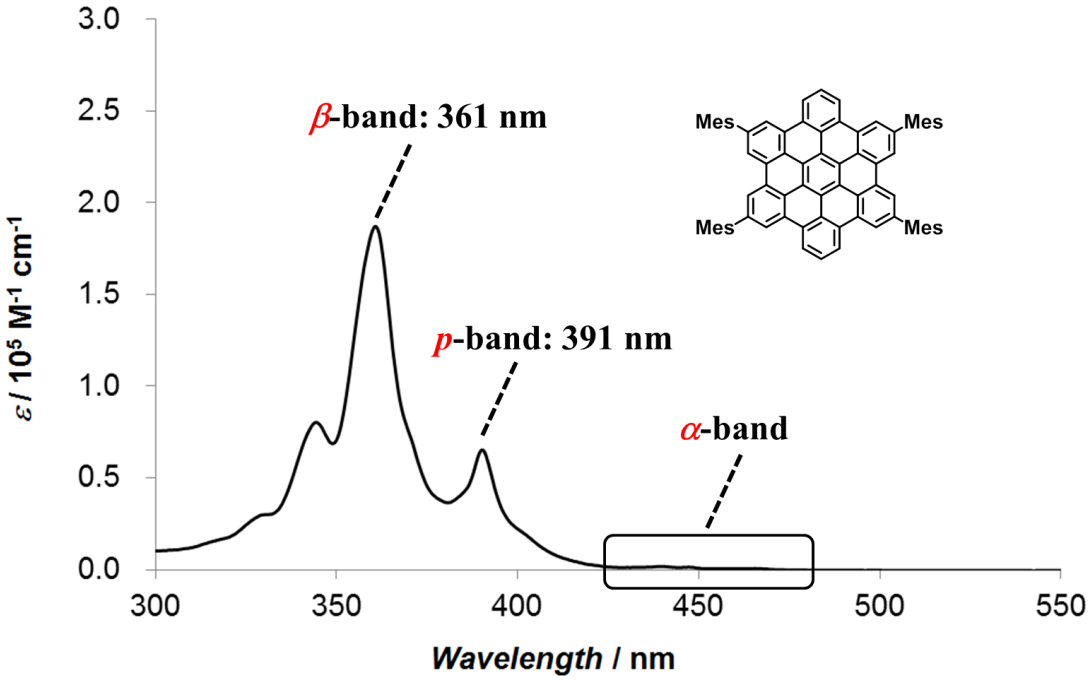

Figure 1-4. UV/vis absorption spectrum of HBC in CH_2Cl_2.

1-3. Substituent effect on HBCs

The HBC unit is often employed as a building block for discotic liquid crystals and supramolecular structures.[12] A variety of HBCs have been synthesized to investigate their aggregation structures, which are deeply affected by the peripheral substituents. Introduction of flexible aliphatic chains to the HBC periphery is a typical strategy to attain liquid crystallinity.[13] A substituent group with a high degree of freedom enables fine-tuning of the stability of the mesophase. In solution, substituted HBCs assemble into a columnar structure due to π-stacking interactions (Figure 1-5).[14] At higher concentrations or decreased temperatures, the sizes of the columnar aggregates are increased in solution.

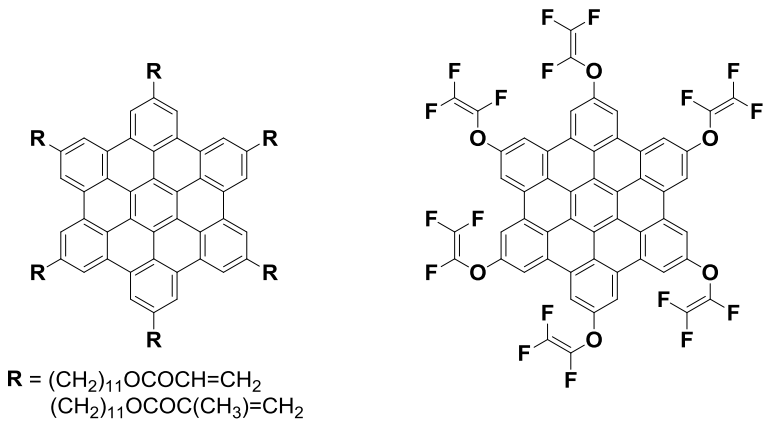

Figure 1-5. Alkyl- and trifluoroethenyl-substituted HBCs.

Aggregation states of HBC are also affected by the position of substituents. Figure 1-6 shows *para*-, *ortho*-, and *meta*-substituted HBCs, in analogy with substituted benzene derivatives.

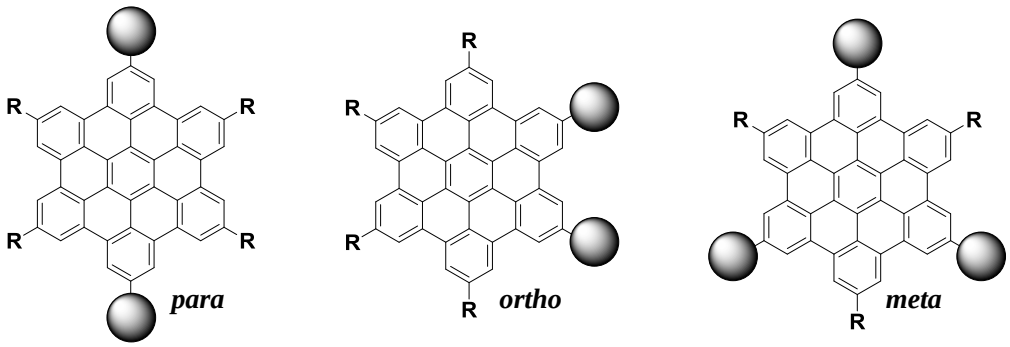

Figure 1-6. *para*-, *ortho*-, and *meta*-HBCs.

Müllen and coworkers have reported trimethoxy-substituted HBC, which forms a helical packing layer in liquid crystalline mesophases (Figure 1-7).[15] Influence of methoxy groups and the intermolecular interactions were investigated in the formation of the helical superstructure in the solid state.

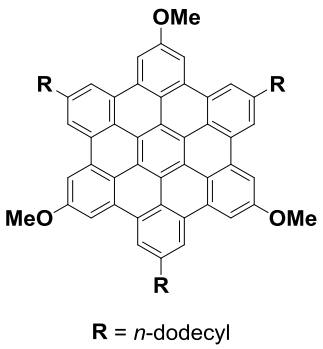

Figure 1-7. C_3-symmetrrical trimethoxy-substituted HBC.

As a representative example of a self-assembly of HBCs, Aida and coworkers reported a supramolecular nanotube assembly of a HBC derivative, which was decorated by hydrophilic and hydrophobic substituents.[16] In a polar solvent, the amphiphilic HBC derivative was aggregated spontaneously to form supramolecular nanotube with a diameter of 20 nm.

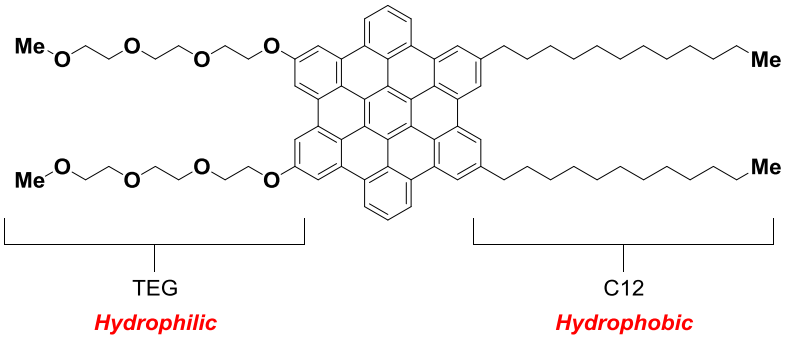

Figure 1-8. Amphiphilic HBC**.**

As demonstrated by these previous works, the aggregate state of HBCs can be effectively controlled by proper design of the substituents of the HBC core. Consequently, versatile methodologies to introduce a variety of substituents to the HBC core are required.

1-4. Conventional functionalization methods and their drawbacks

Müllen and coworkers have developed a general synthetic route to prepare HBC through Scholl oxidative fusion of hexaphenylbenzenes (HPBs) with $FeCl_3$ as an oxidant (Scheme 1-1 and Scheme 1-2). Sixfold symmetric HPBs were first prepared by $Co_2(CO)_8$-catalyzed cyclotrimerization of substituted

diphenylacetylenes followed by oxidative cyclization. This method allowed the synthesis of the parent HBC as well as symmetric substituted HBCs.[17,18] Lower symmetric HBCs were synthesized by an alternative route (Scheme 1-2). Diels–Alder cycloaddition between tetraphenylcyclopentadienones and diphenylacetylenes afforded the lower symmetric HPBs, which further underwent oxidative cyclization to furnish HBCs.

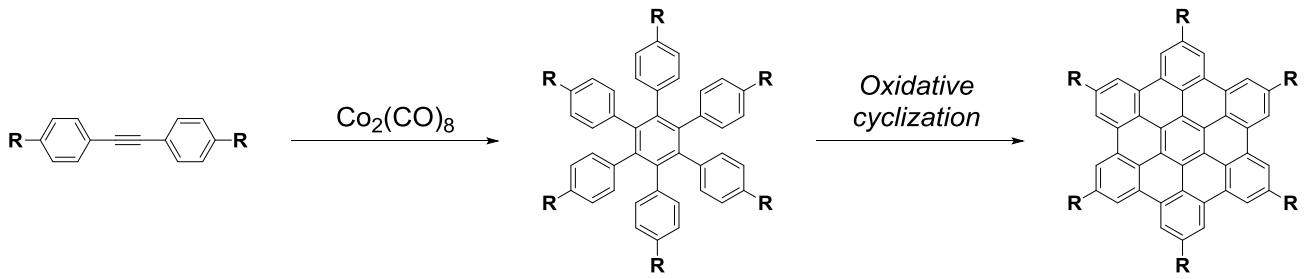

Scheme 1-1. General synthetic route (Sixfold Symmetric HBCs).

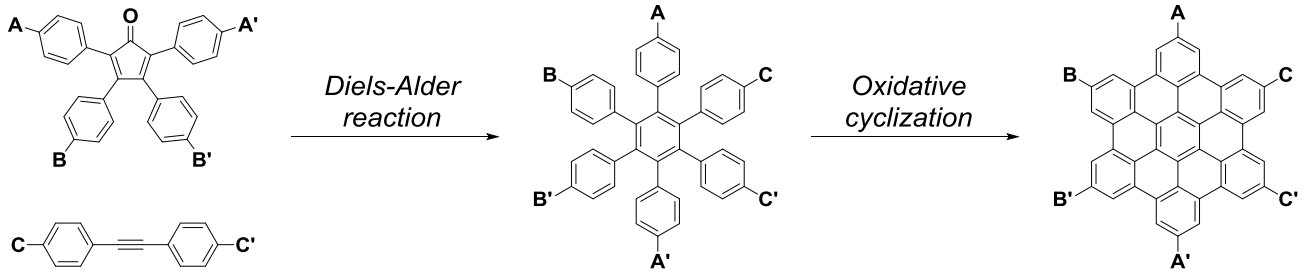

Scheme 1-2. General synthetic route (Lower symmetric HBCs).

These synthetic approaches are useful and have been successful for several HBCs. However, a serious drawback exists: It is not possible to introduce unstable substituents under oxidative cyclization reaction to HBCs. For example, synthesis of *para*-methoxy-substituted HBCs is difficult because of the formation of bis-spirocyclic dienone (Scheme 1-3).[19]

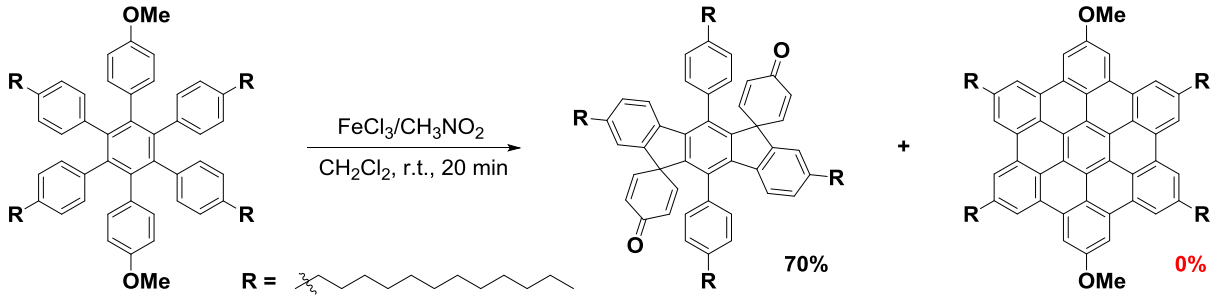

Scheme 1-3. Oxidative cyclization of *para*-methoxy-substituted HPB.

To overcome this drawback, introduction of substituents to HBC core after oxidative cyclization reaction is desirable (Figure 1-9). To achieve this purpose, a new synthetic concept is required.

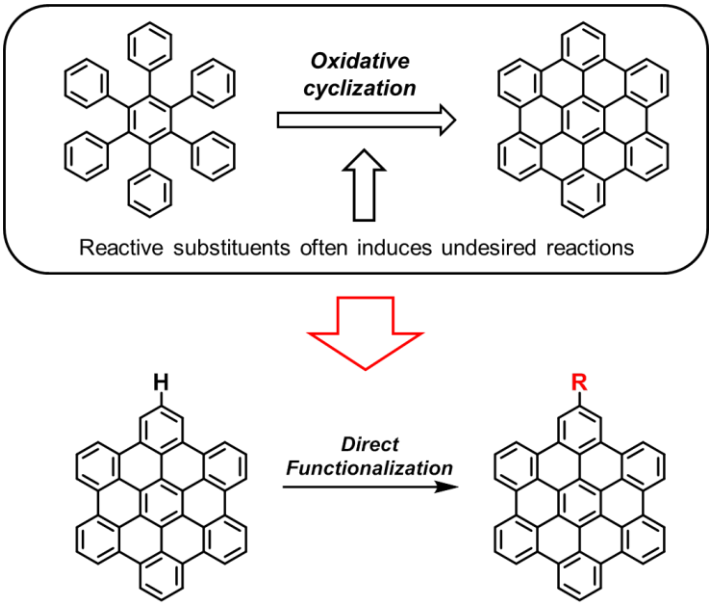

Figure 1-9. Direct functionalization of the HBC core.

1-5. Late-stage functionalization

Recently, the concept of late-stage functionalization of a molecule has received much attention. In the late-stage functionalization strategy, a basic skeleton of a molecule is constructed at first and then is subjected to modification. For examples, total syntheses of eudesmane terpenes by Baran and coworkers[20] and (+)-Lithospermic acid Yu and coworkers[21] were accomplished via late-stage functionalization. In the former example, the core skeleton was regioselectively oxidized to afford a library of analogues in a highly efficient manner (Scheme 1-4).

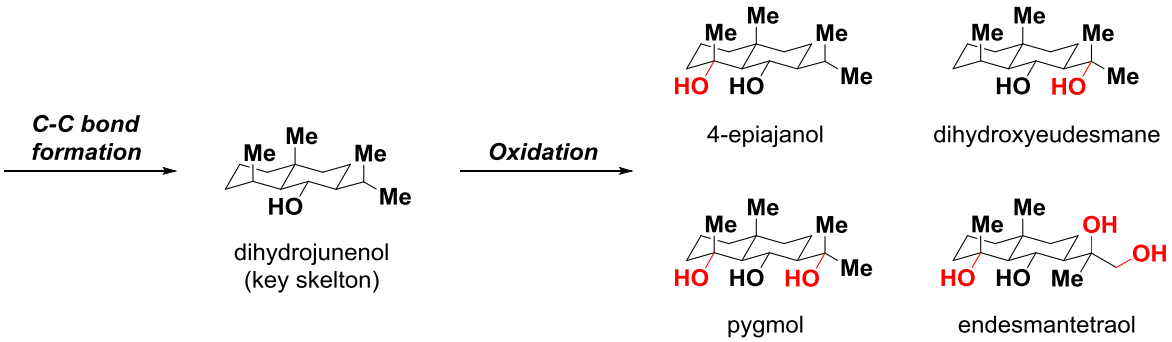

Scheme 1-4. Direct functionalization of basic skeleton.

In the latter example, they achieved to improve the overall yield and the convergence in the synthesis of the target molecule by using C–H olefination[22] at the end of the synthesis (Scheme 1-5).

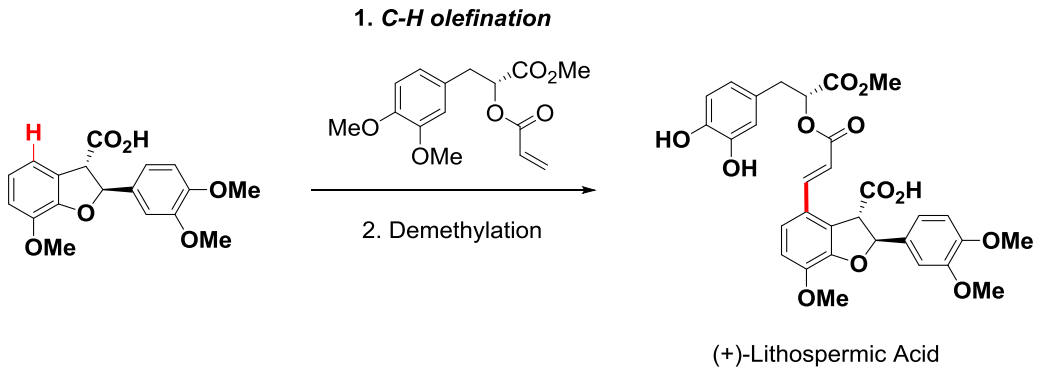

Scheme 1-5. Synthesis of (+)-Lithospermic Acid through C–H olefination.

In addition to these examples, Ritter and coworkers advocated "late-stage fluorination".[23] This can also be considered as an example of late-stage functionalization.

As shown in the examples above, late-stage functionalization thorough C–H activation not only solves the problems of modification of a molecular framework but also allows the expansion of freedom in the synthetic route.

In this study, the author attempted to develop a new methodology in modification of the HBC core through a late-stage functionalization approach. The author believes that the result of this study not only allows facile introduction of various functional groups to HBC but also leads to the creation of novel aggregate structures based on novel HBCs.

1-6. References

[1] (a) M. M. Haley, R. R. Tykwinski, Eds. *Carbon-Rich Compound*; Wiley-VCH: Weinheim, **2006**. (b) R. G. Harvey, *Polycyclic Aromatic Hydrocarbons*; Wiley-VCH: New York, **1997**.

[2] X. Feng, W. Pisula, K. Müllen, *Pure. Appl. Chem.* **2009**, *81*, 2203.

[3] T. M. Figueira-Duarte, K. Müllen, *Chem. Rev.* **2011**, *111*, 7260.

[4] A. Yadav, P. C. Mishra, *J. Phys. Chem. A.* **2013**, *117*, 8958.

[5] (a) G. Portella1, J. Poater, M. Solà, *J. Phys. Org. Chem.* **2005**, *18*, 785. (b) M. Randić, *Chem. Rev.* **2003**, *103*, 3449. (c) M. D. Watson, A. Fechtenkötter, K. Müllen, *Chem. Rev.* **2001**, *101*, 1267. (d) S. W. Slayden, J. F. Liebman, *Chem. Rev.* **2001**, *101*, 1541.

[6] (a) M. Abe, *Chem. Rev.* **2013**, *113*, 7011. (b) A. Konishi, Y. Hirao, M. Nakano, A. Shimizu, E. Botek, B. Champagne, D. Shiomi, K. Sato, T. Takui, K. Matsumoto, H. Kurata, T. Kubo, *J. Am. Chem. Soc.* **2010**, *132*, 11021.

[7] (a) A. Konishi, Y. Hirao, K. Matsumoto, H. Kurata, R. Kishi, Y. Shigeta, M. Nakano, K. Tokunaga, K. Kamada, T. Kubo, *J. Am. Chem. Soc.* **2013**, *135*, 1430. (b) Z. Sun, S. Lee, K. H. Park, X. Zhu, W. Zhang, B. Zheng, P. Hu, Z. Zeng, S. Das, Y. Li, C. Chi, R. Li, K. Huang, J. Ding, D. Kim, J. Wu, *J. Am. Chem. Soc.* **2013**, *135*, 18229.

[8] (a) W. Pisula, M. Kastler, D. Wasserfallen, T. Pakula, K. Müllen, *J. Am. Chem. Soc.* **2004**, *126*, 8074. (b) J. Wu, A. Fechtenkötter, J. Gauss, M. D. Watson, M. Kastler, C. Fechtenkötter, M. Wagner, K. Müllen, *J. Am. Chem. Soc.* **2004**, *126*, 11311.

[9] J. Wu, W. Pisula, K. Müllen, *Chem. Rev.* **2007**, *107*, 718.

[10] (a) E. Clar, C. T. Ironside, *Proc. Chem. Soc.* **1958**, 150. (b) E. Clar, C. T. Ironside, M. Zander, *J. Chem. Soc.* **1959**, 142.

[11] M. Kastler, J. Schmidt, W. Pisula, D. Sebastiani, K. Müllen, *J. Am. Chem. Soc.* **2006**, *128*, 9526.

[12] W. Pisula, Ž. Tomović, C. Simpson, M. Kastler , T. Pakula, K. Müllen, *Chem. Mater.* **2005**, *17*, 4296.

[13] I. Fischbach, T. Pakula, P. Minkin, A. Fechtenkötter, K. Müllen, H. W. Spiess, *J. Phys. Chem. B* **2002**, *106*, 6408.

[14] J. D. Brand , C. Kübel, S. Ito , K. Müllen, *Chem. Mater.* **2000**, *12*, 1638.

[15] X. Feng, W. Pisula, M. Takase, X. Dou, V. Enkelmann, M. Wagner, N. Ding, K. Müllen, *Chem. Mater.* **2008**, *20*, 2872.

[16] J. P. Hill, W. Jin, A. Kosaka, T. Fukushima, H. Ichihara, T. Shimomura, K. Ito, T. Hashizume, N. Ishii, T. Aida, *Science* **2004**, *304*, 1481.

[17] P. Herwig, C. W. Kayser, K. Müllen, H. W. Spiess, *Adv. Mater.* **1996**, *8*, 510.

[18] A. Fechtenkötter, K. Saalwächter, M. A. Harbison, K. Müllen, H. W. Spiess, *Angew. Chem. Int. Ed.* **1999**, *38*, 3039.

[19] X. Dou, X. Yang, G. J. Bodwell, M. Wagner, V. Enkelmann, K. Müllen, *Org. Lett.* **2007**, *9*, 2485.

[20] K. Chen, P. S. Baran, *Nature*, **2009**, *459*, 824.

[21] D.-H. Wang, J.-Q. Yu, *J. Am. Chem. Soc.* **2011**, *133*, 5767.

[22] D.-H. Wang, K. M. Engle, B.-F. Shi, J.-Q. Yu, *Science* **2010**, *327*, 315.

[23] (a) P. Tang, T. Furuya, T. Ritter, *J. Am. Chem. Soc.* **2010**, *132*, 12150. (b) F. Sladojevich, S. I. Arlow, P. Tang, T. Ritter, *J. Am. Chem. Soc.* **2013**, *135*, 2470.

Chapter 2.

Synthesis of Oxygen-Substituted Hexa-*peri*-hexabenzocoronenes through Iridium-Catalyzed Direct Borylation

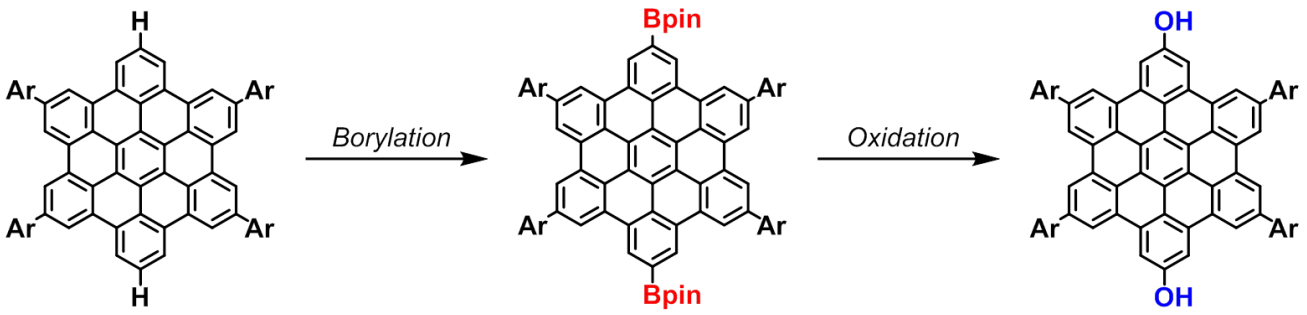

C–H borylation of HBCs with an iridium catalyst provided borylated HBCs regioselectively, which were converted to hydroxy HBCs via oxidation of the boryl groups. Treatment of dihydroxy HBC with a hypervalent iodine reagent afforded tetraoxo HBC with *syn*-selectivity.

·Contents

1. Introduction

As discussed in Chapter 1, introduction of various substituents to the HBC core is an important issue. However, introduction of functional groups to the HBC core has been limited because of its low solubility. Moreover, the presence of reactive substituents causes side reactions during Scholl reaction of HPB derivatives.[1]

Recently, transition metal catalyzed direct functionalization has been a hot topic in organic chemistry.[2] Among them, Ir-catalyzed direct borylation is a convenient method to functionalize PAHs.[3] Direct borylation of pyrene,[4] perylene,[5] acene,[6] phenacene,[7] and anthanthrenylene[8] have been reported so far (Scheme 2-1). As can be seen from these examples, regioselectivity of direct borylation is determined by the steric factor of the substrates.

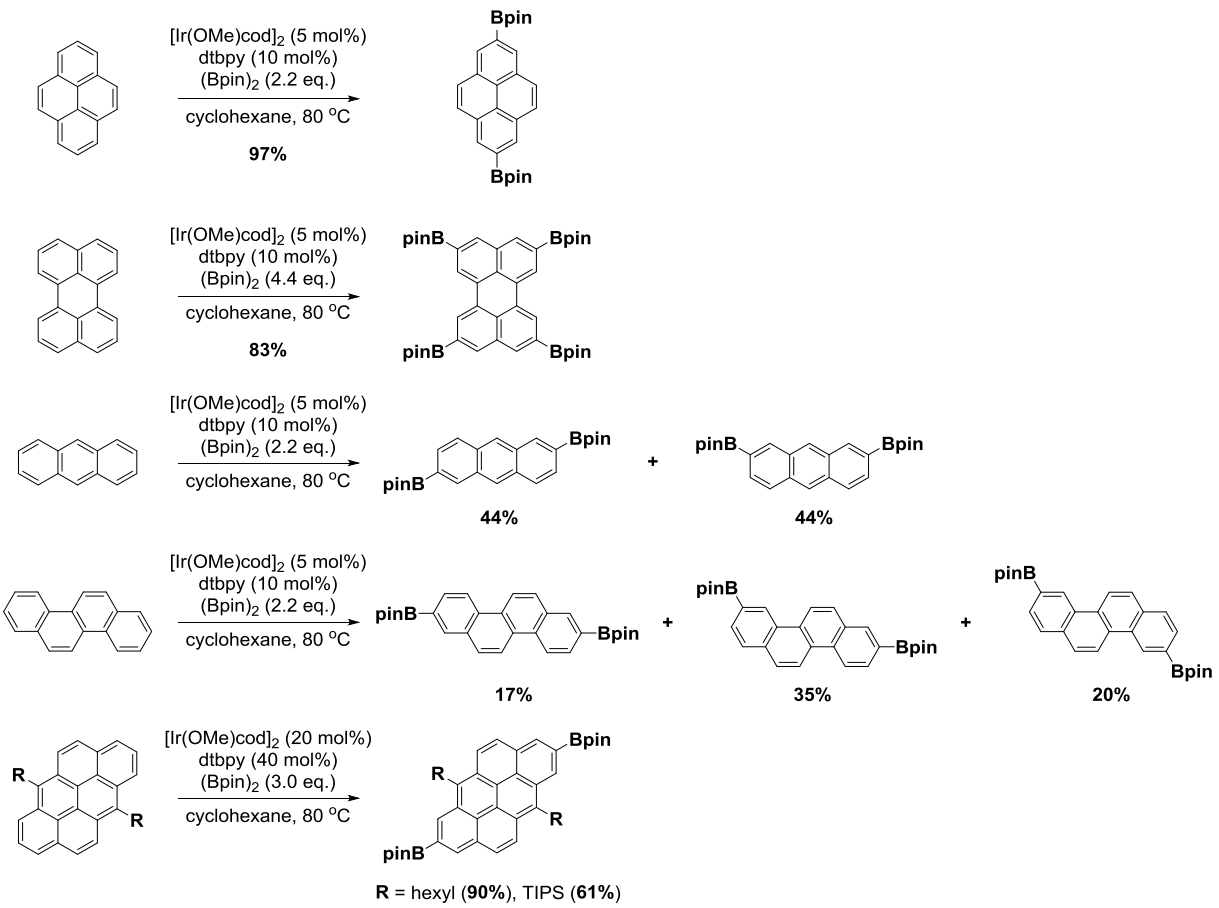

Scheme 2-1. Direct borylation of several PAHs.

The borylated PAHs are convenient intermediates for Suzuki–Miyaura coupling or oxidation to the corresponding alcohols. By using the direct borylation, the author expected to achieve selective modification of HBCs.

2. Synthesis of soluble-HBC

HBCs with bulky substituents were prepared to increase the solubility. 2,5,11,14-Tetra-*tert*-butyl HBC was tested as a substrate (Scheme 2-2).[9] However, iridium-catalyzed direct borylation did not proceed due to the insolubility of this compound in reaction solvents.

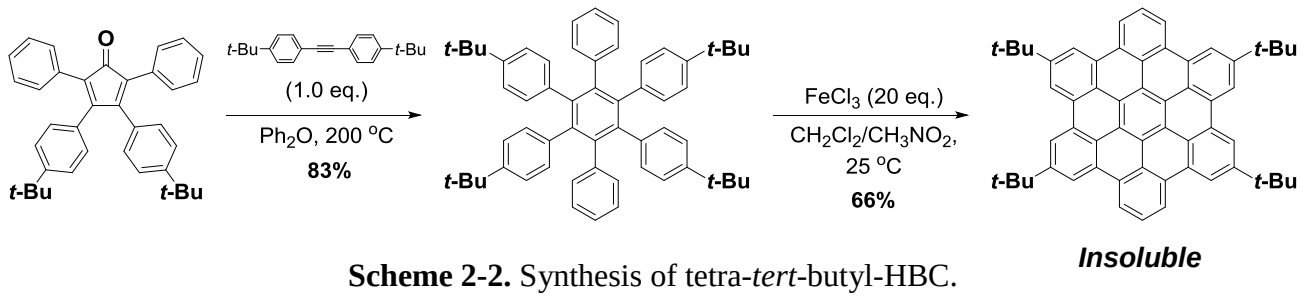

Scheme 2-2. Synthesis of tetra-*tert*-butyl-HBC.

To improve the solubility of the substrate, the introduction of more bulky substituents were required. Mesityl groups were introduced by Kumada–Tamao–Corriu coupling of 1,2,4,5-tetra(4-bromophenyl)-3,6-diphenylbenzene with 8.0 equiv of mesitylmagnesium bromide (Scheme 2-3).[10] Scholl reaction of 1,2,4,5-tetra(4-mesitylphenyl)-3,6-diphenylbenzene with 20 equiv of $FeCl_3$ in CH_2Cl_2/EtOH (2000/1) provided mesityl-substituted HBC **1a** in 96% yield. This compound was soluble in organic solvents such as dichloromethane, chloroform, toluene, and THF.[11] HBCs **1b** and **1c** provided under similar reaction conditions, and these compounds also showed high solubility for various organic solvents. These three types of mesityl-substituted HBCs were employed for direct C–H borylation.

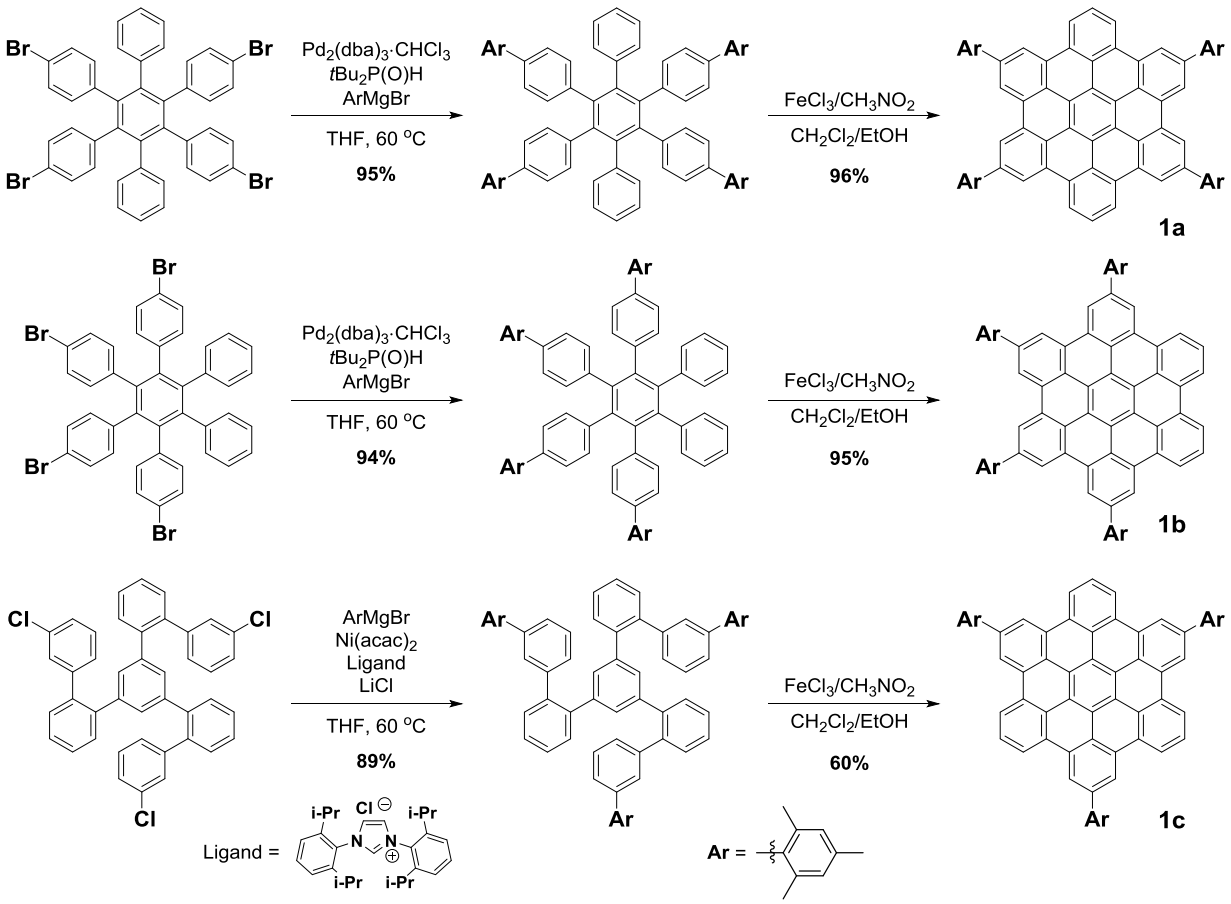

Scheme 2-3. Synthesis of mesityl-substituted HBCs.

3. Direct borylation and oxidation

Iridium-catalyzed direct borylation of **1a**, **1b,** and **1c** was then investigated (Scheme 2-4). Direct borylation of the **1a** and **1b** were carried out with bis(pinacolate)diboron (4.0 equiv), in the presence of catalytic amount of $[Ir(OMe)(cod)]_2$ (3 mol%), and dtbpy (6 mol%) as a ligand.[12] The use of mesitylene/*tert*-butyl methyl ether furnished the borylated product **2a** and **2b** in good yields.[13] Direct borylation of **1c** was performed with bis(pinacolate)diboron (6.0 equiv) and $[Ir(OMe)(cod)]_2$ (5 mol%), and dtbpy (10 mol%) in *tert*-butyl methyl ether at reflux to provide the *tri*-borylated product **3c** in 73% yields. Oxidation of **2a** and **2c** with basic hydrogen peroxide provided **3a** and **3c** in 85% and 69% yields, respectively.[14] However, **2b** was not oxidized under same reaction condition. After several trials, oxidation of the boryl groups in **2b** by Oxone/acetone furnished **3b** in 79% yields.

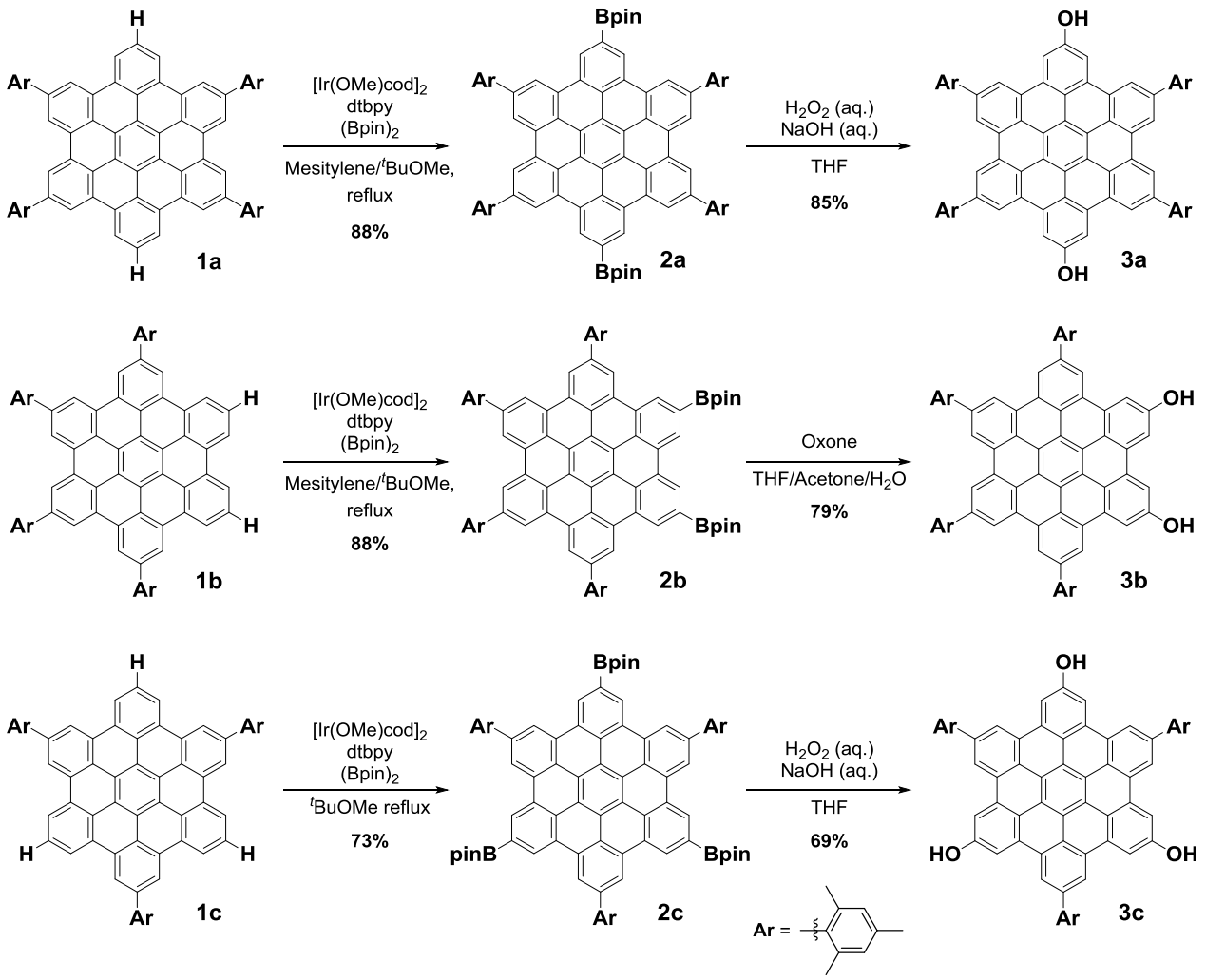

Scheme 2-4. Direct borylation and oxidation of *para*-, *ortho*-, and *meta*-HBC.

The structures of **3a**, **3b,** and **3c** were unambiguously determined by X-ray diffraction analysis (Figures 2-1, 2-2, and 2-3). The HBC plane of **3a** and **3c** were slightly distorted, and the mean plane deviations were 0.045 Å and 0.049 Å, respectively. In crystal packing of **3a** and **3c**, existence of hydrogen bonding is suggested by short distances (2.68 Å and 2.76 Å) between two oxygen atoms on the adjacent molecules. Notably, a 1D chain network of **3a** was constructed in crystal by the hydrogen bonding interactions. In contrast to **3a** and **3c**, **3b** formed a columnar π–π stacking structure. The distances between the two closest HBC planes are 3.35 and 3.25 Å. The difference in packing among the three types of HBCs **3a**, **3b**, and **3c** is probably related to the presence of π–π interactions.

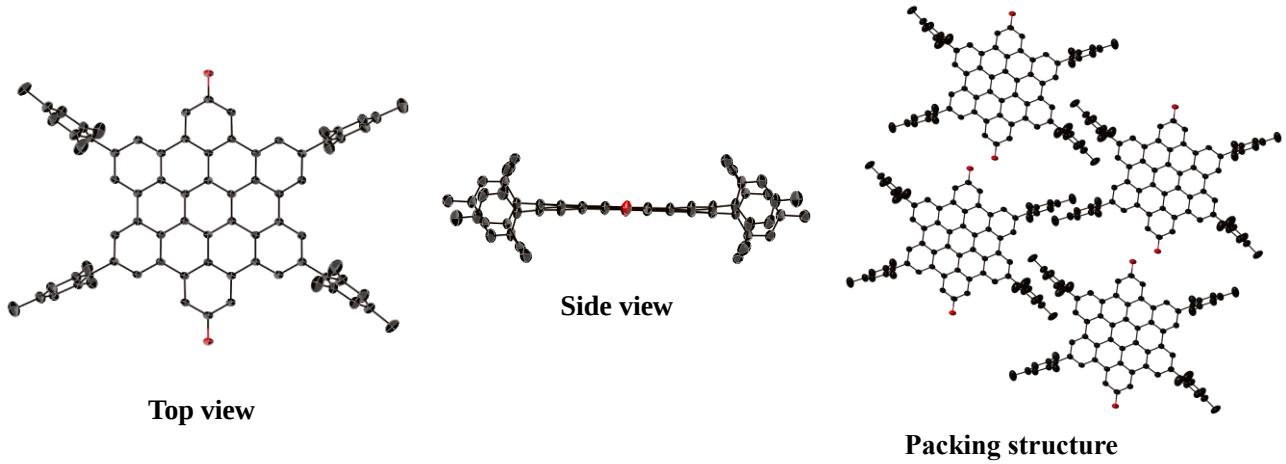

Figure 2-1. X-ray crystal structure of **3a**. The thermal ellipsoids are scaled to the 50% probability level.

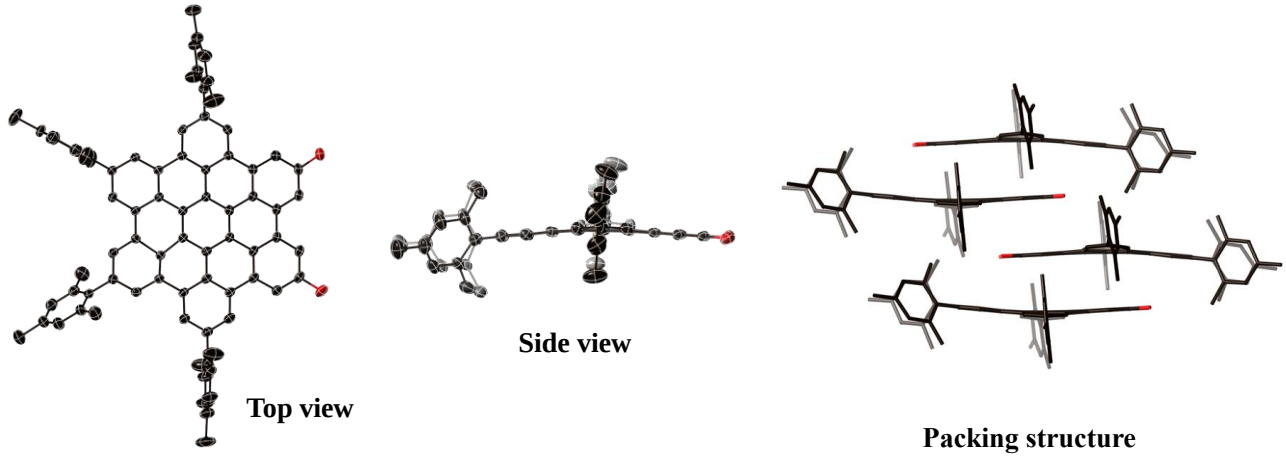

Figure 2-2. X-ray crystal structure of **3b**. The thermal ellipsoids are scaled to the 50% probability level.

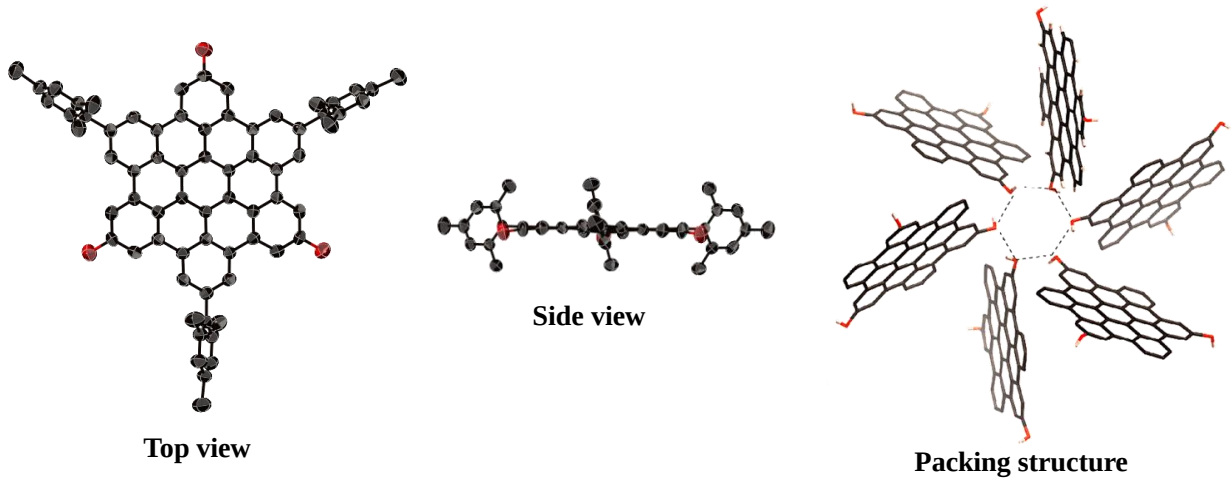

Figure 2-3. X-ray crystal structure of **3c**. The thermal ellipsoids are scaled to the 50% probability level.

4. Synthesis of π-extended quinone

To synthesize a π-extended quinone from HBCs, further oxidation of **3a** was investigated. Unfortunately, the expected quinone product could not be isolated due to its low stability. On the other hand, oxidation of **3a** with 4.4 equiv of phenyliodine bis(trifluoroacetate) (PIFA) efficiently afforded the tetraoxo product **9** regioselectively (Scheme 2-5).[15]

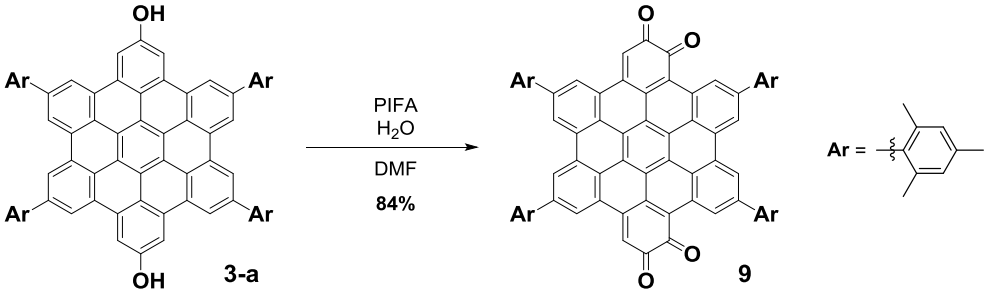

Scheme 2-5. Synthesis of HBC-tetraone **9**.

Regioselectivity of oxidation was determined on the basis of tetrahydroxy HBC **10**, which was obtained by the reduction of HBC-tetraone **9** with $NaBH_4$ in 79% (Scheme 2-6).[16] The structure of **10** was determined by the NOESY experiment. The syn-regioselectivity was also confirmed by X-ray diffraction analysis of the tetraacetylate **11** (Figure 2-4).

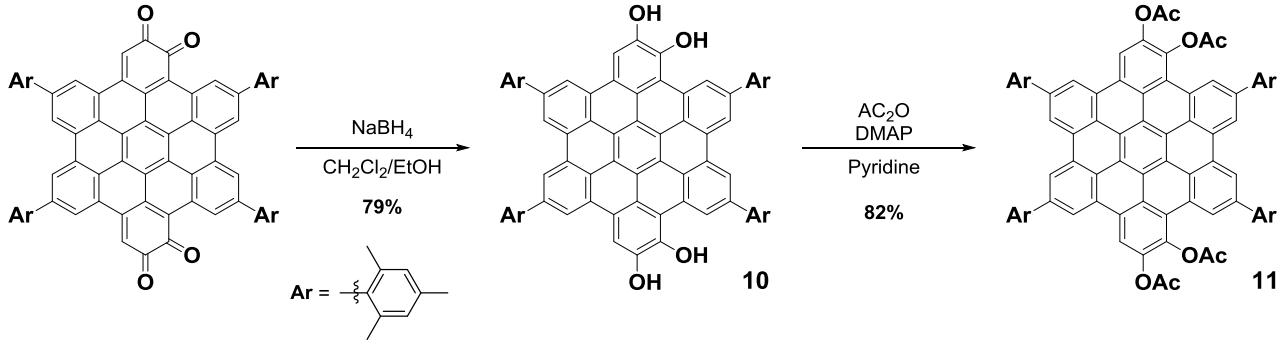

Scheme 2-6. Reduction and acetylation of **9**.

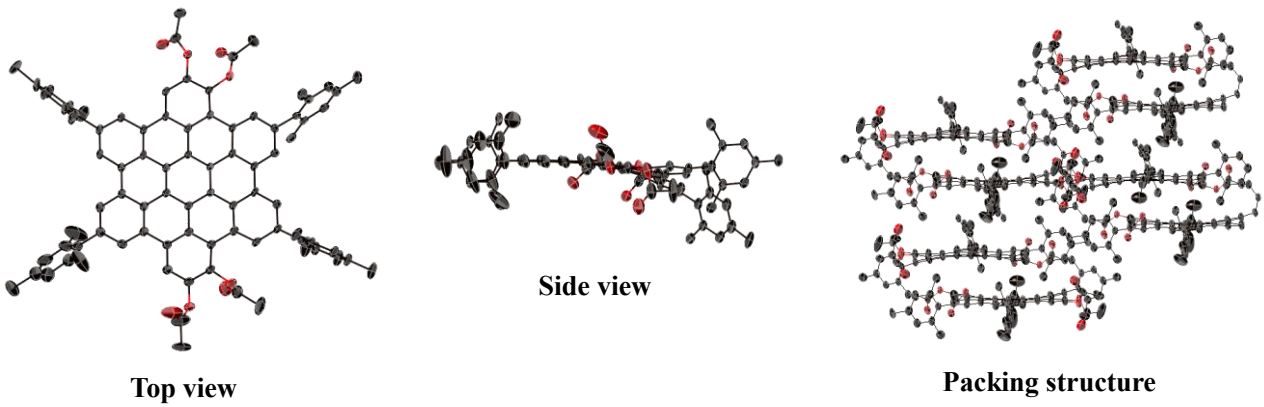

Figure 2-4. X-ray crystal structure of **11**. The thermal ellipsoids are scaled to the 50% probability level.

The plausible reaction mechanism of the formation of **9** was proposed in Scheme 2-7. Nucleophilic addition of water to the HBC-dione yields *ortho*-quinone intermediate **a**. In fact, the generation of intermediate **a** was confirmed by the ^{1}H NMR spectrum. Then, the reaction of **a** with PIFA affords the intermediate **b**, which is then selectively attacked by water to provide HBC-tetraone. DFT calculations suggest that the LUMO of **b** has a large MO coefficient only at the *syn*-carbon atom (Figure 2-5). From these results, the author concluded that the distribution of the LUMO of **b** determines the regioselectivity of the formation of HBC-tetraone.

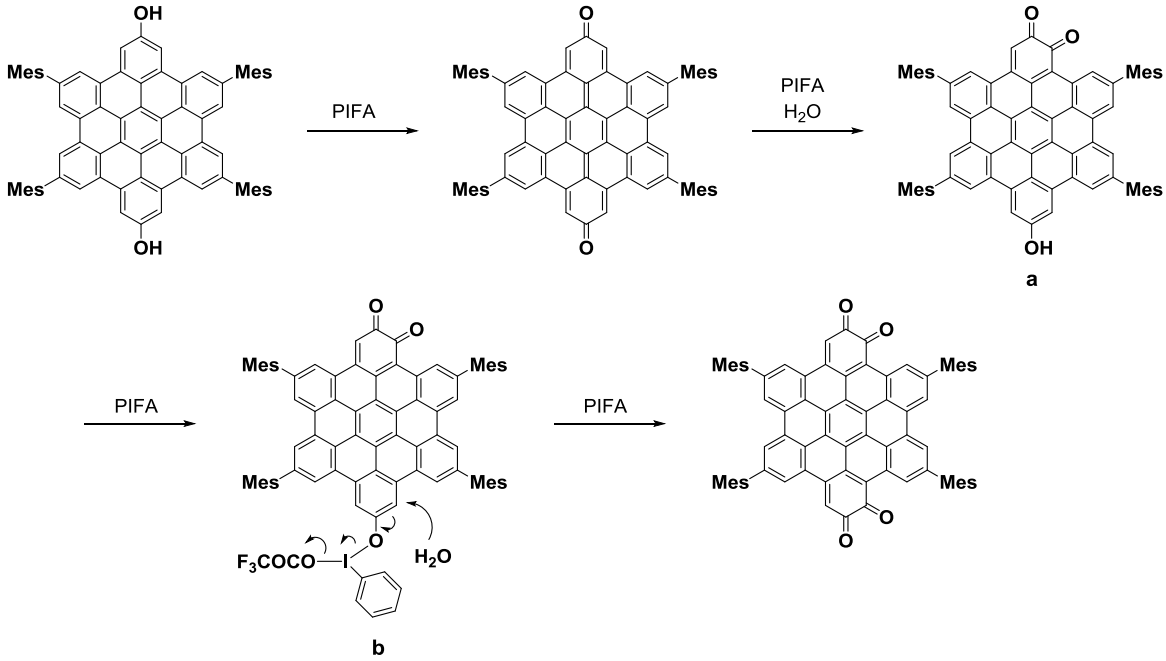

Scheme 2-7. Plausible reaction mechanism of **9**.

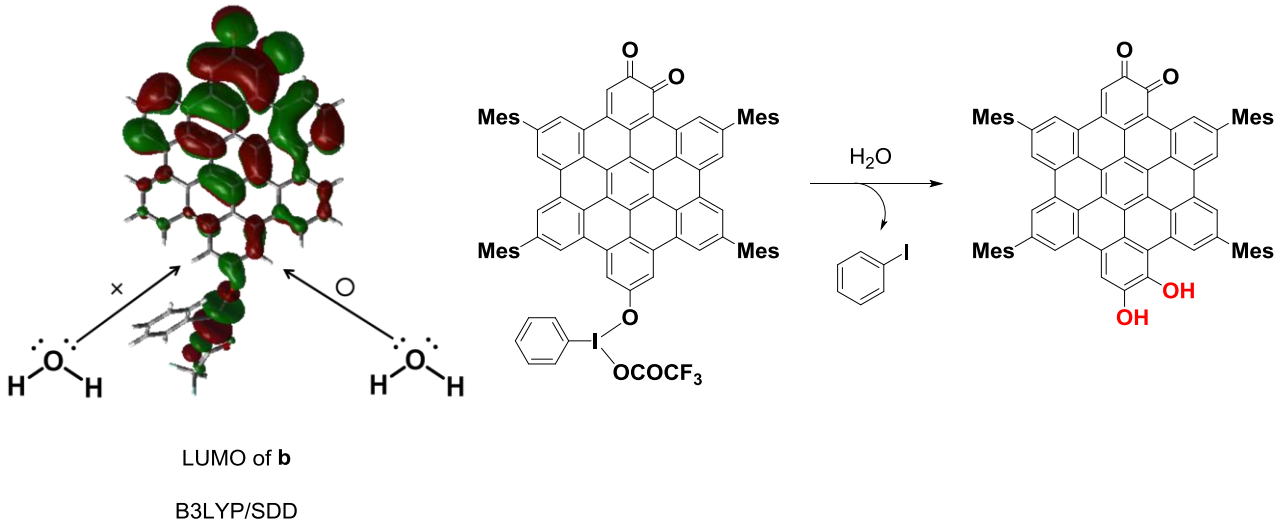

Figure 2-5. Calculated LUMO of intermediate **b**.

5. UV/vis absorption spectra

Figure 2-6 shows UV/vis absorption spectra of **1a, 3a**, **9**, and **10** in CH_2Cl_2. HBCs **1a**, **3a**, and **10** exhibited typical absorption spectra for HBCs.[17] As compared to **3**, the absorption spectrum of **10** is slightly bathochromic shifted due to electron-donating hydroxy groups. The broadening of the spectrum of **10** is likely because of lowered symmetry. HBC quinone **9** showed a broad band reaching to the near infrared region. The large bathochromic shift can be explained by intramolecular charge-transfer interactions from the core to the carbonyl moieties. According to the TD-DFT calculation, the broad absorption at 571 nm was assigned as the transition of HOMO–1→LUMO+1 and HOMO→LUMO. As shown in Figure 2-7, HOMO–1 and HOMO are separated from LUMO+1 and LUMO of **9**, supporting intramolecular charge-transfer characters in these transitions.

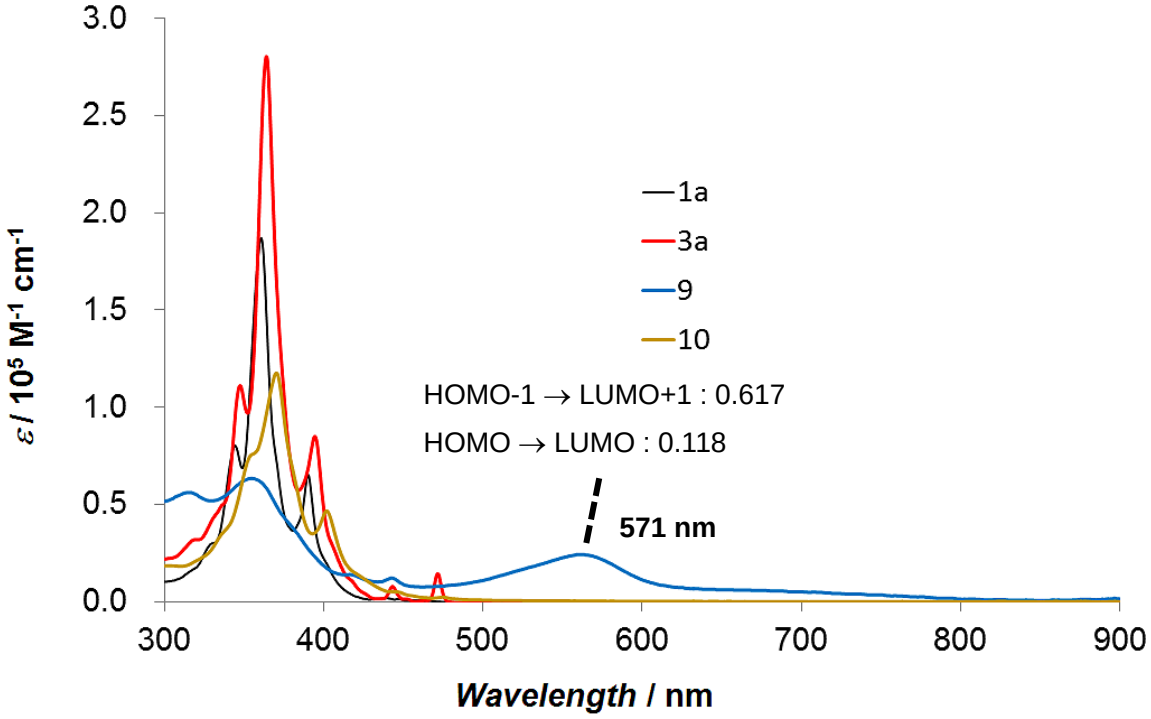

Figure 2-6. UV/vis absorption spectra of **1a**, **3a**, **9**, and **10** in CH_2Cl_2.

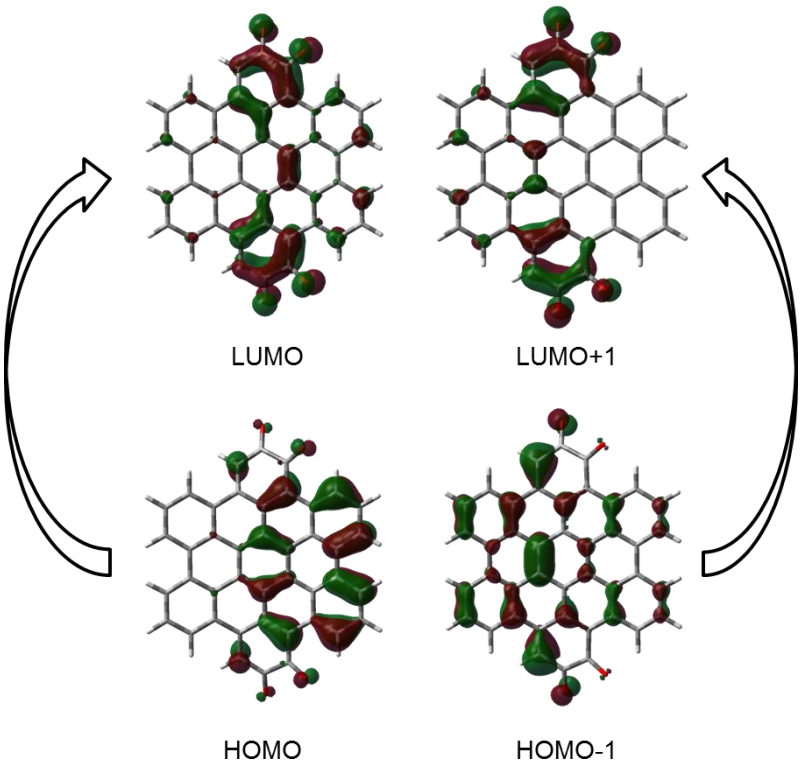

Figure 2-7. UV/vis absorption spectra of **1a**, **3a**, **9**, and **10** in CH_2Cl_2.

6. Cyclic voltammetry

The HOMO and LUMO energies of **3a** and **11** were estimated on the basis of electrochemical analysis by cyclic voltammetry and differential pulse voltammetry (Figures 2-8, 2-10, and Table 2-1). The oxidation and reduction potentials of **9** were determined by differential pulse voltammetry (Figure 2-9, and Table 2-1). Reduction and oxidation waves of **9** were detected at –0.52 and 1.03 V (vs ferrocene/ferrocenium cation), respectively. Compared to **3a** and **11**, the difference between oxidation and reduction potentials of **9** is small (1.55 V).

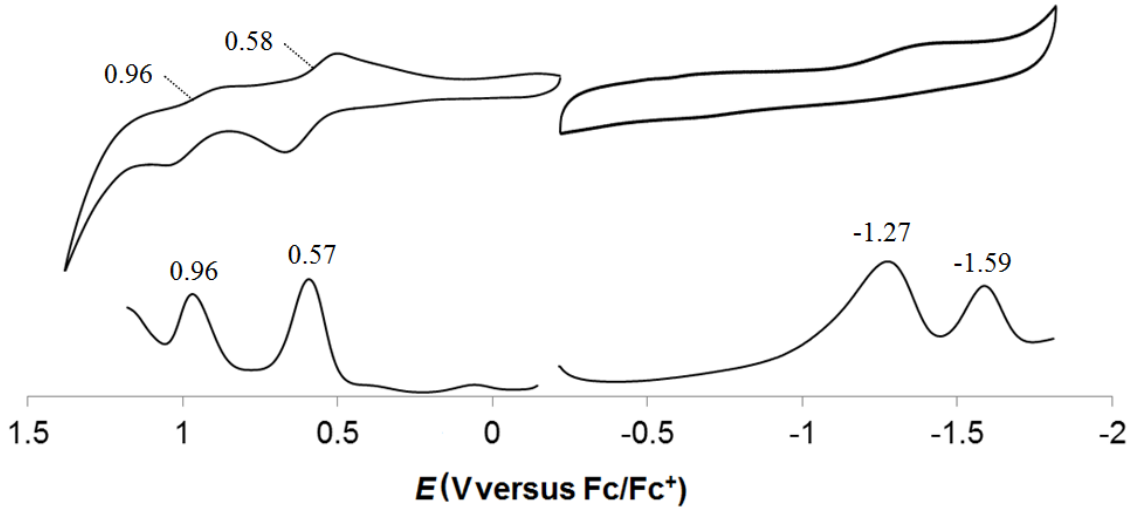

Figure 2-8. Cyclic voltammgram and differential pulse voltammgram of **3a**. Electrolyte: 0.1 M Bu_4NPF_6 in CH_2Cl_2; Working Electrode: Glassy Carbon; Counter Electrode: Pt; Reference Electrode: $Ag/AgClO_4$; Scan rate: 0.1 V/s.

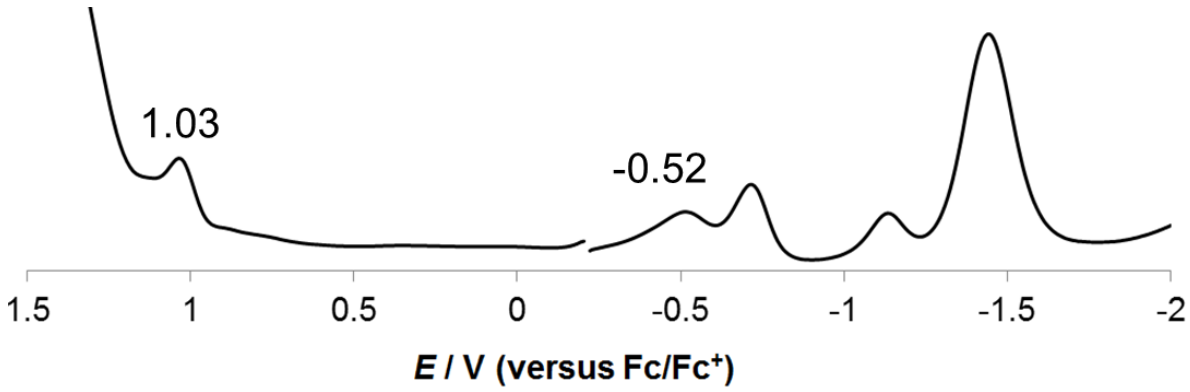

Figure 2-9. Differential pulse voltammgram of **9.** Electrolyte: 0.1 M Bu_4NPF_6 in CH_2Cl_2; Working Electrode: Glassy Carbon; Counter Electrode: Pt; Reference Electrode: $Ag/AgClO_4$; Scan rate: 0.1 V/s.

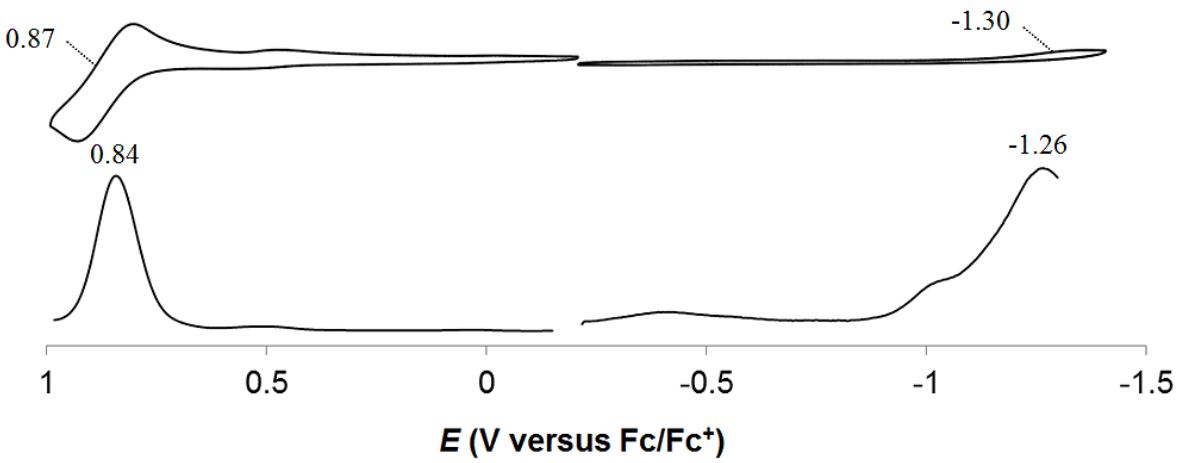

Figure 2-10. Cyclic voltammgram and differential pulse voltammgram of **11.** Electrolyte: 0.1 M Bu_4NPF_6 in CH_2Cl_2; Working Electrode: Glassy Carbon; Counter Electrode: Pt; Reference Electrode: $Ag/AgClO_4$; Scan rate: 0.1 V/s.

Table 2-1. Summary of electrochemical potentials of **3a**, **9** and **11**.

Compounds	E_{ox}^{2} / V	E_{ox}^{1} / V	E_{red}^{1} / V	E_{red}^{2} / V	ΔE^{a} / V
3a	0.96	0.57	–1.27	–1.59	1.84
9	–	1.03	–0.52	-0.72	1.55
11	–	0.84	–1.26	–	2.10

a: $\Delta E = E_{ox}^{1} - E_{red}^{1}$

7. Summary

In this chapter, the author describes that iridium-catalyzed C–H borylation of tetramesityl-, and tri-mesityl-substituted HBCs afforded multi-borylated HBCs in excellent yields. The borylated HBCs were easily transformed into hydroxylated HBCs, which were not accessible by the conventional oxidative fusion reaction. Furthermore, HBC-tetraone **9** was obtained through treatment of dihydroxy HBC **3a** with PIFA. The present late-stage functionalization would be useful for the introduction of a variety of functional groups after construction of the HBC core.

8. References

[1] J. Wu, W. Pisula, K. Müllen, *Chem. Rev.* **2007**, *107*, 718.

[2] D. Alberico, M. E. Scott, M. Lautens, *Chem. Rev.* **2007**, *107*, 174.

[3] I. A. I. Mkhalid, J. H. Barnard, T. B. Marder, J. M. Murphy, J. F. Hartwig, *Chem. Rev.* **2010**, *110*, 890.

[4] Z. Liu, Y. Wang, Y. Chen, J. Liu, Q. Fang, C. Kleeberg, T. B. Marder, *J. Org. Chem.* **2012**, *77*, 7124.

[5] D. N. Coventry, A. S. Batsanov, A. E. Goeta, J. A. K. Howard, T. B. Marder, R. N. Perutzb, *Chem. Commun.* **2005**, 2172.

[6] (a) T. Kimoto, K. Tanaka, Y. Sakai, A. Ohno, K. Yoza, K. Kobayashi, *Org. Lett.* **2009**, *11*, 3658. (b) R. Ozawa, K. Yoza, K. Kobayashi, *Chem. Lett.* **2011**, *40*, 941. (c) Y. Koyama, S. Hiroto, H. Shinokubo, *Angew. Chem. Int. Ed.* **2013**, *52*, 5740.

[7] S. Hitosugi, Y. Nakamura, T. Matsuno, W. Nakanishi, H. Isobe, *Tetrahedron Letters* **2012**, *53*, 1180.

[8] T. Matsuno, S. Kamata, S. Hitosugia, H. Isobe, *Chem. Sci.* **2013**, *4*, 3179.

[9] S. K. Sadhukhan, C. Viala, A. Gourdon, *Synthesis* **2003**, *10*, 1521.

[10] (a) C. Wolf, H. Xu, *J. Org. Chem.* **2008**, *73*, 162. (b) G. Y. Li, *Angew. Chem. Int. Ed.* **2001**, *40*, 1513.

[11] R. Yamaguchi, S. Hiroto, H. Shinokubo, *Org. Lett.* **2012**, *14*, 2472.

[12] T. Ishiyama, J. Takagi, J. F. Hartwig, N. Miyaura, *Angew. Chem. Int. Ed.* **2002**, *41*, 3056.

[13] P. Harrisson, J. Morris, P. G. Steel, T. B. Marder, *Synlett* **2009**, *1*, 147.

[14] R. J. Ely, J. P. Morken, *J. Am. Chem. Soc.* **2010**, *132*, 2534.

[15] A, Wu, Y. Duan, D. Xu, T. M. Penning, R. G. Harvey, *Tetrahedron* **2010**, *66*, 2111.

[16] K. L. Platt, F. Oesch, *J. Org. Chem.* **1983**, *48*, 265.

[17] M. Kastler, J. Schmidt, W. Pisula, D. Sebastiani, K. Müllen, *J. Am. Chem. Soc.* **2006**, *128*, 9526.

Chapter 3.

Functionalization of Hexa-*peri*-hexabenzocoronenes:

Investigation of the Substituent Effects on a Superbenzene

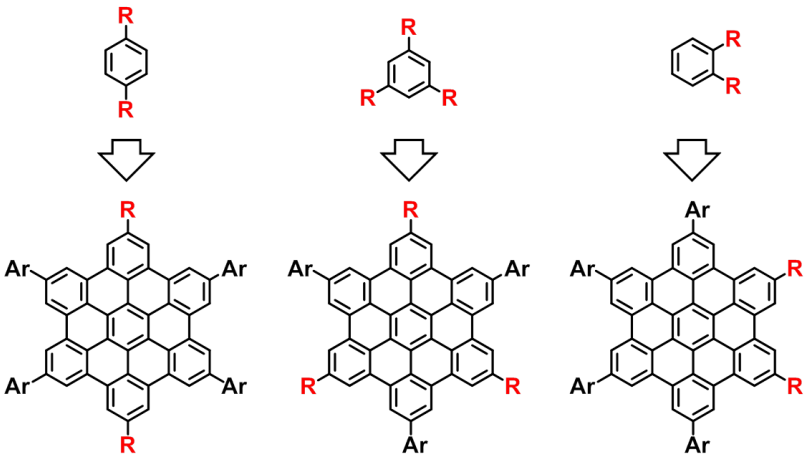

In this chapter, optical properties of HBCs as π-extended benzenes are described. The boryl groups on HBCs could be transformed into various functional groups such as hydroxy, methoxy, cyano, ethynyl, and amino groups. The substituents significantly influenced the α-band of UV/vis absorption spectra and to enhance fluorescence quantum yields of HBCs. Larger two-photon absorption cross-section values were observed for *para*-substituted HBCs than *ortho*- and *meta*-substituted HBCs.

Contents

1. Introduction

Various HBCs have been synthesized to obtain insight on their aggregation structure.[2] On the other hand, the properties of "non-aggregated HBCs" have remained unexplored. The effect of the substituents and their location on the optical properties has not been systematically investigated.

The energy diagrams of benzene and HBC are compared in Figure 3-1. The HOMO–LUMO gap of HBC is much smaller than that of benzene due to π-expansion. However, the pattern of degeneracy in these frontier orbitals is similar. As a result, HBC can be regarded as a π-extended benzene and therefore HBC is sometimes called as superbenzene. Studies on the substituent effects on HBC should be important to understand the properties of superbenzene at the single molecular level.

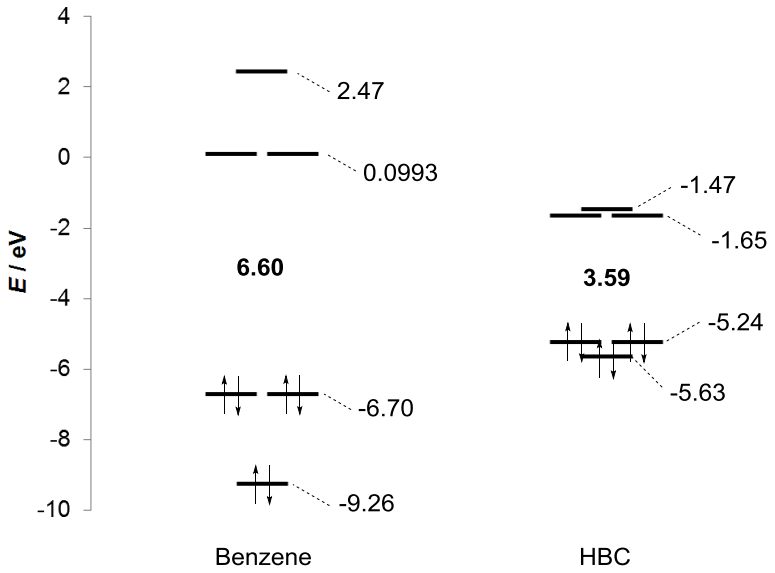

Figure 3-1. Energy diagrams of benzene and HBC calculated at the B3LYP/6-31G(d) level.

Comparison of the optical properties of various substituted HBCs would reveal the substituent effects on the HBC core. To conduct this investigation, there were several considerations. Soluble HBCs often possess long alkyl chains to induce facile aggregation, which prevents thorough studies on the properties of the isolated HBC molecule.[3] In contrast, *para*-, *ortho*-, and *meta*-mesityl-substituted HBCs are fairly soluble in common organic solvents and optimal for investigations on HBCs in the non-aggregated state (Figure 3-2). Herein the author discloses synthetic

methods for functionalized HBCs from hydroxy HBCs **3a**, **3b**, and **3c**. In addition, the effect of the substituents on the optical properties is discussed.

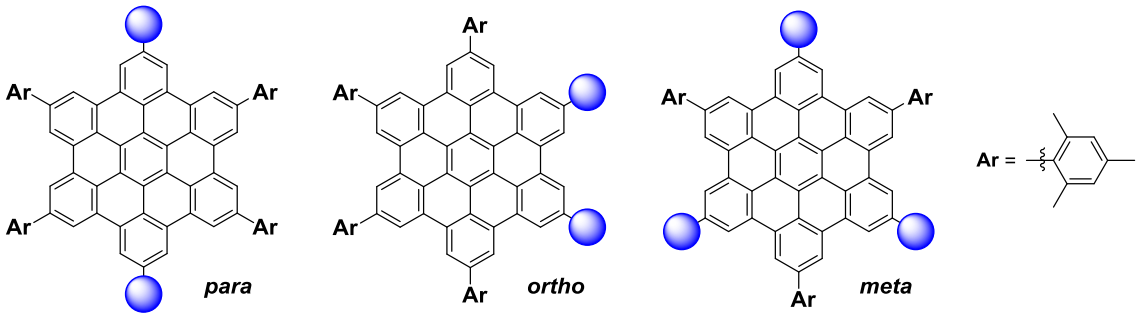

Figure 3-2. *para*-, *ortho*-, and *meta*-mesityl-substituted HBCs.

2. Functional group transformation

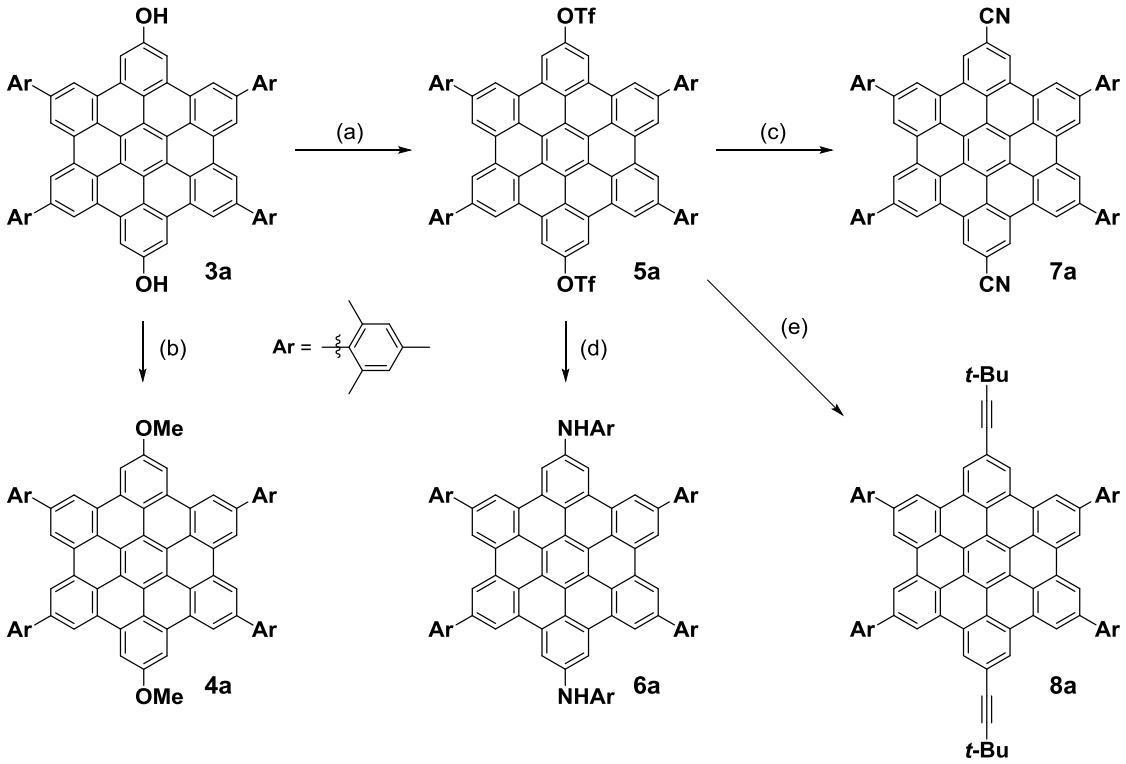

Scheme 3-1. Introduction of various functionalities to *para*-substituted HBC.

Reagents and conditions: (a) Tf_2O (4.0 equiv), pyridine (8.0 equiv), CH_2Cl_2, rt, 3 h; (b) MeI (excess), K_2CO_3 (8.0 equiv), THF/acetone=3/1, reflux, 24 h; (c) KCN (8.0 equiv), $Pd_2dba_3{\cdot}CHCl_3$ (5 mol%), DPPF (10 mol%), Zn (6 mol%), toluene/NMP=1:1, 60 °C, 24 h; (d) 2,4,6-trimethylaniline (8.0 equiv), $Pd_2dba_3{\cdot}CHCl_3$ (5 mol%), DPPF (10 mol%), Cs_2CO_3 (6.0 equiv), toluene, reflux, 30 h; (e)

3,3-dimethyl-1-butyne (4.0 equiv), $PdCl_2(PPh_3)_2$ (3 mol%), CuI (6 mol%), DBU(6.0 equiv), THF, rt, 18 h.

Scheme 3-1 describes introduction of various substituents to *para*-substituted HBCs. Methylation of the hydroxy groups with an excess amount of methyl iodide furnished **4a** in 89% yield.[4] Other substituents were introduced through transition-metal catalyzed processes. The reaction of **3a** with Tf_2O and pyridine provided **5a** in 86% yield,[6] which was employed for palladium-catalyzed reactions.[5]

Introduction of amino groups was conducted through a Buchwald–Hartwig amination.[7] After several trials, 1,1'-diphenylphosphinoferrocene (DPPF) was found to be effective, and the use of Cs_2CO_3 as a base greatly improved the yield of **6a** to 86% yield. *ortho*-Diamino HBC **6b** was also synthesized in 86% yield under the same reaction conditions (Scheme 3-2).

Introduction of cyano substituents to **5a** was conducted according to Takagi's protocol to afford **7a** in 72% yield.[8] Cyano-substituted HBCs **7b** and **7c** were also prepared under the same reaction conditions in 72% and 52% yield, respectively (Schemes 3-2 and 3-3). Notably, the addition of a catalytic amount of zinc powder dramatically enhanced the yield of the cyanation products and no reaction occurred in the absence of zinc.

Sonogashira coupling of **5-a** with 3,3-dimethyl-1-butyne afforded **8a** in 97% yield.[9] Using a similar reaction conditions, alkynyl-substituted HBCs **8b** and **8c** were prepared in 85% and 97% yield, respectively.

Unfortunately, trimethoxy- and triamino-substituted HBCs from **5c** could not be isolated. Probably, these HBCs were easily oxidized due to three electron-donating groups.

All of the obtained products were fully characterized by ^{1}H and ^{13}C NMR spectra and mass spectroscopic analysis.

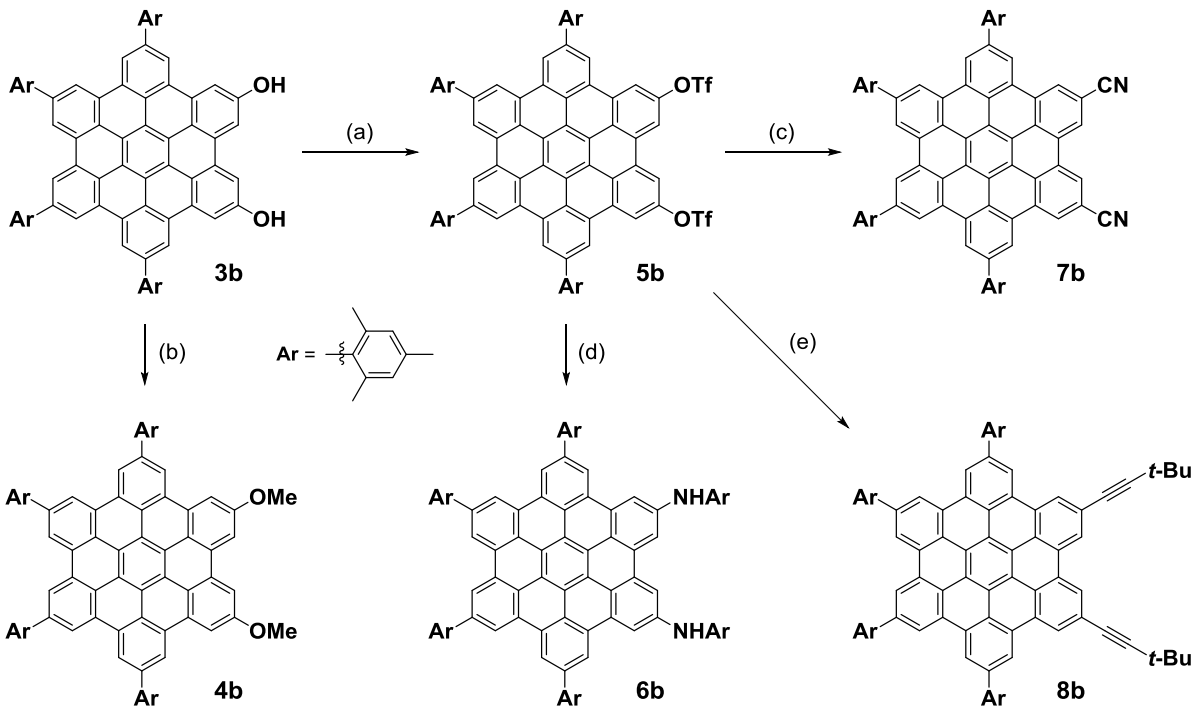

Scheme 3-2. Introduction of various functionalities to *ortho*-substituted HBC.

Reagents and conditions: (a) Tf_2O (4.0 equiv), pyridine (8.0 equiv), CH_2Cl_2, rt, 3 h; (b) MeI (excess), K_2CO_3 (6.0 equiv), THF/acetone=3:1, reflux, 24 h; (c) KCN (8.0 equiv), $Pd_2dba_3{\cdot}CHCl_3$ (3 mol%), DPPF (6 mol%), Zn (6 mol%), toluene/NMP=1/1, 100 °C, 24 h; (d) 2,4,6-trimethylaniline (8.0 equiv), $Pd_2dba_3{\cdot}CHCl_3$ (5 mol%), BINAP (10 mol%), Cs_2CO_3 (6.0 equiv), toluene, reflux, 24 h; (e) 3,3-dimethyl-1-butyne (4.0 equiv), $PdCl_2(PPh_3)_2$ (3 mol%), CuI (6 mol%), DBU (6.0 equiv), THF, rt, 18 h.

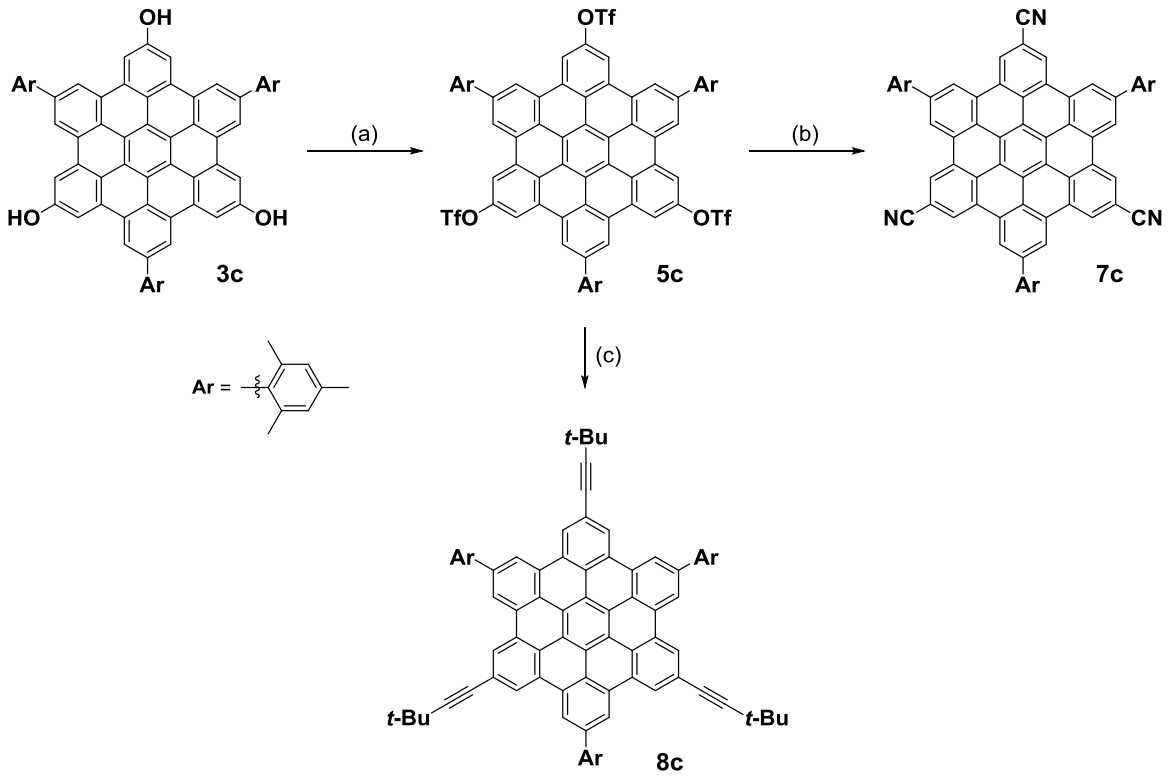

Scheme 3-3. Introduction of various functionalities to *meta*-substituted HBC.

Reagents and conditions: (a) Tf_2O (6.0 equiv), pyridine (8.0 equiv), CH_2Cl_2, rt, 16 h; (b) KCN (12.0 equiv), $Pd_2dba_3{\cdot}CHCl_3$ (5 mol%), DPPF (10 mol%), Zn (6 mol%), toluene/NMP=1/1, 60 °C, 24 h; (c) 3,3-dimethyl-1-butyne (6.0 equiv), $PdCl_2(PPh_3)_2$ (5 mol%), CuI (10 mol%), DBU (6.0 equiv), THF, rt, 24 h.

3. Photophysical properties

Although a number of functionalized HBCs have been reported, there have been rather few studies on their photophysical properties. In particular, emission spectra of HBCs were not known well in the non-aggregated state. The present HBCs are suitable to investigate their unimolecular photophysical properties owing to the mesityl groups that avoid formation of the excimer.

Figure 3-4 shows the UV/Vis absorption spectra of *para*-substituted HBCs in CH_2Cl_2. As shown in Figure 3-4, the α-band is strongly affected by the substituents. In comparison to **1a**, all *para*-substituted HBCs showed bathochromic shifts of the α-bands, indicating decrease of the HOMO-LUMO gaps of *para*-substituted HBCs. In particular, **6a** showed the largest bathochromic shift of the α-band at 491 nm. In addition, intensity of α-bands were increased for **6a**, **7a**, and **8a**.

The amino-substituted HBC **6a** shows the largest α-band (ε = 14000 cm^{-1} M^{-1}), and this implies that the π-donating nature of amino groups significantly influences the transition probability of the α-band.

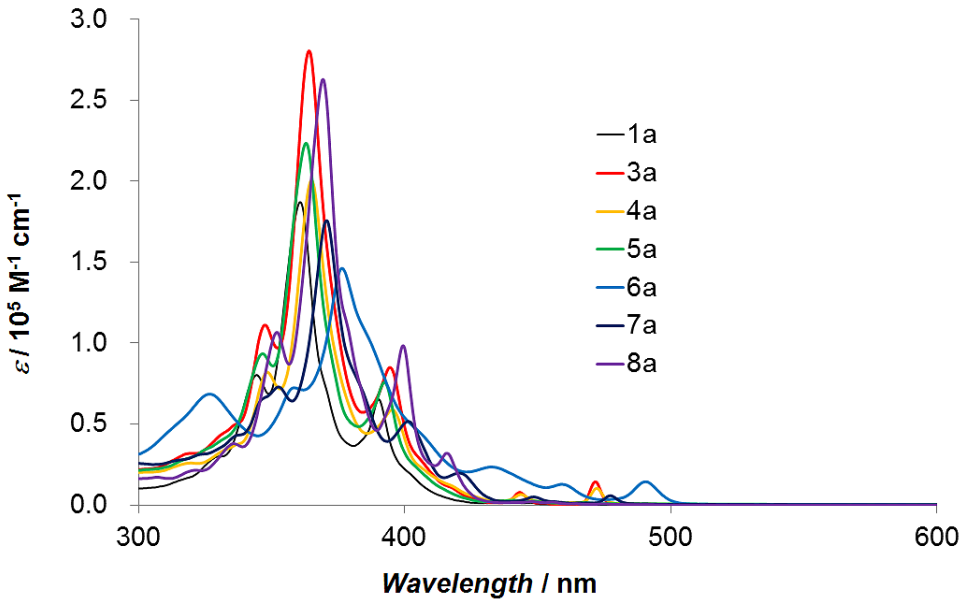

Figure 3-4. UV/vis absorption spectra of *para*-HBCs in CH_2Cl_2.

Figure 3-5 shows UV/vis absorption spectra of *ortho*-substituted HBCs in CH_2Cl_2. A similar trend was observed on the substituent effect on the α-bands. Broadened absorption spectra were obtained as compared to *para*-substituted HBCs. This is probably due to their lower symmetry of *ortho*-substituted HBCs. The degree of the bathochromic shift and enhancement in the α-bands was smaller than that for *para*-substituted HBCs. Only **6b** exhibited α-band at 486 nm with extinction coefficient (ε = 7900 cm^{-1} M^{-1}).

This result indicates that the substituent effects at the *ortho*-position of the HBC core are weaker than those at the *para*-position.

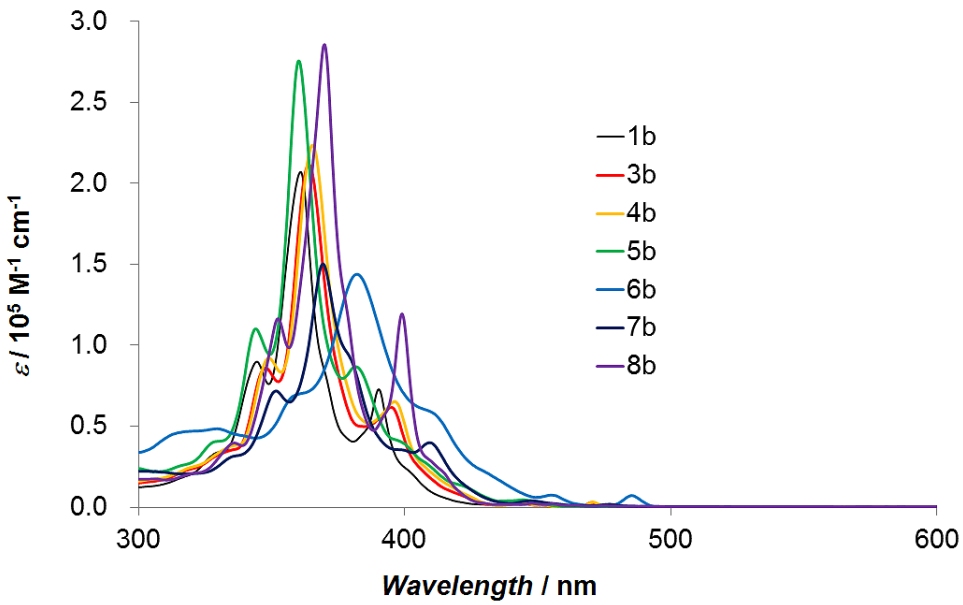

Figure 3-5. UV/vis absorption spectra of *ortho*-HBCs in CH_2Cl_2.

Figure 3-6 shows UV/vis absorption spectra of *meta*-substituted HBCs **1c**, **7c**, and **8c** in CH_2Cl_2. Although *meta*-substituted HBCs have one more additional substituent on HBC compared to *para*- and *ortho*-substituted HBCs, the spectra of *meta*-substituted HBCs were not that different to **1c**. In particular, the α-bands appeared with quite low intensity, thus suggesting that the substituents at the *meta*-positions have a negligible effect on the electronic structure of the HBC core.

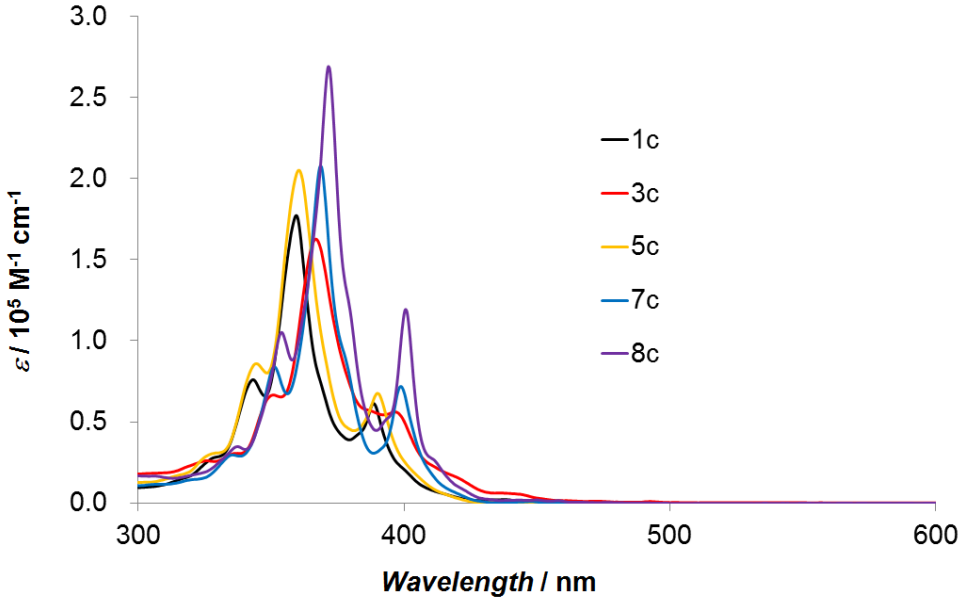

Figure 3-6. UV/vis absorption spectra of *meta*-HBCs in CH_2Cl_2.

Figures 3-7, 3-8, and 3-9 show emission spectra of *para*-, *ortho*-, and *meta*-substituted HBCs in CH_2Cl_2. The shape of the fluorescence spectra of **4a** is similar to that of **1a**. For either electron-donating or electron-withdrawing substituents, the vibronic structures were broadened to show three obvious bands that are attributed to (0–0), (0–1), and (0–2) vibronic transitions for *para*-, *ortho*-, and *meta*-substituted HBCs, respectively. The fluorescence quantum yields were also influenced by the substituents. The fluorescence quantum yield of HBC **1a** was low (Φ = 0.028) and alkynyl substituents did not have much influence on the quantum yield (**8a**; Φ = 0.033). On the other hand, both electron-donating and electron withdrawing substituents improved the quantum yields above 0.10. Amino-substituted HBC **6a** showed the highest quantum yield (Φ = 0.33). These observed quantum yields seem to be related with the intensity of the α-bands. In other words, an increase in transition probability of $S_0 \rightarrow S_1$ leads to the enhancement of fluorescence quantum yield. A similar trend was also observed for *ortho*-substituted HBCs. Fluorescence quantum yields of *ortho*-substituted HBCs showed a smaller enhancement than those of *para*-substituted HBCs: The quantum yield of **6b** is only Φ = 0.20, which is about two-thirds the value of **6a**. For *meta*-substituted HBCs, an improvement in the fluorescence quantum yields with substituents was not observed. A fine vibronic structure was observed for cyano-substituted **7c**, while both **7a** and **7b** showed a rather broad spectrum. These spectroscopic studies elucidated that the substituent effect on the HBC core increases in the order of *meta*-, *ortho*-, and *para*-substituted HBCs.

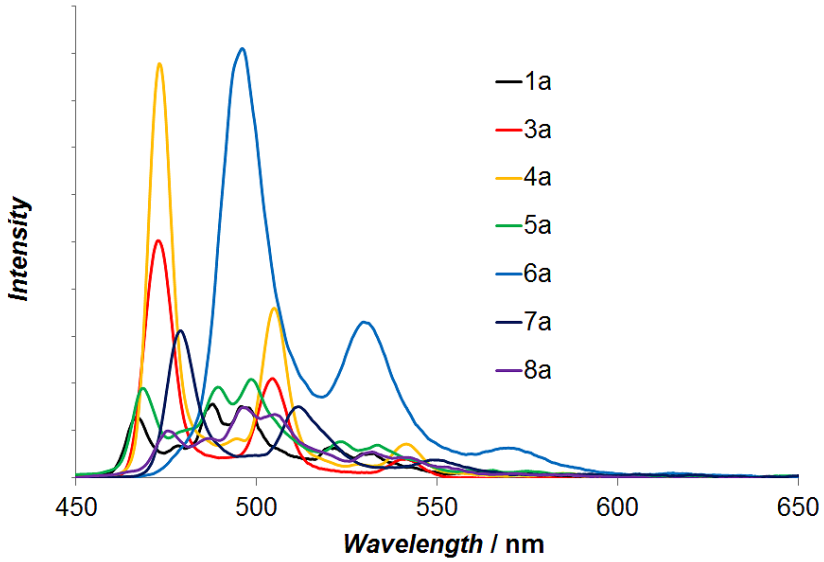

Figure 3-7. Emission spectra of *para*-HBCs in CH_2Cl_2.

All spectra were recorded at 2.0×10^{-6} M in CH_2Cl_2 with excitation at 400 nm.

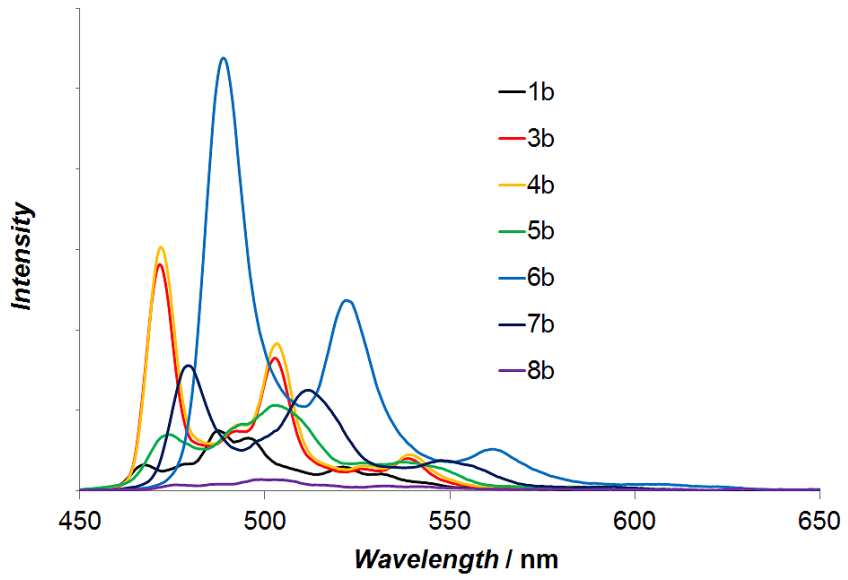

Figure 3-8. Emission spectra of *ortho*-HBCs in CH_2Cl_2.

All spectra were recorded at 2.0×10^{-6} M in CH_2Cl_2 with excitation at 400 nm.

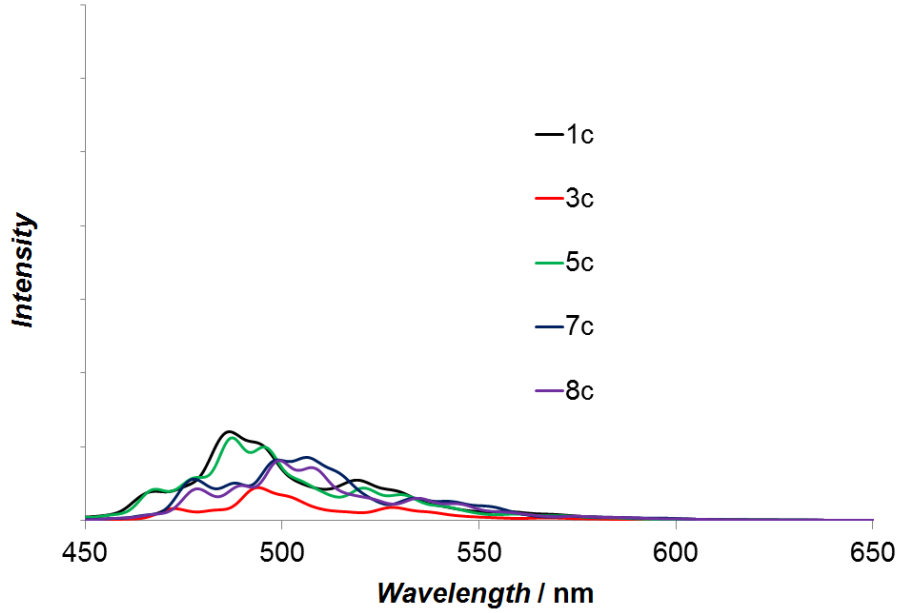

Figure 3-9. Emission spectra of *meta*-HBCs in CH_2Cl_2.

All spectra were recorded at 2.0×10^{-6} M in CH_2Cl_2 with excitation at 400 nm.

4. Theoretical investigations

To reveal the substituent effect on the optical properties of HBCs, the author performed theoretical calculations on substituted-HBCs. Peripheral mesityl and *N*-mesityl groups were replaced with hy-

drogen atoms and methyl groups, respectively, to reduce the calculation cost (Figure 3-10). The molecular geometries were fully optimized by the density-functional theory (DFT) based on B3LYP hybrid functional with the 6–31G(d) basis set.[11] Calculated oscillator strengths were obtained by the time-dependent DFT (TD-DFT) method.

The calculated frontier orbitals and energy diagrams are showed in Figure 3-11. HOMO and HOMO–1 as well as LUMO and LUMO+1 of unsubstituted HBC **I** are two sets of degenerate frontier orbitals. Müllen and co-workers reported both the α-band and β-band result from the transitions between these two degenerated HOMOs and LUMOs.[12] Because of the configuration interaction of these degenerate transitions, α-band shows the forbidden feature (Table 3-1, entry 1).

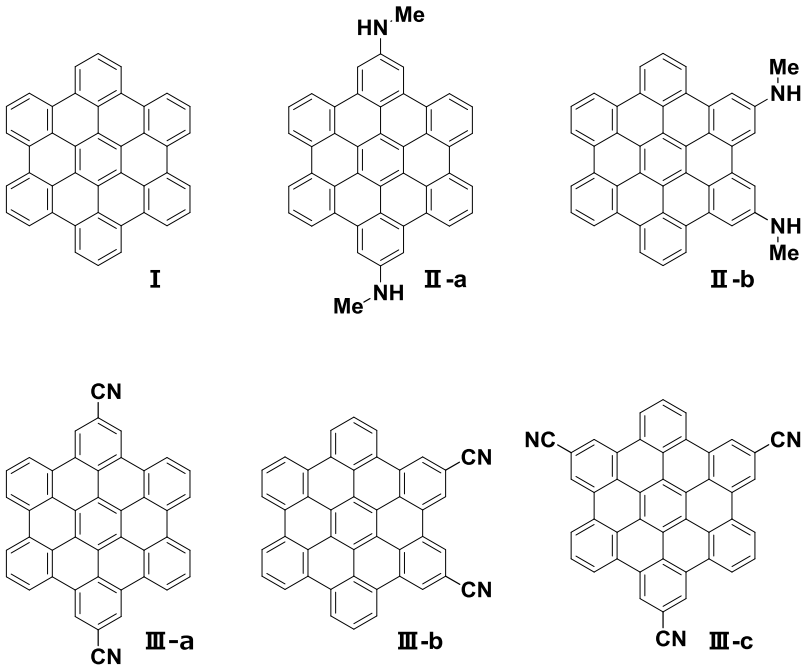

Figure 3-10. The structures of *para*-, *ortho*-, and *meta*-HBCs in DFT calculations.

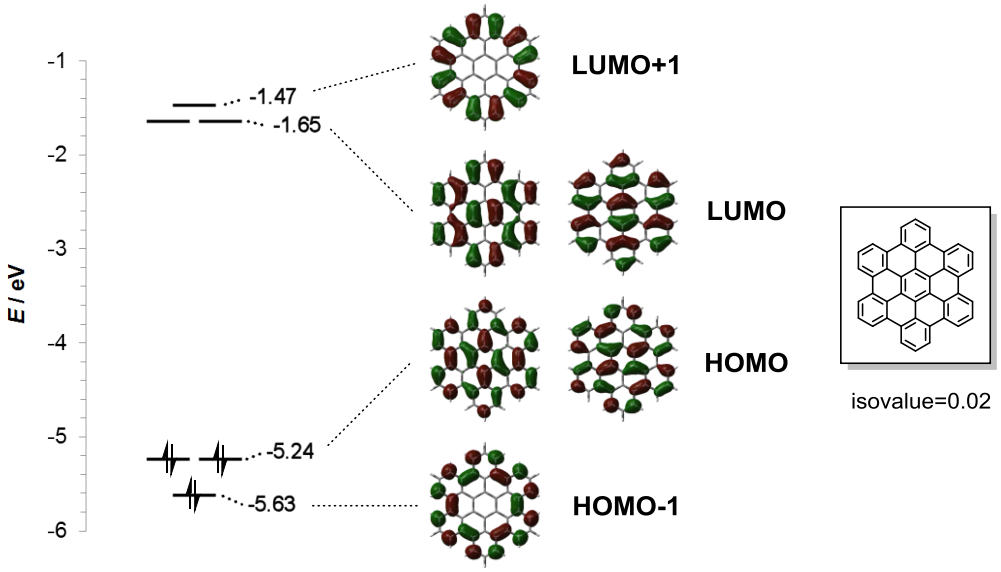

Figure 3-11. Energy diagram of unsubstituted HBC.

Figure 3-12 shows the energy diagrams of *para*- and *ortho*-diamino HBCs **II-a** and **II-b** as well as the parent HBC **I**. The introduction of amino groups destabilizes one of two HOMOs, resulting in splitting of the degenerated orbitals for both **II-a** and **II-b**. The removal of degeneracy can be explained by the interaction of two HOMOs of the parent HBC with the amino groups. One HOMO interacts significantly with the electron-donating amino groups to destabilize the energy level, while the other stays at almost the same energy level owing to the lack of an interaction at the nodal plane position of the molecular orbital. As a result, the two orbitals have different energies. This situation can be confirmed from the molecular orbitals of diamino-HBCs. Figure 3-13 illustrates the HOMO and HOMO–1 of *para*-diamino HBC **II-a**, in which the HOMO has a substantial contribution from the amino groups, while the HOMO–1 has no molecular orbital coefficient on the nitrogen atoms. Oscillator strengths of the α-bands are enhanced because split of HOMO and HOMO–1 weakened the configuration interaction (Table 3-1, entries 2 and 3). Because of the rigid structure of the HBC unit, the higher oscillator strength would lead to the higher radiative rate constant. The observed fluorescence quantum yield of the amino-substituted HBCs was substantially higher than the unsubstituted HBC. In consequence, the enhancement in emission efficiency in amino-substituted HBCs **6a** and **6b** should be related the splitting of HOMO and HOMO-1.

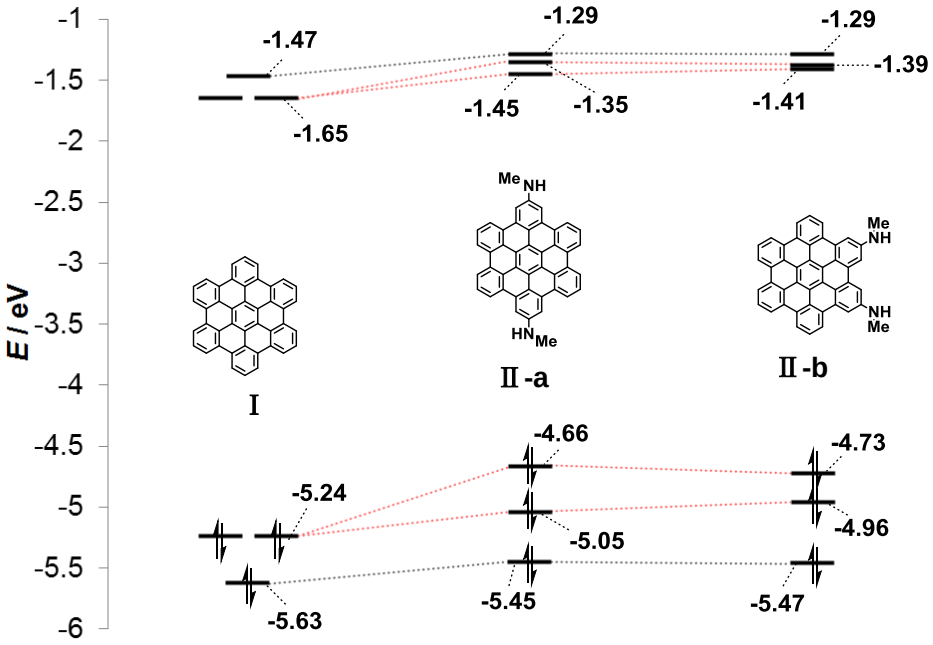

Figure 3-12. Energy diagrams of *para*- and *ortho*-diamino HBCs.

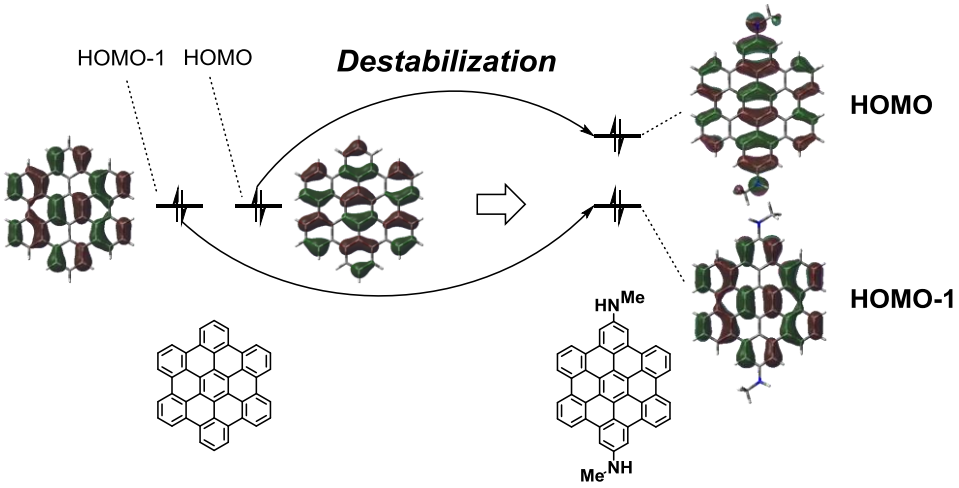

Figure 3-13. Splitting of HOMOs of unsubstituted HBC by amino groups.

Figure 3-14 shows the energy diagrams of cyano HBCs **III-a**, **III-b**, and **III-c**. As compared to **I**, dicyano HBC **III-a** and **III-b** have LUMO and LUMO+1 of different energies, while HOMO and HOMO–1 are almost degenerate. For tricyano HBC **III-c**, both HOMOs and LUMOs are almost degenerate as well as the parent HBC. In the case of *para*-dicyano-substituted HBC **III-a**, the substituent interacts with the LUMO but not with LUMO+1 (Figure 3-15). One of the two degen-

erate LUMOs is stabilized by effective hybridization with the electron-withdrawing cyano groups, thereby resulting in the splitting of LUMO and LUMO+1. Compared to the amino-substituted HBCs, the oscillator strengths of the α-band for the cyano-substituted HBCs are relatively small (Table 3-1, entry 4–6). Furthermore, the oscillator strengths decrease in the order of *para*, *ortho*, and *meta*. This order is the same as that of the energy gaps between LUMO and LUMO+1. This result indicates that the oscillator strength of the α-band responsible for the degree of the splitting in the LUMOs of cyano HBCs. In *meta*-cyano substituted HBC **III-c**, which has almost degenerate LUMOs, transition of the lowest energy band is completely forbidden.

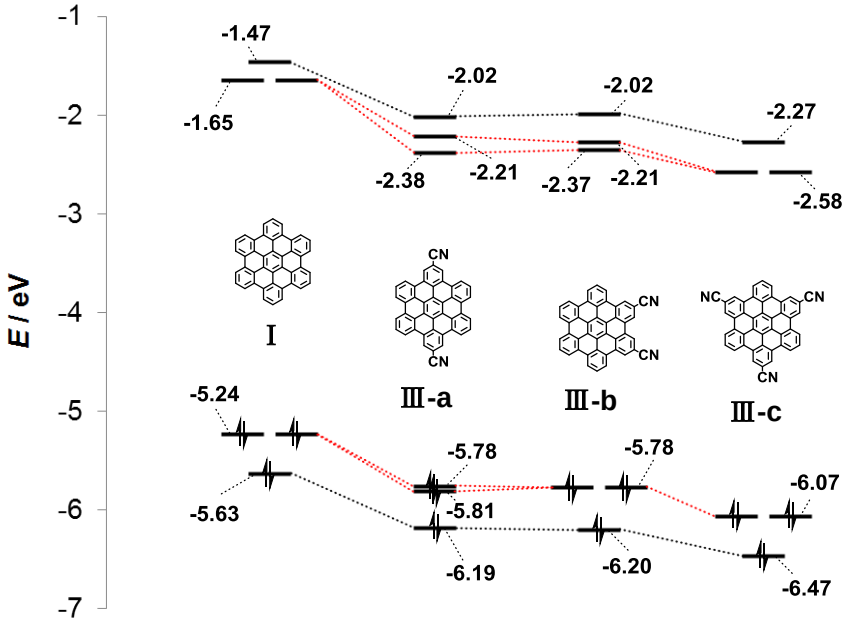

Figure 3-14. Energy diagrams of *para*-dicyano, *ortho*-dicyano, and *meta*-tricyano HBCs.

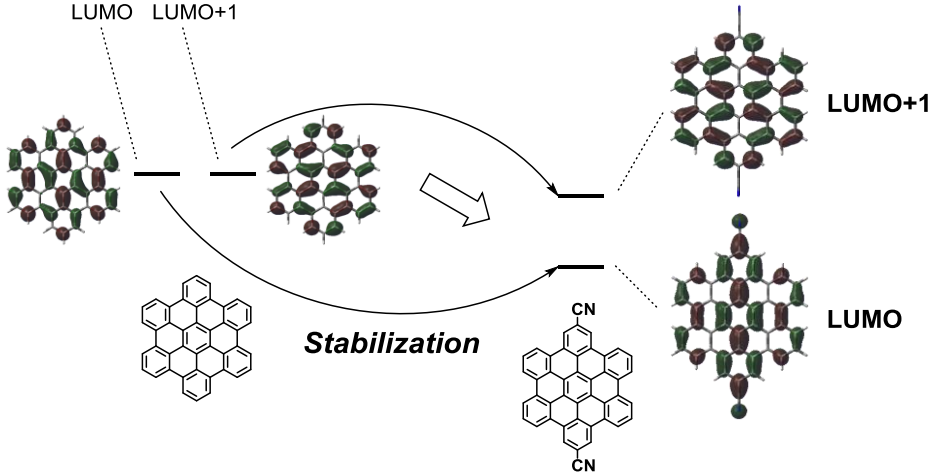

Figure 3-15. Splitting of LUMOs of unsubstituted HBC by cyano groups.

Table 3-1. Calculated wavelengths and oscillator strengths of α-bands of HBC derivatives by the TD-DFT method.

Entry	Compounds	Excitation Wavelength / nm	Excited state	CI coefficient	Oscillator strength,
1	**I**	428	HOMO–1→LUMO	0.50537	0
			HOMO→LUMO+1	0.50532	
		409	HOMO–1→LUMO+1	–0.49275	0
			HOMO→LUMO	0.49464	
2	**II-a**	454	HOMO–1→LUMO+1	0.32398	0.0580
			HOMO→LUMO	0.61536	
		435	HOMO–1→LUMO	–0.32185	0.0923
			HOMO→LUMO+1	0.61147	
3	**II-b**	447	HOMO–1→LUMO+1	–0.39932	0.0267
		432	HOMO→LUMO	0.58068	
			HOMO–1→LUMO	0.37928	0.0467
			HOMO→LUMO+1	0.58068	
4	**III-a**	440	HOMO→LUMO	0.54725	0.0055
			HOMO→LUMO+1	–0.44042	
		424	HOMO–1→LUMO+1	0.37462	0.0584
			HOMO→LUMO	0.59718	
5	**III-b**	442	HOMO–1→LUMO+1	–0.4718	0.0022
			HOMO→LUMO	0.52311	
		426	HOMO–1→LUMO	0.50797	0.0066
			HOMO→LUMO+1	0.48404	
6	**III-c**	441	HOMO–1→LUMO	0.49753	0
			HOMO→LUMO+1	0.49627	
		422	HOMO–1→LUMO	–0.49602	0
			HOMO→LUMO+1	0.50115	

Finally, the oscillator strengths of the α-band by TD-DFT calculations and observed fluorescence quantum yields of substituted HBCs are plotted in Figure 3-16. Interestingly, an almost linear and positive correlation was obtained. This result indicates that the oscillator strength of the α-band is essential to the fluorescence quantum yield of substituted HBCs. The substituents at the *para*- and *ortho*-positions effectively lift the degeneracy of the HOMOs or LUMOs to enhance the oscillator strengths of the lowest energy band, thus increasing fluorescence quantum yields.

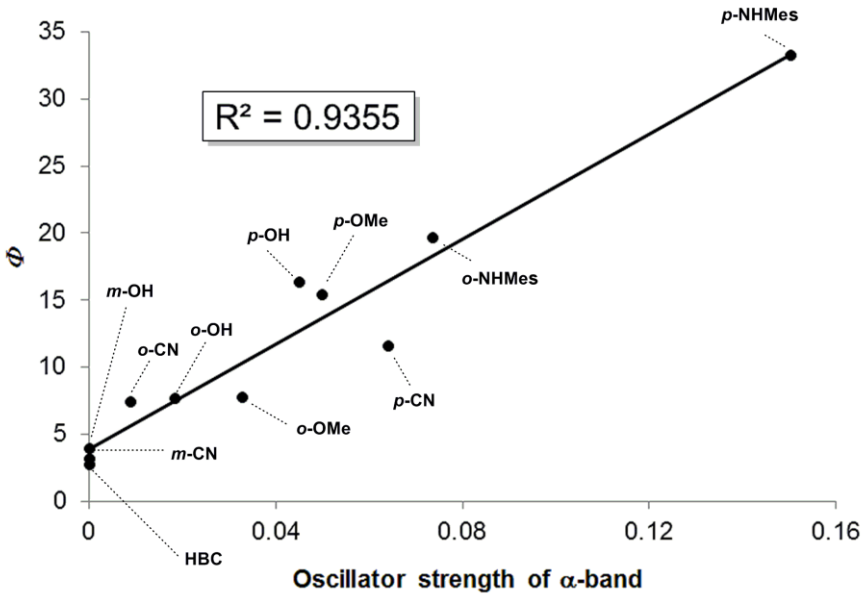

Figure 3-16. Correlation of the calculated oscillator strengths and observed fluorescence quantum yields of the α-band of various HBCs.

5. Non-linear optical property

Recently, Wu and coworkers prepared octupolar HBCs that bear donors and acceptors, thus exhibiting large TPA cross section values.[13] Encouraged by this study, the TPA cross-section values of three-types of substituted HBCs were determined to clarify the regiochemical dependence of the non-linear optical (NLO) properties. Figure 3-17 summarizes the results. The TPA cross-section values were measured at 800 nm in toluene. Among three alkynyl-substituted HBCs, **8a** had the largest TPA cross-section value (700 GM), while **8b** and **8c** showed lower values (400 and 480 GM, respectively). Compared to *ortho*- and *meta*-substituted HBCs, the larger value for *para*-substituted HBC **8a** is probably due to effective conjugation over the HBC plane. This result is consistent with

those obtained by single-photon optical analysis. Another series of HBCs were also observed the same trend. *para*-Substituted HBC **6a** had a larger TPA cross-section value of 910 GM than that of *ortho*-substituted HBC **6b** (440 GM). Due to instability under aerobic conditions, TPA cross-section value of *meta*-amino substituted HBC could not be measured. The author concludes that the NLO properties of HBCs were dependent on the introduced functional groups and their locations.

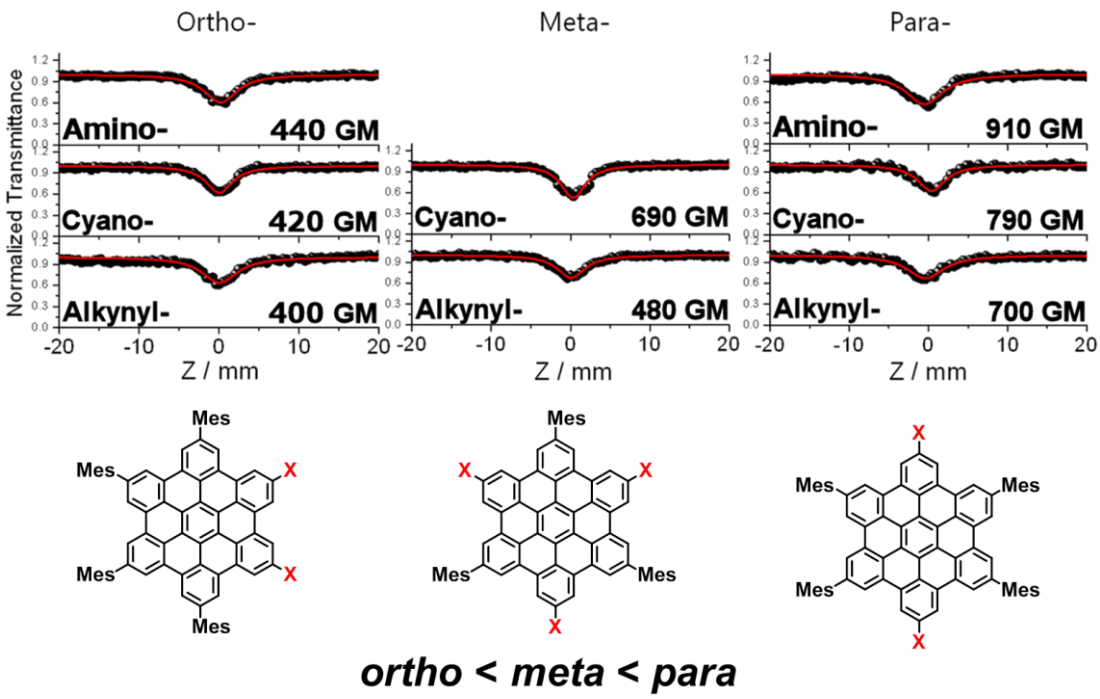

Figure 3-17. Two-photon absorption cross-sections of **6**, **7**, and **8** in toluene.

6. Summary

In this chapter, the introduction of various functional groups after construction of the HBC skeleton was demonstrated. Three types of HBCs, *para*-, *meta*-, and *ortho*-substituted HBCs, could be readily prepared in high yields through functional group transformation of hydroxy-substituted HBC **3**. Electronic structures of HBCs were substantially influenced by the electron-donating and electron-accepting groups, thus showing bathochromic shifts in their absorption and emission spectra. In particular, introduction of amino and cyano groups intensified the α-bands of the absorption spectra and enhanced fluorescence quantum yields of HBCs. Importantly, location of the substituents is

important in the electronic property of HBCs: *para*-disubstituted HBCs experience the largest substituent effects than other HBCs. According to the theoretical analysis, the splitting of degenerate HOMOs with electron-donating substituents or LUMOs with electron-accepting groups enhances transition probability of α-band. Interestingly, the fluorescence quantum yields indicate a linear correlation with oscillator strengths of the α-bands. These results demonstrate that the emission properties of HBCs can be operated by electron-donating and electron-accepting groups at the appropriate positions. The present strategy for functionalization of HBCs should be useful for development in the field of PAHs.

7. References

[1] (a) J. Wu, W. Pisula, K. Müllen, *Chem. Rev.* **2007**, *107*, 718. (b) X. Feng, W. Pisula, K. Müllen, *Pure. Appl. Chem.* **2009**, *81*, 2203.

[2] (a) W. Pisula, X. Feng, K. Müllen, *Adv. Mater.* **2010**, *22*, 3634. (b) W. Pisula, Ž. Tomović, C. Simpson, M. Kastler, T. Pakula, K. Müllen, *Chem. Mater.* **2005**, *17*, 4296. (c) J. P. Hill, W. Jin, A. Kosaka, T. Fukushima, H. Ichihara, T. Shimomura, K. Ito, T. Hashizume, N. Ishii, T. Aida, *Science* **2004**, *304*, 1481.

[3] (a) M. Kastler, W. Pisula, D. Wasserfallen, T. Pakula, K. Müllen, *J. Am. Chem. Soc.* **2005**, *127*, 4286. (b) W. W. H. Wong, D. Vak, Th. B. Singh, S. Ren, C. Yan, D. J. Jones, I. I. Liaw, R. N. Lamb, A. B. Holmes, *Org. Lett.* **2010**, *12*, 5000. (c) W. W. H. Wong, T. B. Singh, D. Vak, W. Pisula, C. Yan, X. Feng, E. L. Williams, K. L. Chan, Q. Mao, D. J. Jones, C.-Q. Ma, K. Müllen, P. Buerle, A. B. Holmes, *Adv. Funct. Mater.* **2010**, *20*, 927.

[4] X. Feng, J. Wu, V. Enkelmann, K. Müllen, *Org. Lett.* **2006**, *8*, 1145.

[5] (a) G. Battagliarin, Y. Zhao, C. Li, K. Müllen, *Org. Lett.* **2011**, *13*, 3399. (b) G. Battagliarin, C. Li, V. Enkelmann, K. Müllen, *Org. Lett.* **2011**, *13*, 3012. (c) J. M. Murphy, X. Liao, J. F. Hartwig, *J. Am. Chem. Soc.* **2007**, *129*, 15434.

[6] T. Peng, D. Yang, *Org. Lett.* **2010**, *12*, 496.

[7] D. S. Surry, S. L. Buchwald, *Chem. Sci.* **2011**, *2*, 27.

[8] (a) K. Takagi, Y. Sakakibara, *Chem. Lett.* **1989**, 1957. (b) R. Chidambaram, *Tetrahedron Lett.* **2004**, *45*, 1441.

[9] M. J. Mio, L. C. Kopel, J. B. Braun, T. L. Gadzikwa, K. L. Hull, R. G. Brisbois, C. J. Markworth , P. A. Grieco, *Org. Lett.* **2002**, *4*, 3199.

[10] M. Kastler, J. Schmidt, W. Pisula, D. Sebastiani, K. Müllen, *J. Am. Chem. Soc.* **2006**, *128*, 9526.

[11] (a) A. D. Becke, *Phys. Rev. A* **1988**, *38*, 3098. (b) C. Lee, W. Yang, R. G. Parr, *Phys. Rev. B* **1988**, *37*, 785.

[12] A. G. Crawford, A. D. Dwyer, Z. Liu, A. Steffen, A. Beeby, L.-O. Plsson, D. J. Tozer, T. B. Marder, *J. Am. Chem. Soc.* **2011**, *133*, 13349.

[13] Z. Zeng, Z. Guan, Q.-H. Xu, J. Wu, *Chem. Eur. J.* **2011**, *17*, 3837.

Chapter 4.

Synthesis of Curved Hexa-*peri*-hexabenzocoronenes

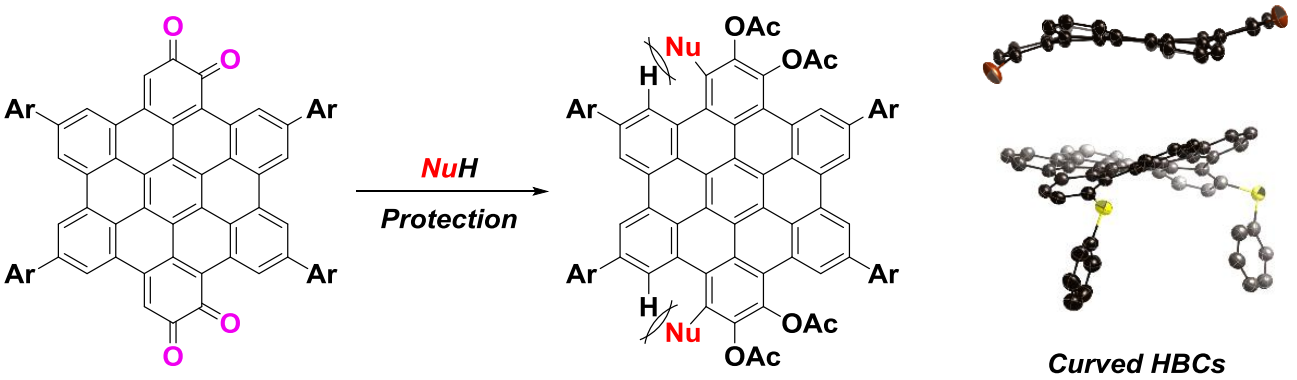

Halogenation and phenylthiolation of HBC-tetraone have been achieved. Introduction of the substituents resulted in curvature of the HBC plane by steric repulsion between hydrogen atoms and the substituents. This method would be useful for construction of curved HBCs, which would allow formation of novel aggregation structures.

Contents

1. Introduction

In chapters 2 and 3, the author has described late-functionalization methods of HBC through iridium-catalyzed C–H borylation.[1] This procedure expanded the flexibility of functionalization, allowing facile introduction of a variety of substituents.[2]

Ortho-quinones are known to react with nucleophilic reagents regioselectively to afford mono-substituted dihydroxybenzenes (Scheme 4-1). For example, Dürckheimer *et al.* reported nucleophilic addition to *ortho*-quinone with hydrochloric acid and hydrogen bromide.[3] It was expected that nucleophilic addition reaction can be applied to HBC-tetraone **9**, of which synthesis was described in Chapter 2.

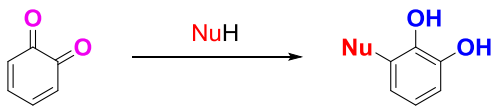

Scheme 4-1. Nucleophilic addition to *ortho*-quinone.

In this chapter, the author describes nucleophilic addition of nucleophiles with **9** and preparation of highly functionalized HBCs (Scheme 4-2). Introduction of substituents to the fjord region of HBCs induces distortion of π-plane, because of repulsion between hydrogen atom and substituents.[4] In other words, a nucleophilic addition to **9** would result in the distorted HBC plane.

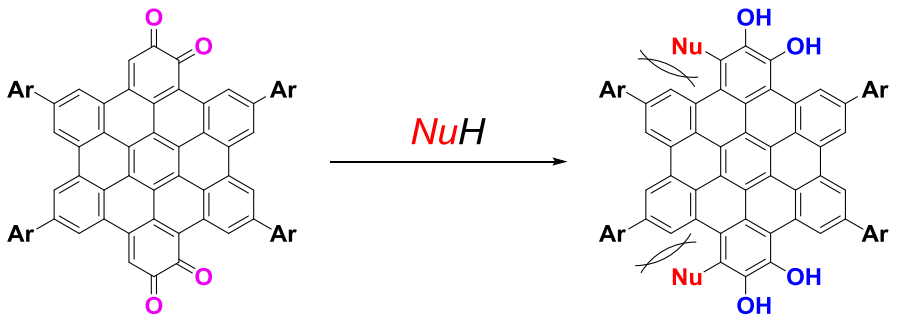

Scheme 4-2. Regioselective nucleophilic addition with HBC-tetraone **9**.

2. Nucleophilic addition with HBC-tetraone 9

To explore the reactivity of **9**, nucleophilic addition of hydrogen halides was investigated. The reaction of **9** with HCl aq. resulted in regioselective chlorination to provide dichloro tetrahydroxy HBC **12a** in 44% yields in CH_2Cl_2 at room temperature (Scheme 4-3).[3] ^{1}H NMR analysis of **12a** revealed disappearance of a singlet peak at 7.27 ppm, which was observed for **9**. The reaction of **9** with aqueous HBr under similar conditions provided **12b** in 70% yield. The use of hydrogen iodide did not afford the corresponding adducts. In addition, treatment of **9** with 4.0 equiv of thiophenol provided dithiolated tetrahydroxy HBC **12c** in 44% yield.[5] Unfortunately, **12a**, **12b**, and **12c** were unstable under aerobic conditions. Therefore, **12a**, **12b**, and **12c** were protected by acetylation. Treatment of **12a**, **12b**, and **12c** with 20.0 equiv of acetic anhydride in pyridine provided **13a**, **13b**, and **13c** in 79%, 78%, and 76% yields, respectively. These compounds were sufficiently stable under aerobic condition.

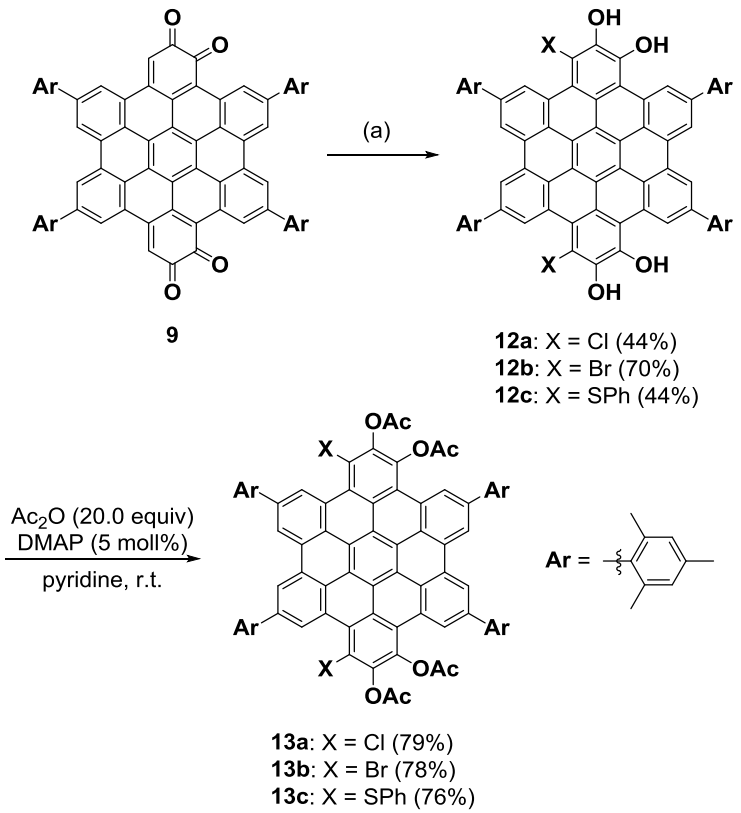

Scheme 4-3. Introduction of substituents to **9** through nucleophilic addition. (a) HCl (35~37% aq.), CH_2Cl_2, r.t., 6 h, for **12a**, HBr (47~49% aq.), CH_2Cl_2, r.t., 12 h, for **12b**, thiophenol (4.0 equiv), THF, r.t., 3 h, for **12c**.

3. X-ray structures of 13b and 13c

The structures of **13b** and **13c** were unambiguously confirmed by X-ray diffraction analysis (Figure 4-2, and 4-3). The positional relationship of the two bromo groups in **13b** was *anti*, while that of two phenylthio groups in **13c** was *syn*. As a result, **13b** formed twisted structure and **13c** formed curved structure. The π-plane of the HBC core was distorted and the mean plane deviations were calculated to be 0.27 Å (**13b**) and 0.48 Å (**13c**), respectively. On the other hand, the mean plane deviations of unsubstituted HBC-tetraacetate **11** was 0.18 Å.[1]

To investigate the origin of the distortion, we performed theoretical calculations by the DFT method. The molecular geometries were fully optimized at the B3LYP/6–31G(d) level.[6] The optimized structures of **11** (X = H), **13b** (X = Br) and **13c** (X = SPh) are matched well with the X-ray structures. The mean plane deviation of calculated structures were calculated to be 0.09 Å (**11**), 0.26 Å (**13b**), and 0.43 Å (**13c**). This result indicates that the curvature of the HBC core was not significantly influenced by crystal packing. Furthermore, a linear correlation between the distortion and the Charton steric parameter was observed.[7] These indicate that the curvatures of **13b** and **13c** are mainly induced by the steric repulsion between the substituent and the proximal protons (Figure 4-4).

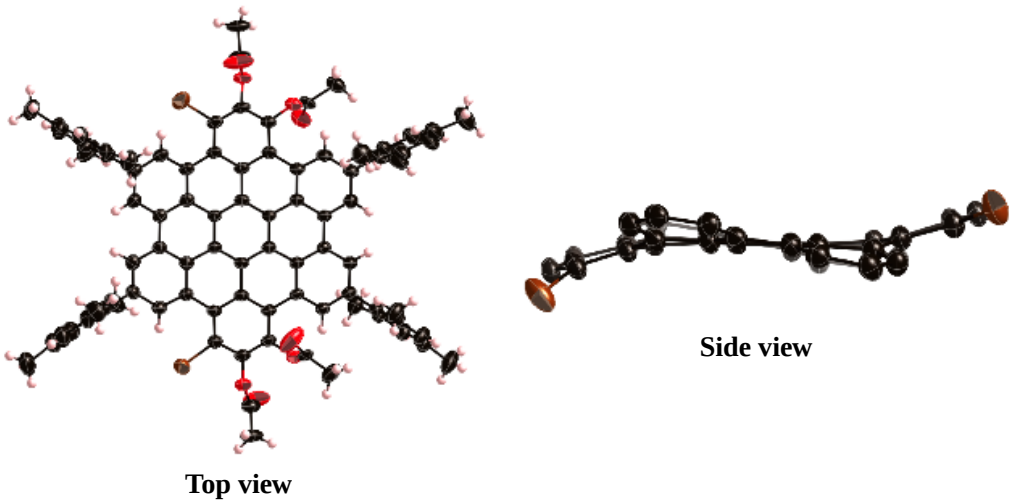

Figure 4-2. X-ray crystal structures of **13b**. The thermal ellipsoids are scaled to 50% probability level. Mesityl groups are omitted for clarity.

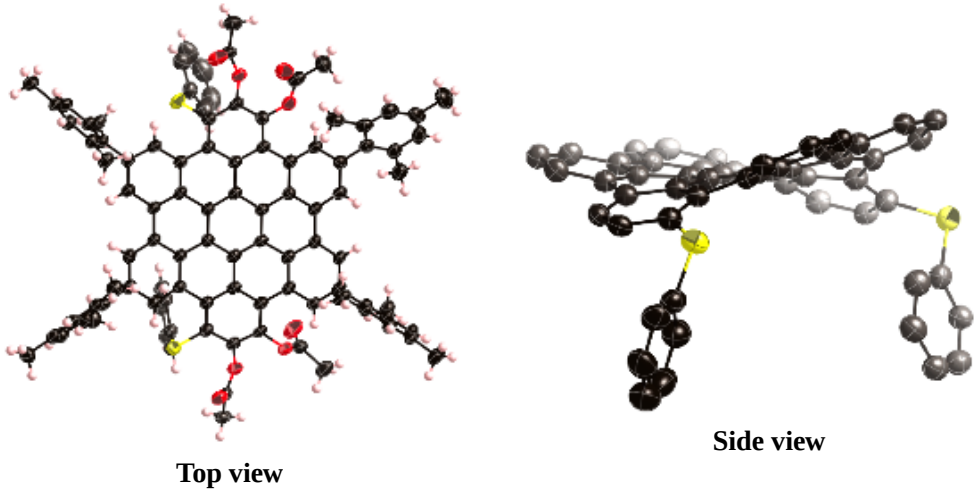

Figure 4-3. X-ray crystal structures of **13c**. The thermal ellipsoids are scaled to 50% probability level. Mesityl groups are omitted for clarity.

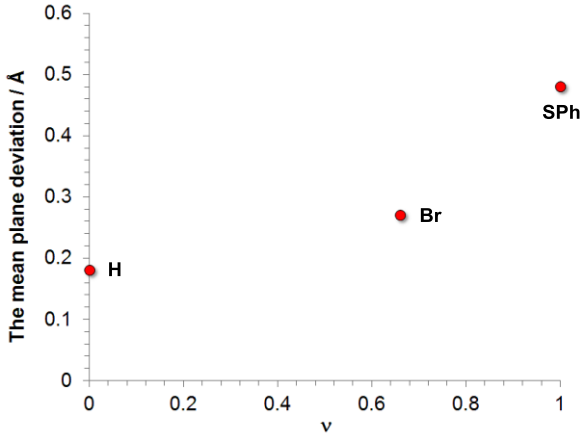

Figure 4-4. Correlation between the mean plane deviation and Charton parameter ν.

4. UV/vis absorption spectra and electrochemical analysis

Figures 4-5 show UV/vis absorption spectra of **11**, **13a**, **13b**, and **13c** in CH_2Cl_2. HBCs **13a**, **13b**, and **13c** exhibited typical absorption spectra for HBCs.[8] Furthermore, because of the degeneracy of the frontier orbital, α-bands were almost forbidden. Compared to **11**, α- and p-bands exhibited red-shift in the order of **13a** < **13b** < **13c**. In particular, phenylthio groups induce slight batho-chromic shift of absorption spectra due to their electron-donating nature.

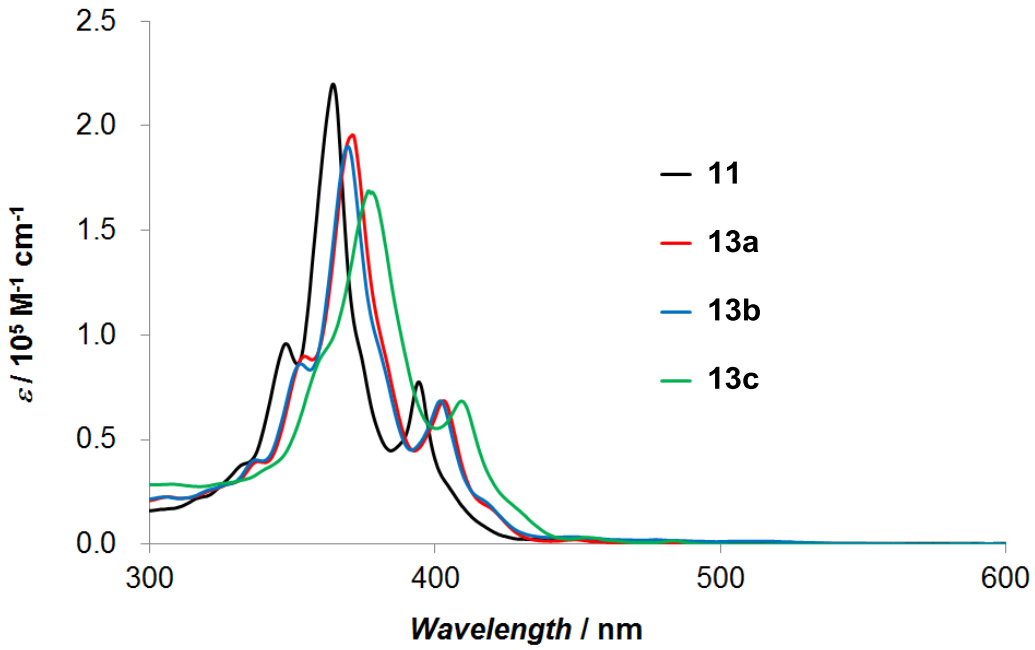

Figure 4-5. UV/vis absorption spectra of **11**, **13a**, **13b**, and **13c** in CH_2Cl_2.

To investigate the electronic structures of **13a**, **13b**, and **13c**, we performed electrochemical analysis by cyclic voltammetry (CV) and differential pulse voltammetry (DPV) (Figure 4-6, 4-7, and 4-8). The results are summarized in Table 1. While the oxidation potentials of **13a** and **13b** are higher than **11**, **13c** has a lower oxidation potential. This can be explained by the electron-withdrawing character of halogen atoms and the electron donating character of the phenylthio group. Compared to the first oxidation potential, the large change in the first reduction potential can be explained molecular orbital of **11**. In the case of compound **11**, orbital coefficient of LUMO of α-carbon is larger than that of HOMO. Therefore, the author considered that the influence of LUMO is larger than HOMO by substituent effect.

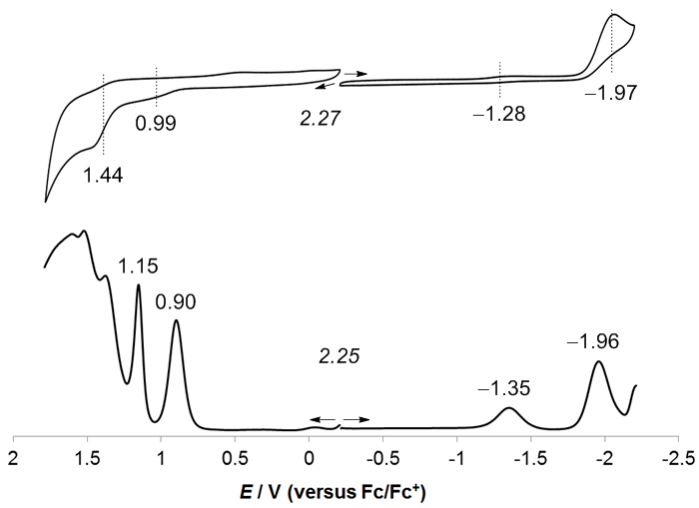

Figure 4-6. Cyclic voltammgram and differential pulse voltammgram of **13a**.

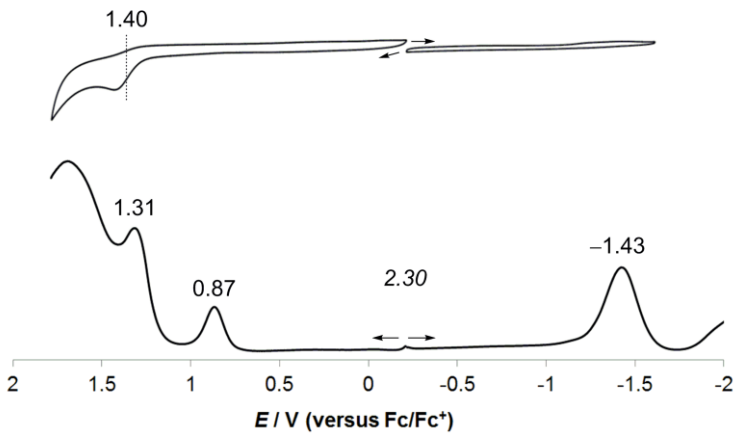

Figure 4-7. Cyclic voltammgram and differential pulse voltammgram of **13b**.

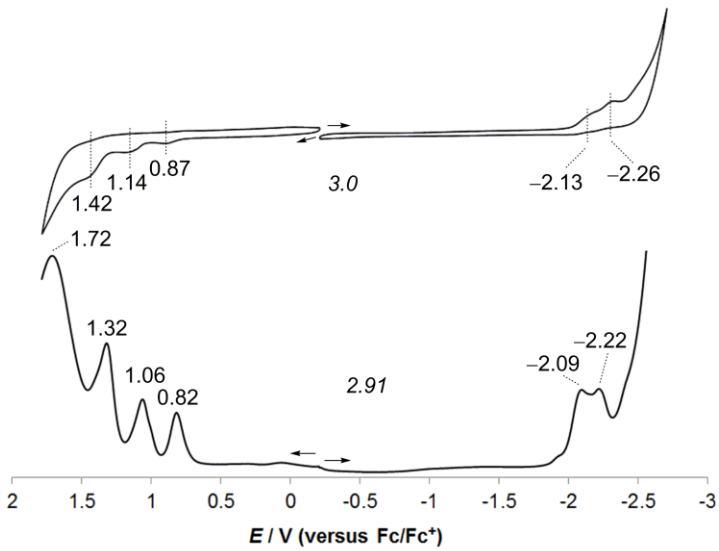

Figure 4-8. Cyclic voltammgram and differential pulse voltammgram of **13c**.

Table 1. Summarized electrochemical data of **11**, **13a**, **13b** and **13c**.

Compound	E_{red}^{1} / V	E_{ox}^{1} / V	ΔE / V
11 (X = H)	–1.26	0.84	2.10
13a (X = Cl)	–1.35	0.90	2.25
13b (X = Br)	–1.43	0.87	2.30
13c (X = SPh)	–2.09	0.82	2.91

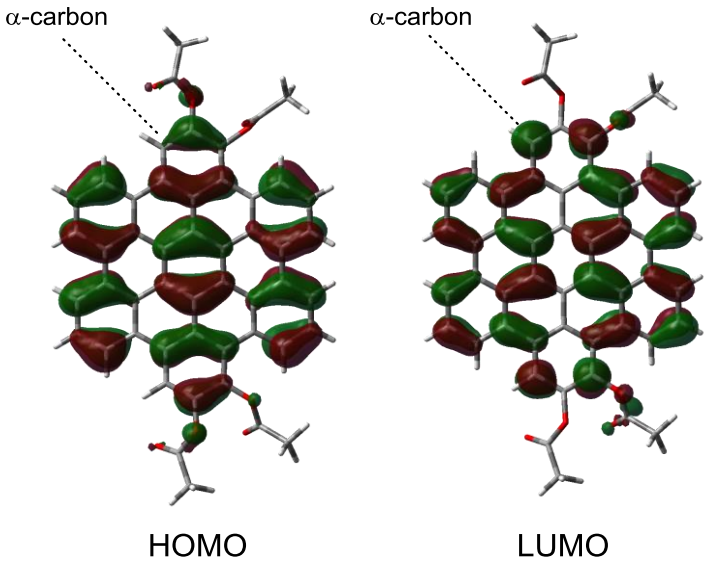

Figure 4-9. HOMO and LUMO orbitals of **11**.

5. Summary

Halogenation and phenylthiolation of HBC-tetraone **9** proceeded regioselectively to afford functionalized HBCs in good yields. Furthermore, curvature of the HBC plane is induced by steric repulsion between hydrogen atoms and the introduced substituents. These synthetic procedures would be useful for preparation of highly functionalized HBCs, of which curved π-systems may allow construction of novel supramolecular architectures.

6. References

[1] R. Yamaguchi, S. Hiroto, H. Shinokubo, *Org. Lett.* **2012**, *14*, 2472.

[2] R. Yamaguchi, S. Ito, B. S. Lee, S. Hiroto, D. Kim, H. Shinokubo, *Chem. Asian. J.* **2013**, *8*, 178.

[3] L. Horner, S. Göwecke, W. Dürckheimer, *Chemische Berichte* **1961**, *94*, 1276.

[4] a) Z. Wang, F. Dötz, V. Enkelmann, K. Müllen, *Angew. Chem. Int. Ed.* **2005**, *44*, 1247. b) J. Luo, X. Xu, R. Mao, Q. Miao, *J. Am. Chem. Soc.* **2012**, *134*, 13796.

[5] (a) K. S. Feldman, S. Quideau, H. M. Appel, *J. Org. Chem.* **1996**, *61*, 6656. (b) C. Kaiser, F. E. Ali, W. E. Bondinell, M. Brenner, K. G. Holden, T. W. Ku, Hye-Ja Oh, S. T. Ross, N. C. F. Yim, C. L. Zirkle *et. al.*, *J. Med. Chem.* **1980**, *23*, 975. (c) L. A. Miller, M. A. Marsini, T. R. R. Pettus, *Org. Lett.* **2009**, *11*, 1955.

[6] (a) A. D. Becke, *Phys. Rev. A* **1988**, *38*, 3098. (b) C. Lee, W. Yang, R. G. Parr, *Phys. Rev. B* **1988**, *37*, 785.

[7] (a) M. Charton, *J. Am. Chem. Soc.* **1975**, *97*, 1552. (b) M. Charton, *J. Org. Chem.* **1976**, *41*, 2217. (c) K. C. Harper, E. N. Bess, M. S. Sigman, *Nat. Chem.* **2012**, *4*, 366.

[8] M. Kastler, J. Schmidt, W. Pisula, D. Sebastiani, K. Müllen, *J. Am. Chem. Soc.* **2006**, *128*, 9526.

Summary

In this thesis, the author has described late-stage functionalization of HBCs through iridium-catalyzed direct borylation. This approach allows overcoming the limitation of the conventional HBC synthesis through the oxidative cyclization. A convenient method for introducing heteroatom substituents such as hydroxy and amino groups has been established.

With various substituted HBCs, a systematic study on the substituent effect of π-extended benzene could be conducted. Furthermore, π-extend HBC-tetraone can be prepared by oxidation of hydroxy HBCs. The late-stage functionalization approach enables introduction of carbonyl groups to the HBC periphery, which was not possible with the conventional method.

Further functionalization of the HBC core through nucleophilic addition to HBC-tetraone allowed facile preparation of distorted HBCs.

Graphical summary

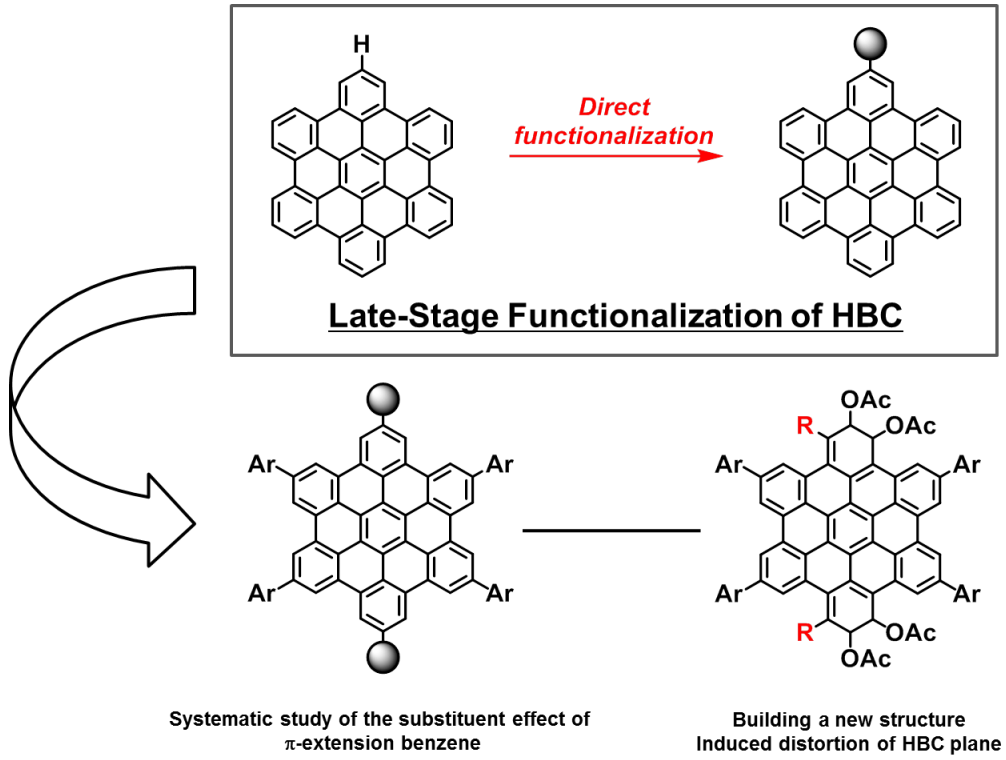

Experimental Section

Instrumentation and materials

^{1}H NMR (500 MHz) and ^{13}C NMR (126 MHz) spectra were recorded on a Varian INOVA-500 spectrometer, and chemical shifts were reported as the delta scale in ppm relative to $CHCl_3$ (δ = 7.260 ppm) and CH_2Cl_2 (δ = 5.320 ppm) for ^{1}H NMR, and $CDCl_3$ (δ = 77.0 ppm) and CD_2Cl_2 (δ = 53.8) for ^{13}C NMR.

UV/vis absorption spectra were recorded on a Shimadzu UV-2550 and JASCO V670 spectrometer. Emission spectra were recorded on a JASCO FP-6500 spectrometer and absolute fluorescence quantum yields were measured by photon-counting method using an integration sphere. The two-photon absorption (TPA) spectrum was measured in the NIR region using the open-aperture Z-scan method with 130 fs pulses from an optical parametric amplifier (Light Conversion, TOPAS) operating at a repetition rate of 2 kHz generated from a Ti:sapphire regenerative amplifier system (Spectra-Physics, Hurricane).

Mass spectra were recorded on a Bruker microTOF using positive and negative mode ESI-TOF method for acetonitrile solutions.

X-ray data were taken on a Bruker SMART APEX X-Ray diffractometer equipped with a large area CCD detector and Rigaku CCD diffractometer (Saturn 724 with MicroMax-007) with Varimax Mo optics.

All calculations were carried out using the Gaussian 09 program.[1] Full optimizations were performed without any symmetry restriction with Becke's three-parameter hybrid exchange functional and the Lee–Yang–Parr correlation functional (B3LYP) and the 6-31G(d) basis set.[2] The calculated absorption wavelengths were obtained with the TD-DFT method at the B3LYP/6–31G(d) level.

Unless otherwise noted, materials obtained from commercial suppliers were used without further purification.

References

[1] M. J. Frisch, G. W. Trucks, H. B. Schlegel, G. E. Scuseria, M. A. Robb, J. R. Cheeseman, G. Scalmani, V. Barone, B. Mennucci, G. A. Petersson, H. Nakatsuji, M. Caricato, X. Li, H. P. Hratchian, A. F. Izmaylov, J. Bloino, G. Zheng, J. L. Sonnenberg, M. Hada, M. Ehara, K. Toyota, R. Fukuda, J. Hasegawa, M. Ishida, T. Nakajima, Y. Honda, O. Kitao, H. Nakai, T. Vreven, J. A. Montgomery, Jr., J. E. Peralta, F. Ogliaro, M. Bearpark, J. J. Heyd, E. Brothers, K. N. Kudin, V. N. Staroverov, R. Kobayashi, J. Normand, K. Raghavachari, A. Rendell, J. C. Burant, S. S. Iyengar, J. Tomasi, M. Cossi, N. Rega, J. M. Millam, M. Klene, J. E. Knox, J. B. Cross, V. Bakken, C. Adamo, J. Jaramillo, R. Gomperts, R. E. Stratmann, O. Yazyev, A. J. Austin, R. Cammi, C. Pomelli, J. W. Ochterski, R. L. Martin, K. Morokuma, V. G. Zakrzewski, G. A. Voth, P. Salvador, J. J. Dannenberg, S. Dapprich, A. D. Daniels, Ö. Farkas, J. B. Foresman, J. V. Ortiz, J. Cioslowski, and D. J. Fox, Gaussian, Inc., Wallingford CT, **2009**.

[2] (a) A. D. Becke, *Phys. Rev. A* **1988**, *38*, 3098. (b) C. Lee, W. Yang, R. G. Parr, *Phys. Rev. B* **1988**, *37*, 785.

Chapter 2

1,2,4,5-Tetra(4-mesitylphenyl)-3,6-diphenylbenzene

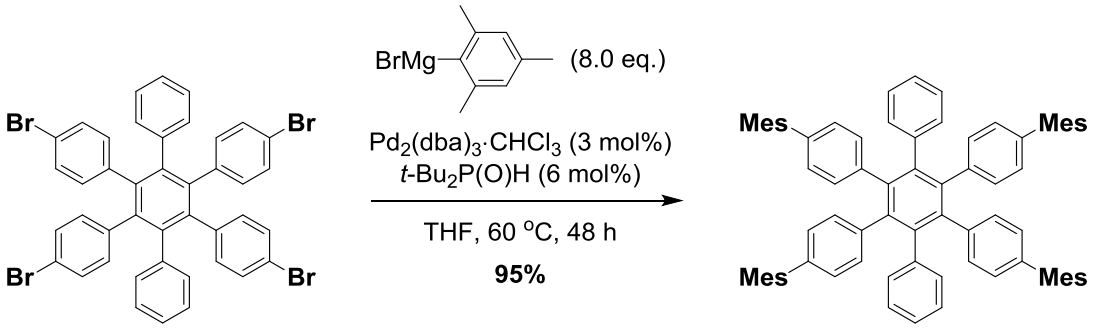

A flask containing 1,2,4,5-tetra(4-bromophenyl)-3,6-diphenylbenzene (2.56 g, 3.0 mmol), $Pd_2(dba)_3{\cdot}CHCl_3$ (82.4 mg, 3 mol%) and di(*tert*-butyl)phosphine oxide (29.2 mg, 6 mol%) was purged with N_2, and then charged with anhydrous and degassed THF (10 mL) and the mixture was stirred for 15 min. To this mixture was added dropwise a solution of mesitylmagnesium bromide prepared prior from mesityl bromide (4.78 g, 8.0 equiv) and magnesium (0.874 g, 12.0 equiv) in anhydrous degassed THF (30 mL) at room temperature. The mixture was then stirred at 60 °C for 72

h, quenched with aqueous HCl aq. (1 M), extracted with CH_2Cl_2, and then dried over Na_2SO_4. The solvents were removed under vacuum, and the crude product was purified by silica gel column chromatography with $CHCl_3$ as eluent and recrystallization from diethyl ether to afford 1,2,4,5-Tetra(4-mesitylphenyl)-3,6-diphenylbenzene (2.86 g, 2.84 mmol) in 95% yield as a white solid. Mp >300 °C; ^{1}H NMR ($CDCl_3$): δ 6.97 (d, J = 8.5 Hz, 8H), 6.90–6.93 (m, 4H), 6.84–6.89 (m, 14H), 6.66 (d, J = 8.5 Hz, 8H), 2.29 (s, 12H), 1.80 (s, 12H), 1.77 (s, 12H) ppm; ^{13}C NMR ($CDCl_3$): δ 140.7, 140.6, 140.3, 139.2, 139.0, 137.8, 136.14, 136.11, 135.7, 131.72, 131.68, 127.75, 127.66, 127.5, 126.5, 124.9, 21.0, 20.33, 20.27 ppm; HR-MS (ESI-MS): m/z = 1006.5477, calcd for $(C_{78}H_{70})^+$ = 1006.5472 [$(M)^+$].

2,5,11,14-Tetramesitylhexabenzo[*bc,ef,hi,kl,no,qr*]coronene (1a).

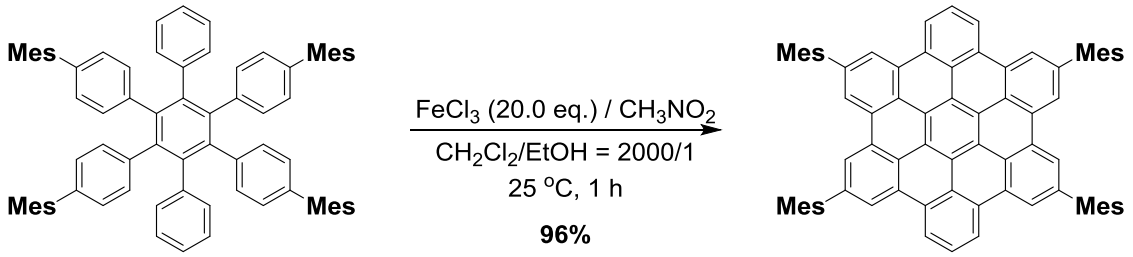

A solution of $FeCl_3$ (3.89 g, 20.0 equiv) in CH_3NO_2 (8 mL) was added to a stirred solution of 1,2,4,5-tetra(4-mesitylphenyl)-3,6-diphenylbenzene (1.21 g, 1.20 mmol) in anhydrous CH_2Cl_2/EtOH (200 mL/0.1 mL), the reaction mixture was stirred for 1 h with continuous N_2 bubbling through the reaction mixture. The mixture was poured into MeOH (100 mL) and concentrated by rotary evaporator. The crude product was purified by silica-gel column chromatography (CH_2Cl_2/hexane = 1/1) and recrystallization from toluene/MeOH to afford **1a** (1.14 g, 1.15 mmol) in 96% yield as a yellow solid. This product was soluble enough in organic solvent such as CH_2Cl_2, $CHCl_3$, and toluene. Mp >300 °C; ^{1}H NMR ($CDCl_3$): δ 9.24 (d, J = 8.0 Hz, 4H), 9.12 (s, 4H), 9.03 (s, 4H), 8.22 (t, J = 8.0 Hz, 2H), 7.14 (s, 8H), 2.46 (s, 12H), 2.26 (s, 24H) ppm; ^{13}C NMR ($CDCl_3$): δ 140.0, 139.2, 137.2, 136.3, 130.96, 130.91, 130.8, 128.4, 127.1, 125.9, 124.4, 123.47, 123.41, 122.35, 121.42, 121.37, 21.3, 21.2 ppm; HR-MS (ESI-MS): m/z = 994.4511, calcd for $(C_{78}H_{58})^+$ = 994.4533 [$(M)^+$]; UV/Vis (CH_2Cl_2): λ_{max} (ε [M^{-1} cm^{-1}]) = 329 (30000), 344 (80000), 361 (190000), 391 (64000) nm.

1,2,3,4-Tetra(4-bromophenyl)-5,6-diphenylbenzene

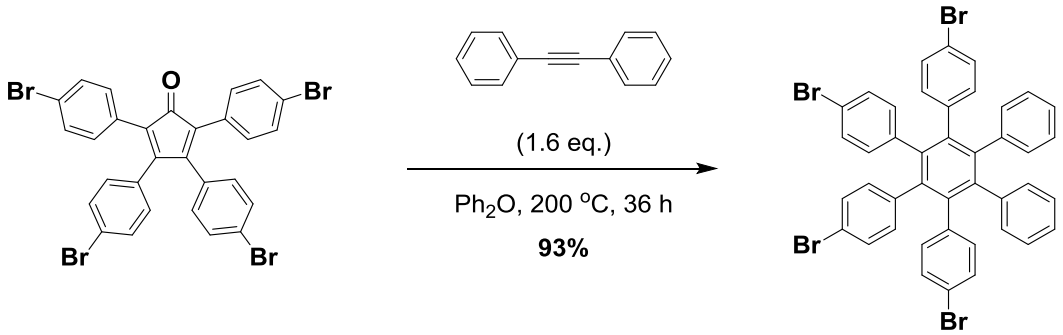

2,3,4,5-Tetrakis(4-bromophenyl)cyclopenta-2,4-dienone (3.10 g, 4.39 mmol) and 1,2-diphenylethyne (1.25 g, 1.6 equiv) in diphenyl ether (8 mL) was heated at 200 °C under N_2 for 36 h. The resulting mixture was cooled to room temperature and then diluted with diethyl ether. The precipitate was collected by filtration, washed with methanol and hexane, and dried to give 1,2,3,4-tetra(4-bromophenyl)-5,6-diphenylbenzene (3.47 g, 4.08 mmol) in 93% yield as a white solid. ^{1}H NMR ($CDCl_3$): δ 7.06 (d, J = 8.5 Hz, 4H), 7.02 (d, J = 8.5 Hz, 4H), 6.85–6.90 (m, 6H), 6.72–6.78 (m, 4H), 6.66 (d, J = 2.5 Hz, 4H), 6.64 (d, J = 2.0 Hz, 4H) ppm; ^{13}C NMR ($CDCl_3$): δ 141.0, 139.7, 139.4, 138.94, 138.91, 138.8, 132.7, 131.1, 130.3, 130.1, 126.9, 125.7, 120.1, 119.9 ppm; HR-MS (ESI-MS): m/z = 884.8457, calcd for $(C_{42}H_{26}Br_4)^-$ = 884.8425 [$(M + Cl)^-$].

1,2,3,4-Tetra(4-mesitylphenyl)-5,6-diphenylbenzene.

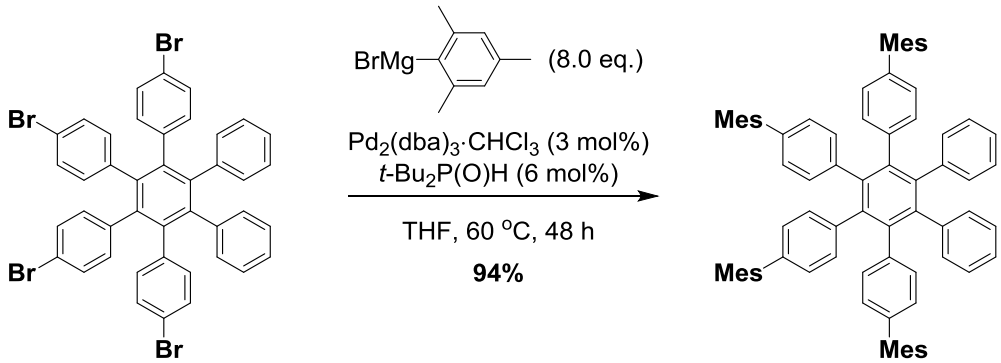

A flask containing 1,2,3,4-tetra(4-bromophenyl)-5,6-diphenylbenzene (2.56 g, 3.0 mmol), $Pd_2(dba)_3{\cdot}CHCl_3$ (82.4 mg, 3 mol%) and di(*tert*-butyl)phosphine oxide (29.2 mg, 6 mol%) was purged with N_2, and then charged with anhydrous and degassed THF (10 mL) and the mixture was

stirred for 15 min. To this mixture was added dropwise a solution of mesitylmagnesium bromide prepared prior from mesityl bromide (4.78 g, 8.0 equiv) and magnesium (0.874 g, 12.0 equiv) in anhydrous degassed THF (30 mL) at room temperature. The mixture was then stirred at 60 °C for 48 h, quenched with aqueous HCl (1 M), extracted with CH_2Cl_2, and then dried over Na_2SO_4. The solvents were removed under vacuum, and the crude product was purified by silica gel column chromatography ($CHCl_3$) and recrystallization from diethyl ether to afford 1,2,3,4-Tetra(4-mesitylphenyl)-5,6-diphenylbenzene (2.83 g, 2.82 mmol) in 94% yield as a white solid. ^{1}H NMR ($CDCl_3$): δ 7.02 (d, J = 8.5 Hz, 4H), 6.82–6.96 (m, 22H), 6.69 (d, J = 8 Hz, 4H), 6.64 (d, J = 8.5 Hz, 4H), 2.291 (s, 6H), 2.286 (s, 6H), 1.81 (s, 6H), 1.80 (s, 6H), 1.78 (s, 6H), 1.76 (s, 6H) ppm; ^{13}C NMR ($CDCl_3$): δ 140.8, 140.6, 140.5, 140.1, 139.2, 139.13, 139.06, 139.0, 137.9, 137.8, 136.23, 136.16, 135.95, 135.89, 135.6, 131.9, 131.7, 131.6, 127.75, 127.69, 127.5, 126.6, 125.1, 21.0, 20.4, 20.3 ppm; HR-MS (ESI-MS): m/z = 1006.5502, calcd for $(C_{78}H_{70})^+$ = 1006.5472 [$(M)^+$].

2,5,8,11-Tetramesitylhexabenzo[*bc,ef,hi,kl,no,qr*]coronene (1b).

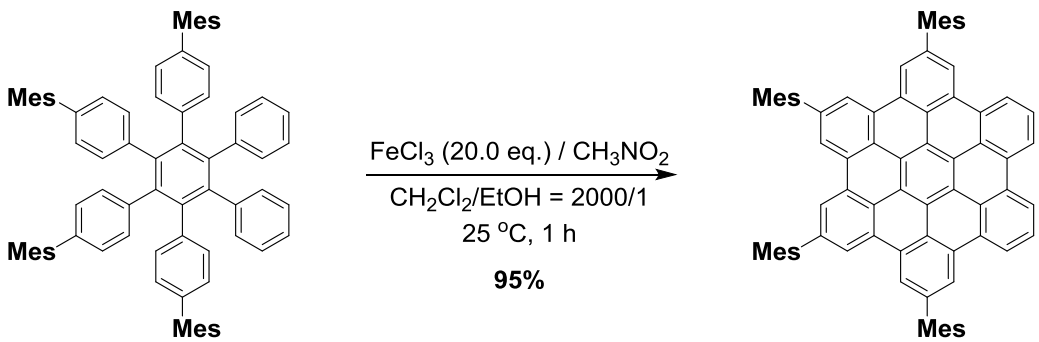

A solution of $FeCl_3$ (4.87 g, 20.0 equiv) in CH_3NO_2 (8 mL) was added to a stirred solution of 1,2,3,4-tetra(4-mesitylphenyl)-5,6-diphenylbenzene (1.51 g, 1.50 mmol) in anhydrous CH_2Cl_2/EtOH (150 mL/0.075 mL). The reaction mixture was stirred for 1 h with continuous N_2 bubbling through the reaction mixture. The mixture was poured into MeOH (100 mL) and concentrated by rotary evaporator. The crude product was purified by silica-gel column chromatography (CH_2Cl_2/hexane = 1/2) and recrystallization from CH_2Cl_2/MeOH to afford **1b** (1.42 g, 1.43 mmol) in 95% yield as a yellow solid. This product was soluble enough in organic solvent such as CH_2Cl_2, $CHCl_3$, and tol-

uene. ^{1}H NMR ($CDCl_3$): δ 9.06 (s, 2H), 9.03 (s, 2H), 8.99 (s, 2H), 8.93 (s, 2H), 8.91 (d, J = 8 Hz, 2H), 8.77 (d, J = 8 Hz, 2H), 7.87 (t, J = 8 Hz, 2H), 7.13 (s, 4H), 7.12 (s, 4H), 2.48 (s, 6H), 2.45 (s, 6H), 2.29 (s, 12H), 2.25 (s, 12H) ppm; ^{13}C NMR ($CDCl_3$): δ 139.9, 139.7, 139.2, 139.1, 137.1, 136.3, 136.1, 131.0, 130.9, 130.8, 130.7, 130.2, 130.1, 128.42, 128.39, 126.6, 125.2, 124.5, 124.2, 123.5, 123.4, 123.3, 123.2, 121.9, 121.7, 121.1, 121.0, 21.35, 21.29, 21.19, 21.17 ppm; HR-MS (ESI-MS): m/z = 995.4634, calcd for $(C_{78}H_{58})^+$ = 995.4611 [$(M + H)^+$]; UV/vis (CH_2Cl_2): λ_{max} (ε [M^{-1} cm^{-1}]) = 345 (90000), 361 (210000), 391 (71000) nm.

1,3,5-Tri(3'-chlorobiphen-2-yl)benzene.

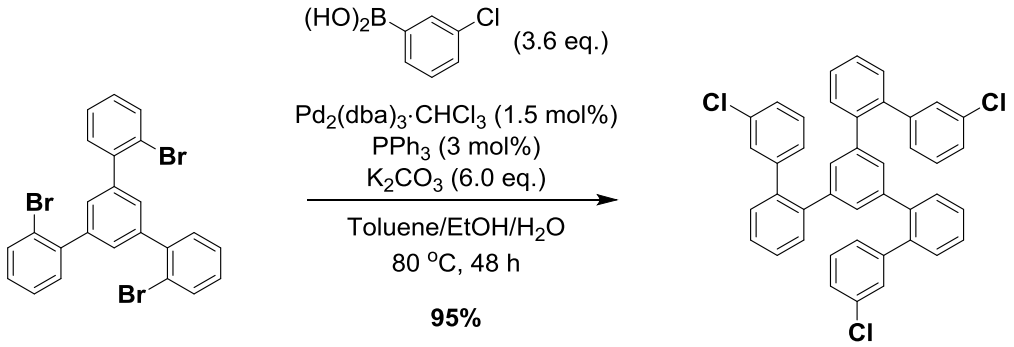

A flask containing 1,3,5-tri(2-bromophenyl)benzene (2.72 g, 5.0 mmol), 3-chlorophenylboronic acid (2.81 g, 3.6 equiv), potassium carbonate (4.15 g, 6.0 equiv), $Pd_2(dba)_3$•$CHCl_3$ (77.6 mg, 1.5 mol%), triphenylphosphine (39.3 mg, 3 mol%) was charged with toluene (50 mL) and EtOH/H_2O = 1/1 (24 ml). The resulting solution was degassed by thrice "freeze-pump-thaw" cycle and then stirred at 80 °C under N_2 for 48 h. The reaction mixture was slowly diluted with aqueous HCl (1 M). The mixture was extracted with CH_2Cl_2, dried over Na_2SO_4 and concentrated with rotary evaporator. The crude reaction mixture was purified by silica gel column chromatography ($CHCl_3$) and recrystallization from CH_2Cl_2/MeOH to afford 1,3,5-Tri(3'-chlorobiphen-2-yl)benzene (3.03 g, 4.75 mmol) in 95% yield as a white solid. Mp 214-229 °C; ^{1}H NMR (CD_2Cl_2): δ 7.3–7.4 (m, 9H), 7.2–7.3 (m, 9H), 6.84–6.9 (m, 6H), 6.79 (s, 3H) ppm; ^{13}C NMR ($CDCl_3$): δ 143.9, 140.9, 140.3, 139.3, 134.2, 130.9, 130.6, 130.3, 130.1, 129.6, 129.1, 128.3, 128.0, 127.0 ppm; HR-MS (ESI-MS): m/z = 636.1199, calcd for $(C_{42}H_{27}Cl_3)^+$ = 636.1173 [$(M)^+$].

1,3,5-Tri(3'-mesitylbiphen-2-yl)benzene.

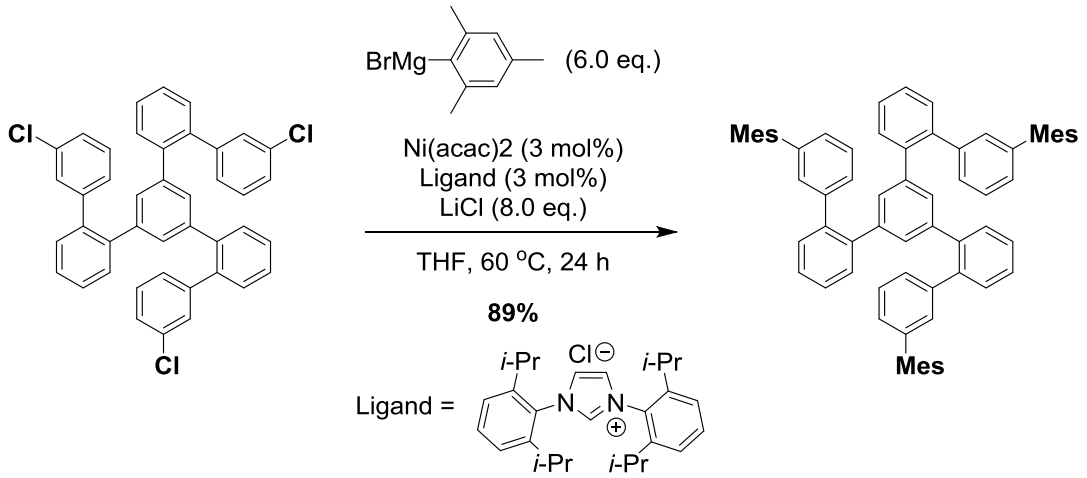

A flask containing 1,3,5-tri(3'-chlorobiphen-2-yl)benzene (2.56 g, 4.0 mmol), $Ni(acac)_2$ (30.8 mg, 3 mol%), 1,3-bis(2,6-diisopropylphenyl)imidazolium chloride (40.9 mg, 3 mol%), LiCl (1.36 g, 8.0 equiv) was purged with N_2, and then charged with anhydrous THF (10 mL) and the mixture was stirred for 15 min. To this mixture was added dropwise a solution of mesitylmagnesium bromide prepared prior from mesityl bromide (4.78 g, 6.0 equiv) and magnesium (0.758 g, 7.8 equiv) in anhydrous THF (30 mL) at room temperature. The mixture was then stirred at 60 °C for 24 h, quenched with aqueous HCl (1 M), extracted with $CHCl_3$, and then dried over Na_2SO_4. The solvents were removed under vacuum, and the crude product was purified by silica gel column chromatography ($CHCl_3$) and recrystallization from diethyl ether/MeOH to afford 1,3,5-Tri(3'-mesitylbiphen-2-yl)benzene (3.16 g, 3.55 mmol) in 89% yield as a white solid. Mp 247-257 °C; ^{1}H NMR (CD_2Cl_2): δ 7.31–7.36 (m, 6H), 7.24–7.29 (m, 3H), 7.04–7.11 (m, 3H), 6.90–6.98 (m, 9H), 6.89-6.82 (br, 3H), 6.86 (s, 6H), 6.84 (s, 3H), 2.27 (s, 9H), 1.78 (s, 18H) ppm; ^{13}C NMR ($CDCl_3$): δ 142.6, 141.5, 141.2, 141.0, 140.6, 139.2, 136.8, 136.1, 131.0, 130.7, 130.6, 130.5, 129.0, 128.2, 128.1, 127.8, 127.7, 127.5, 21.1, 20.8 ppm; HR-MS (ESI-MS): *m/z* = 888.4734, calcd for $(C_{69}H_{60})^+$ = 888.4690 [$(M)^+$].

2,8,14-Trimesitylhexabenzo[*bc,ef,hi,kl,no,qr*]coronene (1c).

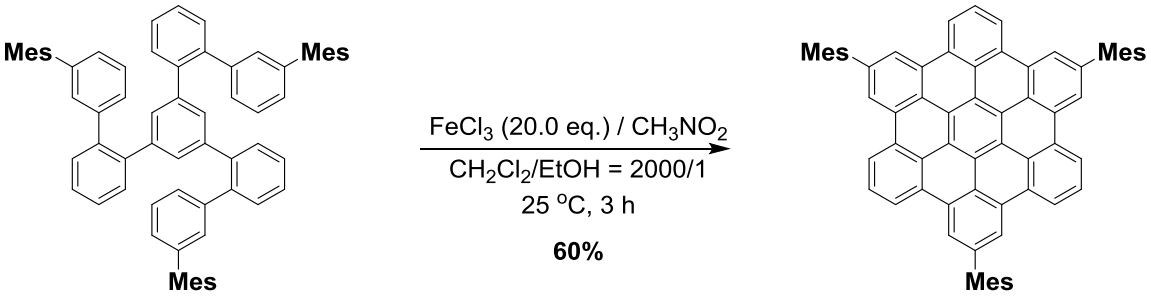

A solution of $FeCl_3$ (3.89 g, 20.0 eq.) in CH_3NO_2 (10 mL) was added dropwise to a stirred solution of 1,3,5-tri(3'-mesitylbiphen-2-yl)benzene (1.07 g, 1.2 mmol) in anhydrous CH_2Cl_2/EtOH (200 mL/0.1 mL), the reaction mixture was stirred for 3 h with continuous N_2 bubbling through the reaction mixture. After the mixture was poured into MeOH, the resulting solution was washed with water, dried over Na_2SO_4, and then concentrated with rotary evaporator. The crude product was purified by column chromatography (toluene/hexane = 1/9) and recrystallization from $CHCl_3$/MeOH several times to afford **1c** (626 mg, 0.72 mmol) in 60% yield as a yellow solid. Mp >300 °C; ^{1}H NMR ($CDCl_3$): δ 9.22 (d, J = 8.0 Hz, 6H), 9.10 (s, 6H), 8.20 (t, J = 8.0 Hz, 3H), 7.18 (s, 6H), 2.49 (s, 9H), 2.28 (s, 18H) ppm; ^{13}C NMR ($CDCl_3$): δ 140.0, 139.4, 137.3, 136.5, 131.0, 130.7, 128.4, 127.1, 125.9, 124.3, 123.3, 122.4, 121.6, 121.3, 21.3, 21.2 ppm; UV/Vis (CH_2Cl_2): λ_{max} (ε [M^{-1} cm^{-1}]) = 343 (76000), 360 (180000), 389 (61000) nm; HR-MS (ESI-MS): *m/z* = 876.3727, calcd for $(C_{69}H_{48})^+$ = 876.3751 [$(M)^+$].

2,11-Diboryl-5,8,14,17-tetramesitylhexabenzo[*bc,ef,hi,kl,no,qr*]coronene (2a).

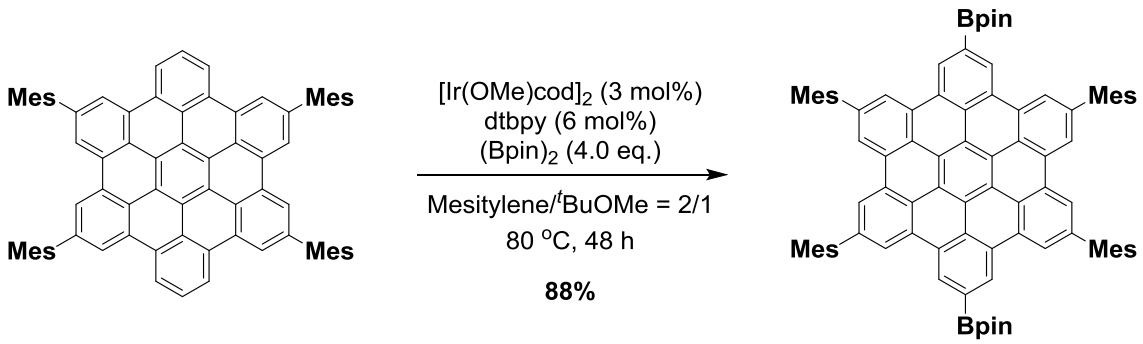

A flask containing 2,5,11,14-tetramesitylhexabenzo[*bc,ef,hi,kl,no,qr*]coronene **1a** (1.19 g, 1.20 mmol), bis(pinacolato)diboron (1.22 g, 4.0 equiv), 4,4'-di-*tert*-butyl-2,2'-bipyridyl (19.3 mg, 6

mol%), and $[Ir(OMe)cod]_2$ (23.9 mg, 3 mol%) was purged with N_2, and then charged with degassed anhydrous mesitylene/*tert*-butyl methyl ether (20 mL/10 mL). The mixture was then stirred at 80 °C for 48 h. The crude product was purified by silica gel column chromatography ($CHCl_3$) and recrystallization from $CHCl_3$/MeOH to afford **2a** (1.32 g, 1.06 mmol) in 88% yield as a yellow solid. Mp >300 °C; ^{1}H NMR ($CDCl_3$): δ 9.64 (s, 4H), 9.21 (s, 4H), 9.00 (s, 4H), 7.15 (s, 8H) 2.47 (s, 12H), 2.24 (s, 24H), 1.50 (s, 24H) ppm; ^{13}C NMR ($CDCl_3$): δ 140.1, 139.4, 137.3, 136.4, 131.2, 130.9, 129.9, 128.7, 128.4, 127.7, 124.4, 123.5, 123.2, 121.8, 121.6, 84.4, 25.0, 21.3, 21.2 ppm; HR-MS (ESI-MS): *m/z* = 1245.6293, calcd for $(C_{78}H_{80}B_2O_4)^+$ = 1245.6281 [$(M)^+$]; UV/Vis (CH_2Cl_2): λ_{max} (ε [M^{-1} cm^{-1}]) = 330 (39000), 348 (110000), 365 (270000), 394 (82000), 444 (3800), 472 (5500) nm.

5,8,14,17-Tetramesitylhexabenzo[*bc,ef,hi,kl,no,qr*]coronene-2,11-diol (3a).

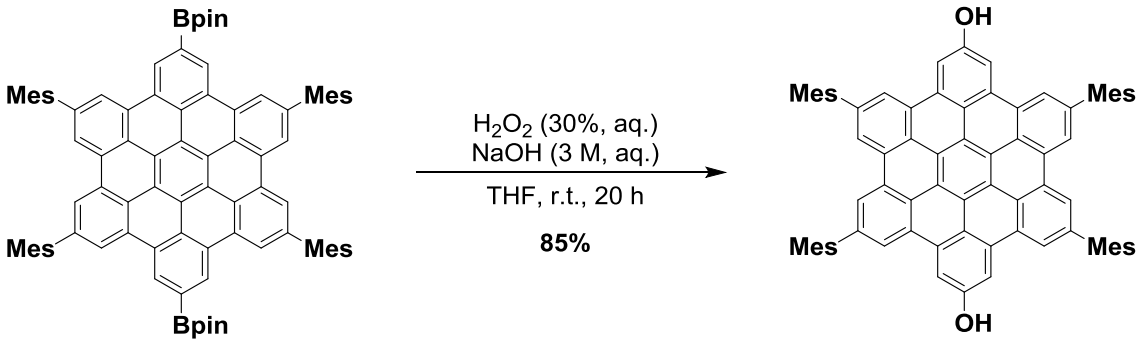

2,11-Diboryl-5,8,14,17-tetramesitylhexabenzo[*bc,ef,hi,kl,no,qr*]coronene **2a** (1.87 g, 1.5 mmol) was placed in a 100-mL flask and dissolved in THF (40 mL) and then cooled to 0 °C (ice/water). To the solution, aqueous sodium hydroxide (3 M, 10 mL) and aqueous hydrogen peroxide (30%, 10 mL) were added. The reaction mixture was gradually warmed to room temperature and stirred for 20 h. The flask was cooled to 0 °C (ice/water) and saturated aqueous sodium thiosulfate (10 mL) was added dropwise. The reaction mixture was diluted with $CHCl_3$ and the organic layers were separated. The aqueous layer was extracted with $CHCl_3$. The combined organic layers were dried over Na_2SO_4, and concentrated with rotary evaporator. The crude reaction mixture was purified by silica gel column chromatography (CH_2Cl_2/hexane = 2/1) and recrystallization from $CHCl_3$/hexane to afford **3a** (1.31 g, 1.28 mmol) in 85% yield as a yellow solid. Mp 240 °C (decomp.); ^{1}H NMR ($CDCl_3$): δ 9.00 (s, 4H), 8.97 (s, 4H), 8.64 (s, 4H), 7.12 (s, 8H) 5.57 (s, 2H), 2.45 (s, 12H), 2.23 (s, 24H) ppm; ^{13}C NMR ($CDCl_3$): δ 154.9, 139.8, 139.1, 137.2, 136.3, 132.8, 130.9, 130.4, 128.4, 124.7,

123.7, 123.5, 120.8, 120.5, 109.5, 21.3, 21.2 ppm; HR-MS (ESI-MS): *m/z* = 1026.4447, calcd for $(C_{78}H_{58}O_2)^+$ = 1026.4431 [$(M)^+$]; UV/Vis (CH_2Cl_2): λ_{max} (ε [M^{-1} cm^{-1}]) = 347 (110000), 364 (280000), 395 (85000), 443 (7800), 472 (14000) nm.; Crystal data: Single crystals were grown from $CHCl_3/CH_3OH$ solution. $C_{82.45}H_{64.20}Cl_{7.74}O_{6.26}$, M_w = 1429.56, Monoclinic, space group $P2_1/n$, a = 15.513(3) Å, b = 13.049(2) Å, c = 18.801(3) Å, β = 105.283(4)º, V = 3671.4(11) Å^3, Z = 2, D_{calc}= 1.293 g/cm^3, R_1 = 0.0884 ($I > 2.0\sigma(I)$), wR_2 = 0.2916 (all data), GOF = 1.037 ($I > 2.0\sigma(I)$).

2,5-Diboryl-8,11,14,17-tetramesitylhexabenzo[*bc,ef,hi,kl,no,qr*]coronene (2b)

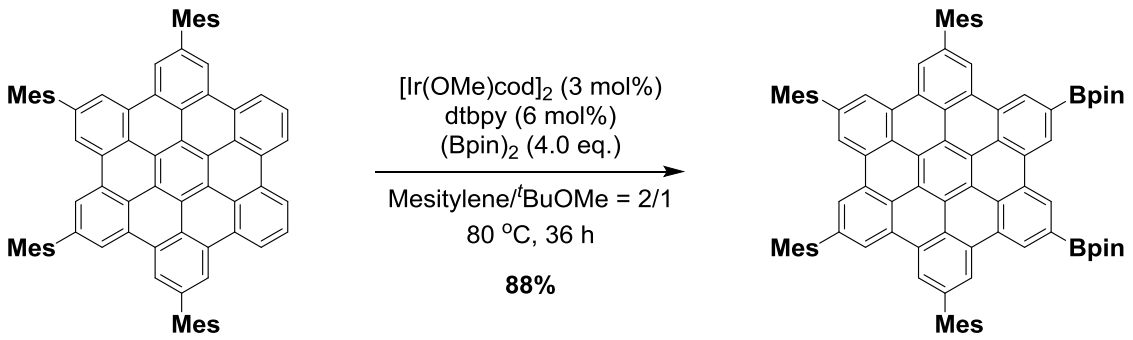

A flask containing **1b** (1.19 g, 1.20 mmol), bis(pinacolato)diboron (1.22 g, 4.0 equiv), 4,4'-di-*tert*-butyl-2,2'-bipyridyl (19.3 mg, 6 mol%), and $[Ir(OMe)cod]_2$ (23.9 mg, 3 mol%) was purged with N_2, and then charged with degassed anhydrous mesitylene/*tert*-butyl methyl ether (20 mL/10 mL). The mixture was then stirred at 80 °C for 36 h. The crude product was purified by silica gel column chromatography (CH_2Cl_2/hexane = 1/2) and recrystallization from CH_2Cl_2/MeOH to afford **2b** (1.32 g, 1.06 mmol) in 88% yield as a yellow solid. ^{1}H NMR ($CDCl_3$): δ 9.84 (s, 2H), 9.69 (s, 2H), 9.24 (s, 2H), 9.01 (s, 2H), 9.00 (s, 2H), 8.99 (s, 2H), 7.16 (s, 4H), 7.08 (s, 4H), 2.48 (s, 6H), 2.42 (s, 6H), 2.25 (s, 12H), 2.23 (s, 12H), 1.57 (s, 24H) ppm; ^{13}C NMR ($CDCl_3$): δ 140.1, 140.0, 139.4, 139.0, 137.3, 137.1, 136.5, 136.1, 131.2, 131.0, 130.98, 130.86, 130.1, 129.6, 128.9, 128.8, 127.7, 124.42, 124.38, 123.52, 123.48, 123.1, 121.8, 121.7, 121.6, 84.4, 25.1, 21.31, 21.29, 21.19, 21.14 ppm; HR-MS (ESI-MS): *m/z* = 1247.6294, calcd for $(C_{90}H_{80}B_2O_4)^+$ = 1247.6341 [$(M + H)^+$]; UV/vis (CH_2Cl_2): λ_{max} (ε [M^{-1} cm^{-1}]) = 349 (100000), 366 (240000), 396 (83000) nm.

8,11,14,17-Tetramesitylhexabenzo[*bc,ef,hi,kl,no,qr*]coronene-2,5-diol (3b)

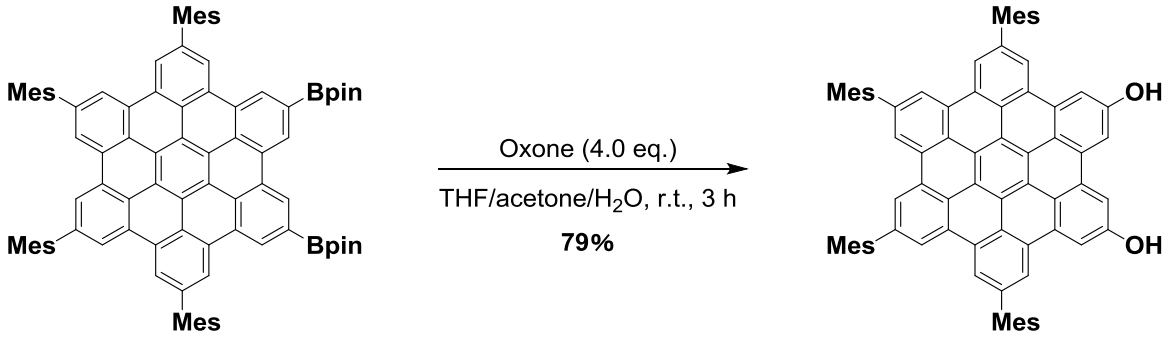

A flask containing **2b** (624 mg, 0.5 mmol) was purged with N_2, and then charged with degassed THF/acetone/H_2O (30 mL/4 mL/2 mL). To this mixture was added Oxone (1.23 g, 4.0 equiv) and was then stirred at room temperature for 3 h. The flask was cooled to 0 °C (ice/water) and saturated aqueous sodium thiosulfate was added dropwise. The reaction mixture was diluted with CH_2Cl_2 and the organic layers were separated. The aqueous layer was extracted with CH_2Cl_2. The combined organic layers were dried over Na_2SO_4, and concentrated with rotary evaporator. The crude product was purified by silica gel column chromatography (CH_2Cl_2/ethyl acetate = 1/1) and recrystallization from CH_2Cl_2/hexane to afford **3b** (405 mg, 0.40 mmol) in 79% yield as a yellow solid. ^{1}H NMR ($CDCl_3$): δ 9.04 (s, 2H), 9.01 (s, 2H), 8.99 (s, 2H), 8.78 (s, 2H), 8.31 (s, 2H), 8.01 (s, 2H), 7.10 (s, 8H), 5.27 (s, 2H, OH), 2.46 (s, 6H), 2.43 (s, 6H), 2.27 (s, 12H), 2.23 (s, 12H) ppm; ^{13}C NMR ($CDCl_3$): δ 154.22, 154.15, 139.7, 139.6, 139.0, 137.11, 137.08, 136.17, 136.09, 132.3, 132.2, 131.48, 131.38, 130.9, 130.7, 124.6, 124.5, 123.6, 123.4, 123.3, 120.5, 120.3, 120.2, 120.1, 120.0, 109.3, 109.0, 21.4, 21.3, 21.18, 21.15 ppm; HR-MS (ESI-MS): *m/z* = 1027.4488, calcd for $(C_{78}H_{58}O_2)^+$ = 1027.4510 [$(M + H)^+$]; UV/vis (CH_2Cl_2): λ_{max} (ε [M^{-1} cm^{-1}]) = 348 (86000), 364 (210000), 395 (62000) nm. $C_{80}H_{60}Cl_6O_2$, M_w = 1265.98, Monoclinic, space group $P2_1/n$, a = 8.099(4) Å, b = 22.002(11) Å, c = 35.641(18) Å, β = 92.477(10)º, V = 6346 (6) Å^3, Z = 4, D_{calc}= 1.325 g/cm^3, R_1 = 0.0704 ($I > 2.0\sigma(I)$), wR_2 = 0.2471 (all data), GOF = 1.050 ($I > 2.0\sigma(I)$).

2,8,14-Triboryl-5,11,17-trimesitylhexabenzo[*bc,ef,hi,kl,no,qr*]coronene (2c).

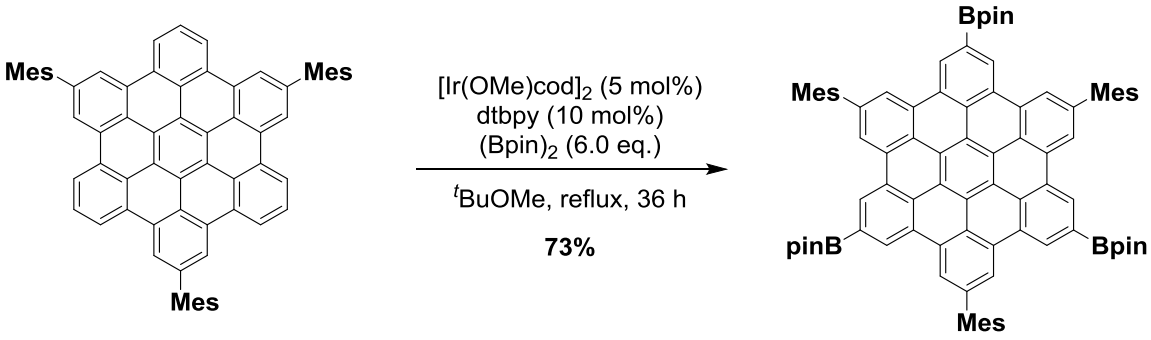

A flask containing 2,8,14-trimesitylhexabenzo[*bc,ef,hi,kl,no,qr*]coronene **1c** (743 mg, 0.847 mmol), bis(pinacolato)diboron (1.29 g, 6.0 equiv), 4,4'-di-*tert*-butyl-2,2'-bipyridyl (22.7 mg, 10 mol%), and $[Ir(OMe)cod]_2$ (28.1 mg, 5 mol%) was purged with N_2, and then charged with anhydrous degassed *tert*-butyl methyl ether (20 mL). The mixture was then stirred at 60 °C for 24 h. The reaction mixture was diluted with $CHCl_3$ and passed through a short plug of Celite, and then concentrated with rotary evaporator. The crude product was purified by silica gel column chromatography (CH_2Cl_2/hexane = 1/2) and recrystallization from $CHCl_3$/MeOH to afford **2c** (777 mg, 0.619 mmol) in 73% yield as a yellow solid. Mp >300 °C; ^{1}H NMR ($CDCl_3$): δ 9.63 (s, 6H), 9.20 (s, 6H), 7.22 (s, 6H), 2.52 (s, 9H), 2.28 (s, 18H), 1.51 (s, 36H) ppm; ^{13}C NMR ($CDCl_3$): δ 140.1, 139.7, 137.4, 136.8, 131.3, 129.7, 128.7, 128.4, 127.6, 124.3, 123.1, 122.8, 121.1, 84.4, 25.0, 21.3, 21.2 ppm; UV/Vis (CH_2Cl_2): λ_{max} (ε [M^{-1} cm^{-1}]) = 349 (99000), 366 (250000), 396 (88000) nm; HR-MS (ESI-MS): *m/z* = 1252.6304, calcd for $(C_{87}H_{81}B_3O_6)^+$ = 1252.6385 [$(M)^+$].

5,11,17-Trimesitylhexabenzo[*bc,ef,hi,kl,no,qr*]coronene-2,8,14-triol (3c).

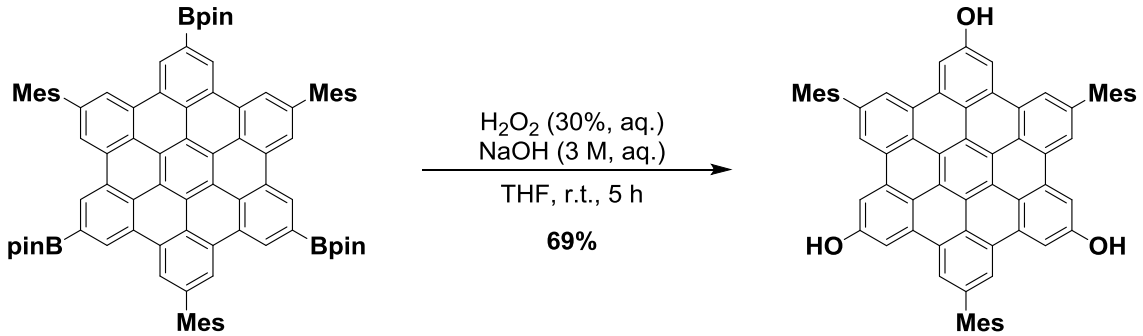

2,8,14-Triboryl-5,11,17-trimesitylhexabenzo[*bc,ef,hi,kl,no,qr*]coronene **2c** (62.8 mg, 0.05 mmol) was placed in a 100 ml flask and dissolved with THF (5 mL) and then cooled to 0 °C (ice/water). To

the solution, aqueous sodium hydroxide (3 M, 1 mL) and aqueous hydrogen peroxide (30%, 1 mL) were added. The reaction was gradually warmed to room temperature and stirred for 5 h. After the flask was cooled to 0 °C (ice/water) and aqueous sodium thiosulfate (1 M, 5 mL) was added dropwise. The reaction mixture was diluted with $CHCl_3$ and the organic layers were separated. The aqueous layer was extracted with $CHCl_3$ and the combined organic layers were dried over Na_2SO_4, and concentrated with rotary evaporator with protecting from light. The crude reaction mixture was purified by silica gel column chromatography (CH_2Cl_2) and recrystallization from CH_2Cl_2/hexane to afford **3c** (32.1 mg, 0.035 mmol) in 69% as a yellow solid. Mp 200 °C (de-comp.); ^{1}H NMR ($CDCl_3$): δ 8.96 (s, 6H), 8.63 (s, 6H), 7.15 (s, 6H), 5.53 (s, 3H, OH), 2.47 (s, 9H), 2.25 (s, 18H) ppm; A well-resolved ^{13}C NMR spectrum could not be obtained because of the poor solubility and instability; UV/Vis (CH_2Cl_2): λ_{max} (ε [M^{-1} cm^{-1}]) = 351 (54000), 367 (130000), 397 (46000) nm; HR-MS (ESI-MS): *m/z* = 924.3609, calcd for $(C_{69}H_{48}O_3)^+$ = 924.3598 [$(M)^+$]; Crystal data: Single crystals were grown from $CHCl_3/CH_3OH$ solution. $C_{71.63}H_{53.50}Cl_{1.25}O_{4.38}$, M_w = 1028.46, Rhombohedral, space group *Pa*-3, a = 21.814(2) Å, V = 10380.2(16) Å^3, Z = 8, D_{calc}= 1.316 g/cm^3, R_1 = 0.0590 ($I > 2.0\sigma(I)$), wR_2 = 0.1987 (all data), GOF = 0.894 ($I > 2.0\sigma(I)$).

5,8,14,17-Tetramesitylhexabenzo[*bc,ef,hi,kl,no,qr*]coronene-1,2,10,11-tetraone (9).

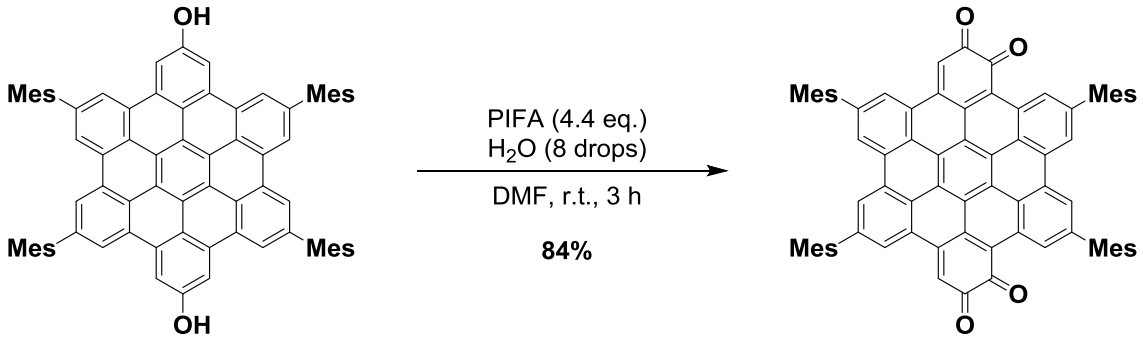

A flask containing 5,8,14,17-tetramesitylhexabenzo[*bc,ef,hi,kl,no,qr*]coronene-2,11-diol **3a** (412 mg, 0.4 mmol) and PIFA (757 mg, 4.4 equiv) was purged with N_2, and then charged with anhydrous de-gassed DMF (14 mL) and pure water (8 drops). The resulting solution was stirred at room temper-ature under light shielding for 3 h. The reaction mixture was diluted with EtOAc/hexane (4/1, v/v) and washed with H_2O several times to remove DMF. The combined organic layers were diluted with CH_2Cl_2 and dried over Na_2SO_4, and concentrated with rotary evaporator under light shielding.

The crude reaction mixture was purified by silica gel column chromatography (CH_2Cl_2) and recrystallization from CH_2Cl_2/hexane to afford **9** (356 mg, 0.336 mmol) in 84% yield as a purple solid. Mp 200 °C (decomp.); ^{1}H NMR (CD_2Cl_2): δ 9.43 (s, 2H), 8.90 (s, 2H), 8.80 (s, 2H), 8.42 (s, 2H) 7.27 (s, 2H), 7.08 (s, 8H), 2.39 (s, 12H), 2.18 (s, 12H), 2.16 (s, 12H) ppm; ^{13}C NMR spectrum could not be recorded due to seriously broadened signals; HR-MS (ESI-MS): *m/z* = 1055.4025, calcd for $(C_{78}H_{54}O_4)^+$ = 1055.4095 [$(M + H)^+$]; UV/Vis (CH_2Cl_2): λ_{max} (ε [M^{-1} cm^{-1}]) = 313 (52000), 354 (59000), 571 (22000) nm; IR (Solid): 2953, 2920, 2857, 2365, 1645 (C=O), 1589, 1447, 1375, 1333, 1271, 1238, 1101, 1034, 895, 849 cm^{-1}.

5,8,14,17-Tetramesitylhexabenzo[*bc,ef,hi,kl,no,qr*]coronene-1,2,10,11-tetraol (10).

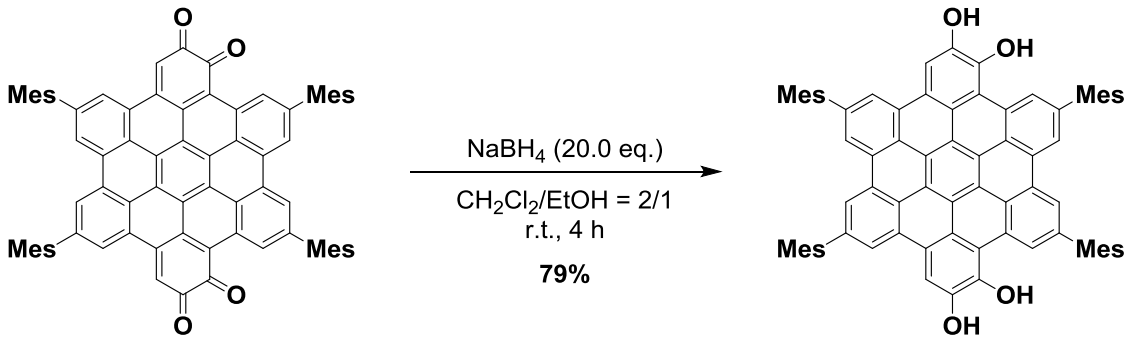

A flask containing 5,8,14,17-tetramesitylhexabenzo[*bc,ef,hi,kl,no,qr*]coronene-1,2,10,11-tetraone **9** (106 mg, 0.1 mmol) and $NaBH_4$ (75.7 mg, 20.0 equiv) was purged with N_2, and then charged with degassed CH_2Cl_2/EtOH (14 mL/7 mL). The resulting solution was stirred at room temperature under light shielding for 4 h. The reaction mixture was slowly diluted with aqueous HCl (1 M) and stirred for 15 min. The resulting solution was extracted with CH_2Cl_2, dried over Na_2SO_4, and then concentrated with rotary evaporator at 30 °C under light shielding. The crude reaction mixture was purified by silica gel column chromatography (CH_2Cl_2) and recrystallization from CH_2Cl_2/hexane to afford **10** (84.0 mg, 0.079 mmol) in 79% yield as a yellow solid. Mp 180 °C (decomp.); ^{1}H NMR (CD_2Cl_2): δ 10.07 (s, 2H), 9.05 (s, 2H), 8.95 (s, 2H), 8.86 (s, 2H), 8.78 (s, 2H), 7.25 (s, 2H, OH), 7.10 (s, 8H), 6.11 (s, 2H, OH), 2.42 (s, 12H), 2.25 (s, 12H), 2.21 (s, 12H) ppm; ^{13}C NMR ($CDCl_3$): δ 143.9, 142.8, 140.3, 140.1, 139.9, 139.7, 137.4, 137.2, 136.6, 131.2, 130.8, 130.53, 130.45, 129.0, 128.7, 128.6, 125.0, 123.9, 123.7, 123.6, 123.2, 123.0, 122.9, 121.8, 121.2, 121.1, 118.2, 109.2,

21.41, 21.36, 21.27 ppm; HR-MS (ESI-MS): *m/z* = 1058.4350, calcd for $(C_{78}H_{58}O_4)^+$ = 1058.4330 [$(M)^+$]; UV/Vis (CH_2Cl_2): λ_{max} (ε [M^{-1} cm^{-1}]) = 354 (75000), 371 (120000), 402 (46000) nm.

5,8,14,17-Tetramesitylhexabenzo[*bc,ef,hi,kl,no,qr*]coronene-1,2,10,11-tetrayl tetraacetate (11).

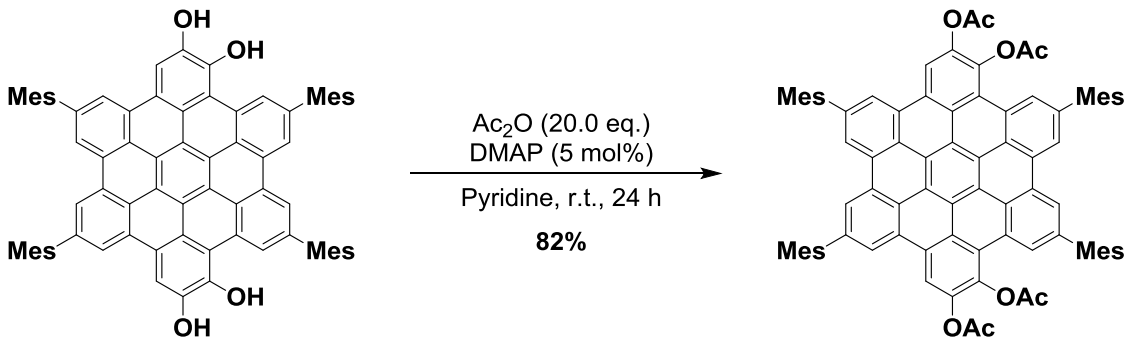

A flask containing 5,8,14,17-tetramesitylhexabenzo[*bc,ef,hi,kl,no,qr*]coronene-1,2,10,11-tetraol **10** (106 mg, 0.1 mmol), acetic anhydride (204 mg, 20 equiv) and 4-(*N,N*-dimethylamino)pyridine (0.06 mg, 5 mol%) was purged with N_2, and then charged with anhydrous and degassed pyridine (10 mL). The resulting solution was stirred at room temperature with protecting from light for 24 h. The reaction mixture was diluted with CH_2Cl_2 and washed with aqueous HCl (1 M) several times to remove pyridine. The combined organic layers were dried over Na_2SO_4, and concentrated with rotary evaporator. The crude reaction mixture was purified by silica gel column chromatography (CH_2Cl_2/hexane = 4/3) and recrystallization from $CHCl_3$/MeOH to afford **11** (101 mg, 0.082 mmol) in 82% yield as a yellow solid. Mp >300 °C; ^{1}H NMR ($CDCl_3$): δ 9.47 (s, 2H), 9.04 (s, 2H), 9.02 (s, 2H), 8.99 (s, 2H), 8.94 (s, 2H), 7.11 (s, 4H), 7.08 (s, 4H), 2.40–2.58 (m, 24H), 2.11–2.29 (m, 24H) ppm; ^{13}C NMR ($CDCl_3$): δ 169.0, 168.0, 142.5, 140.4, 140.0, 139.3, 139.1, 138.9, 137.3, 137.1, 136.3, 135.9, 130.7, 130.5, 130.0, 129.5, 128.7, 128.4, 128.3, 127.3, 125.7, 125.1, 125.0, 124.2, 124.1, 123.8, 121.4, 121.2, 121.1, 117.0, 21.3, 21.2, 21.1, 20.9 ppm; HR-MS (ESI-MS): *m/z* = 1226.4800, calcd for $(C_{86}H_{66}O_8)^+$ = 1226.4752 [$(M)^+$]; UV/Vis (CH_2Cl_2): λ_{max} (ε [M^{-1} cm^{-1}]) = 348 (96000), 365 (220000), 395 (78000) nm. $C_{94}H_{65}Cl_{16}O_8$, M_w = 1889.66, Triclinic, space group *P*-1, a = 14.851(5) Å, b = 16.799(6) Å, c = 17.678(6) Å, α = 68.827(7)º, β = 84.940(8)º, γ = 80.653(7)º, V = 4056(2) Å^3, Z = 2, D_{calc}= 1.547 g/cm^3, R_1 = 0.1005 (I > 2.0σ(I)), wR_2 = 0.3037 (all data), GOF = 0.966 (I > 2.0σ(I)).

Chapter 3

2,5,11,14-Tetramesityl-8,17-dimethoxyhexabenzo[*bc,ef,hi,kl,no,qr*]coronene (4a)

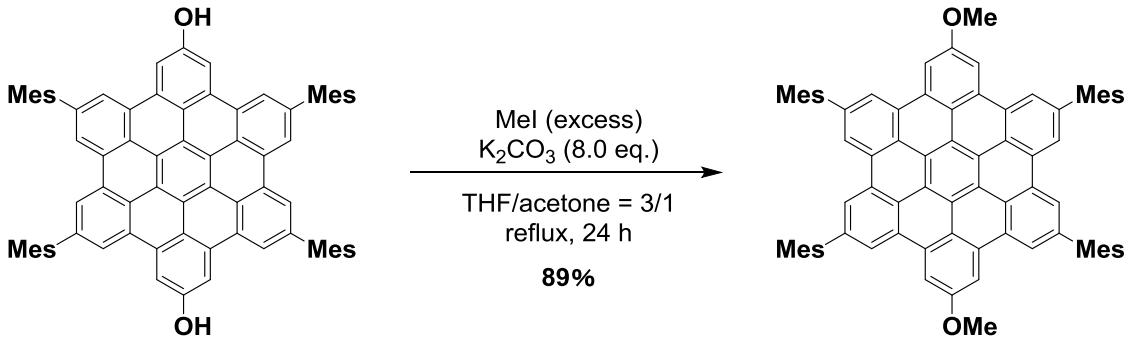

A flask containing **3a** (20.5 mg, 0.02 mmol) and potassium carbonate (22.1 mg, 8.0 equiv) was purged with N_2, and then charged with anhydrous and degassed THF/acetone = 3/1 (4 mL). To this mixture was added iodomethane (0.4 mL, excess) dropwise at room temperature. The mixture was then stirred under reflux for 24 h, quenched with aqueous HCl (1 M), extracted with CH_2Cl_2, and then dried over Na_2SO_4. The solvents were removed under vacuum, and the crude product was purified by silica gel column chromatography (CH_2Cl_2/hexane = 1/2) and recrystallization from CH_2Cl_2/MeOH to afford **4a** (18.7 mg, 0.018 mmol) in 89% yield as a yellow solid. ^{1}H NMR ($CDCl_3$): δ 9.02 (s, 4H), 9.00 (s, 4H), 8.71 (s, 4H), 7.14 (s, 8H), 4.24 (s, 6H), 2.46 (s, 12H), 2.25 (s, 24H) ppm; ^{13}C NMR ($CDCl_3$): δ 158.8, 139.8, 139.2, 137.3, 136.4, 132.4, 131.0, 130.7, 128.4, 124.8, 123.6, 123.4, 120.8, 120.5, 108.2, 56.0, 21.3, 21.2 ppm; HR-MS (ESI-MS): HR-MS (ESI-MS): *m/z* = 1055.4775, calcd for $(C_{80}H_{62}O_2)^+$ = 1055.4823 [$(M + H)^+$]; UV/vis (CH_2Cl_2): λ_{max} (ε [M^{-1} cm^{-1}]) = 349 (82000), 365 (200000), 396 (58000), 444 (6500), 472 (10000) nm.

5,8,14,17-Tetramesitylhexabenzo[*bc,ef,hi,kl,no,qr*]coronene-2,11-diyl bis(trifluoromethanesulfonate) (5a)

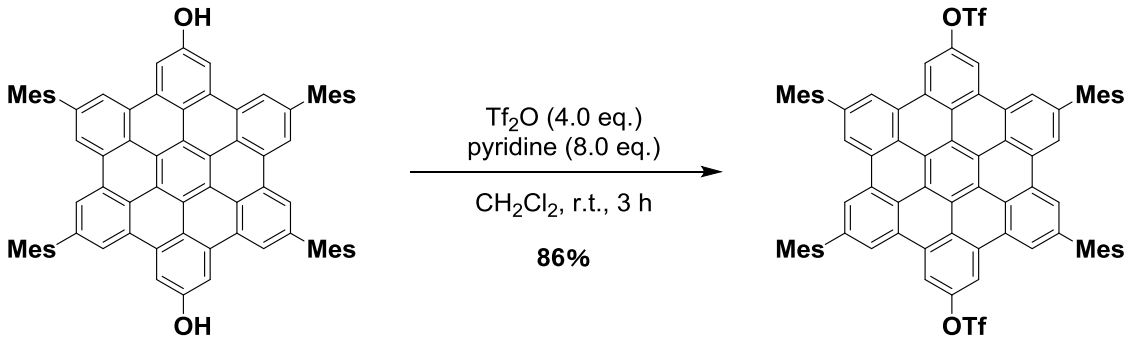

A flask containing **3a** (616 mg, 0.6 mmol) was purged with N_2, and then charged with anhydrous and degassed CH_2Cl_2 (8 mL) and pyridine (0.39 ml, 8.0 equiv). Then the mixture was stirred for 1 min. To this mixture was added trifluoromethanesulfonic anhydride (0.41 ml, 4.0 equiv) dropwise at room temperature. The mixture was then stirred at room temperature for 3 h, quenched with aqueous HCl (1 M), extracted with CH_2Cl_2, and then dried over Na_2SO_4. The solvents were removed under vacuum, and the crude product was purified by silica gel column chromatography (CH_2Cl_2/hexane = 1/2) and recrystallization from CH_2Cl_2/MeOH to afford **5a** (667 mg, 0.52 mmol) in 86% yield as a yellow solid. ^{1}H NMR ($CDCl_3$): δ 9.11 (s, 4H), 9.03 (s, 4H), 9.02 (s, 4H), 7.16 (s, 8H), 2.47 (s, 12H), 2.25 (s, 24H) ppm; ^{13}C NMR ($CDCl_3$): δ 148.9, 140.8, 138.5, 137.7, 136.2, 133.4, 130.9, 129.8, 128.6, 125.1, 124.9, 124.9, 124.6, 124.0, 121.5, 120.9, 114.7, 21.3, 21.2 ppm; HR-MS (ESI-MS): HR-MS (ESI-MS): *m/z* = 1291.3446, calcd for $(C_{80}H_{56}F_6O_6S_2)^+$ = 1291.3495 [$(M + H)^+$]; UV/vis (CH_2Cl_2): λ_{max} (ε [M^{-1} cm^{-1}]) = 347 (93000), 363 (220000), 393 (75000) nm.

***N*2,*N*11,5,8,14,17-Hexamesitylhexabenzo[*bc,ef,hi,kl,no,qr*]coronene-2,11-diamine (6a)**

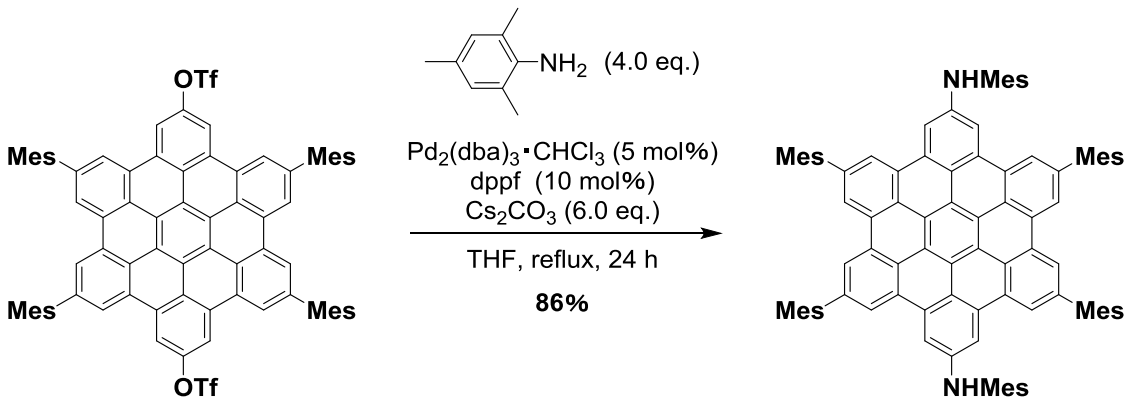

A flask containing **5a** (258 mg, 0.2 mmol), $Pd_2(dba)_3{\cdot}CHCl_3$ (10.4 mg, 5 mol%), 1,1'-bis(diphenylphosphino)ferrocene (11.1 mg, 10 mol%), and cesium carbonate (391 mg, 6.0 equiv) was purged with N_2, and then charged with anhydrous and degassed toluene (15 mL). To this mixture was added 2,4,6-trimethylaniline (216 mg, 8.0 equiv) dropwise at room temperature. The mixture was then stirred under reflux for 24 h, quenched with CH_2Cl_2, and then the solvents were removed under vacuum. The crude product was purified by silica gel column chromatography ($CHCl_3$/hexane = 1/3) and recrystallization from CH_2Cl_2/MeOH to afford **6a** (216 mg, 0.17 mmol) in 86% yield as a yellow solid. ^{1}H NMR ($CDCl_3$): δ 8.92 (s, 4H), 8.81 (s, 4H), 8.28 (s, 4H), 7.10 (s, 8H), 7.04 (s, 4H), 5.73 (s, 2H, NH), 2.44 (s, 12H), 2.38 (s, 6H), 2.34 (s, 12H), 2.22 (s, 24H) ppm; ^{13}C NMR ($CDCl_3$): δ 145.6, 139.4, 139.2, 137.0, 136.4, 135.8, 135.6, 134.9, 132.1, 130.8, 130.6, 129.8, 128.4, 124.8, 123.4, 123.2, 120.7, 120.0, 119.3, 107.5, 21.3, 21.1, 18.6 ppm; HR-MS (ESI-MS): *m/z* = 1260.6331, calcd for $(C_{96}H_{80}N_2)^+$ = 1260.6316 [$(M)^+$]; UV/vis (CH_2Cl_2): λ_{max} (ε [M^{-1} cm^{-1}]) = 327 (68000), 359 (72000), 377 (150000), 433 (24000), 459 (13000), 491 (14000) nm.

5,8,14,17-Tetramesitylhexabenzo[*bc,ef,hi,kl,no,qr*]coronene-2,11-dicarbonitrile (7a)

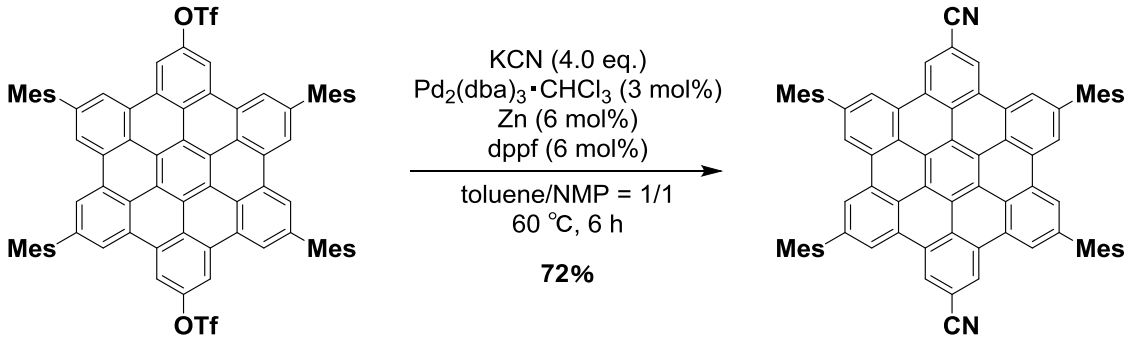

A flask containing **5a** (64.6 mg, 0.05 mmol), $Pd_2(dba)_3{\bullet}CHCl_3$ (2.59 mg, 5 mol%), 1,1'-bis(diphenylphosphino)ferrocene (2.77 mg, 10 mol%), KCN (26.0 mg, 8.0 equiv), and zinc powder (0.19 mg, 6 mol%) was purged with N_2, and then charged with anhydrous and degassed toluene/NMP = 1/1 (4 mL). The mixture was then stirred at 60 °C for 24 h, quenched with aqueous HCl (1 M), extracted with CH_2Cl_2, and then dried over Na_2SO_4. The solvents were removed under vacuum, and the crude product was purified by silica gel column chromatography (CH_2Cl_2/hexane = 2/1) recrystallization from CH_2Cl_2/MeOH to afford **7a** (37.5 mg, 0.036 mmol) in 72% yield as a yellow solid. ^{1}H NMR ($CDCl_3$): δ 9.44 (s, 4H), 9.11 (s, 4H), 9.08 (s, 4H), 7.14 (s, 8H), 2.46 (s, 12H),

2.24 (s, 24H) ppm; ^{13}C NMR ($CDCl_3$): δ 141.1, 138.3, 137.6, 136.0, 131.8, 130.8, 129.5, 128.6, 127.9, 125.2, 124.9, 124.3, 124.0, 122.2, 121.2, 119.4, 111.2, 21.3, 21.2 ppm; HR-MS (ESI-MS): *m/z* = 1044.4451, calcd for $(C_{80}H_{56}N_2)^+$ = 1044.4438 [$(M)^+$]; UV/vis (CH_2Cl_2): λ_{max} (ε [M^{-1} cm^{-1}]) = 353 (73000), 371 (180000), 402 (51000), 421 (20000), 449 (4900), 478 (5600) nm.

2,11-Bis(3,3-dimethylbut-1-yn-1-yl)-5,8,14,17-tetramesitylhexabenzo[*bc,ef,hi,kl,no,qr*]coronene (8a)

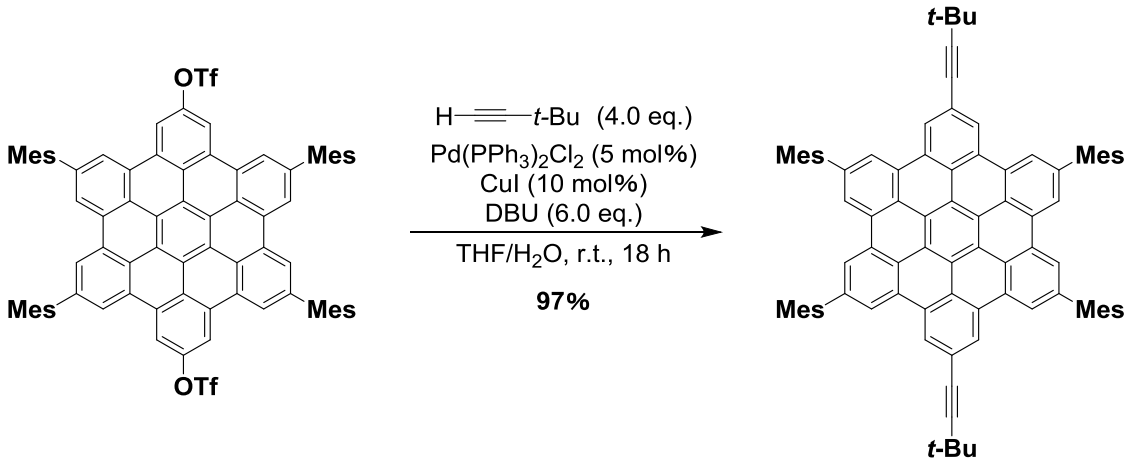

A flask containing **5a** (129 mg, 0.1 mmol), $PdCl_2(PPh_3)_2$ (2.11 mg, 3 mol%), and copper(I) iodide (1.14 mg, 6 mol%) was purged with N_2, and then charged with anhydrous and degassed THF (5 mL). To this mixture was added 1,8-diazabicyclo[5.4.0]undec-7-ene (91.3 mg, 6.0 equiv) and pure water (2 drops) and 3,3-dimethylbut-1-yne (32.9 mg, 4.0 equiv) at room temperature. The mixture was then stirred under room temperature for 18 h, quenched with aqueous HCl (1 M), extracted with CH_2Cl_2, and then dried over Na_2SO_4. The solvents were removed under vacuum, and the crude product was purified by silica gel column chromatography (CH_2Cl_2/hexane = 1/2) and recrystallization from $CHCl_3$/MeOH to afford **8a** (113 mg, 0.097 mmol) in 97% yield as a yellow solid. ^{1}H NMR ($CDCl_3$): δ 9.21 (s, 4H), 9.06 (s, 4H), 9.01 (s, 4H), 7.13 (s, 8H), 2.46 (s, 12H), 2.24 (s, 24H), 1.47 (s, 18H) ppm; ^{13}C NMR ($CDCl_3$): δ 140.2, 139.1, 137.3, 136.3, 130.9, 130.7, 130.4, 128.4, 125.4, 124.9, 124.5, 123.6, 123.5, 122.9, 121.4, 121.2, 99.9, 79.7, 31.2, 28.2, 21.3, 21.2 ppm; HR-MS (ESI-MS): *m/z* = 1155.5855, calcd for $(C_{90}H_{74})^+$ = 1155.5863 [$(M + H)^+$]; UV/vis (Toluene): λ_{max} (ε [M^{-1} cm^{-1}]) = 352 (110000), 372 (260000), 399 (98000), 416 (32000) nm.

2,5,8,11-Tetramesityl-14,17-dimethoxyhexabenzo[*bc,ef,hi,kl,no,qr*]coronene (4b)

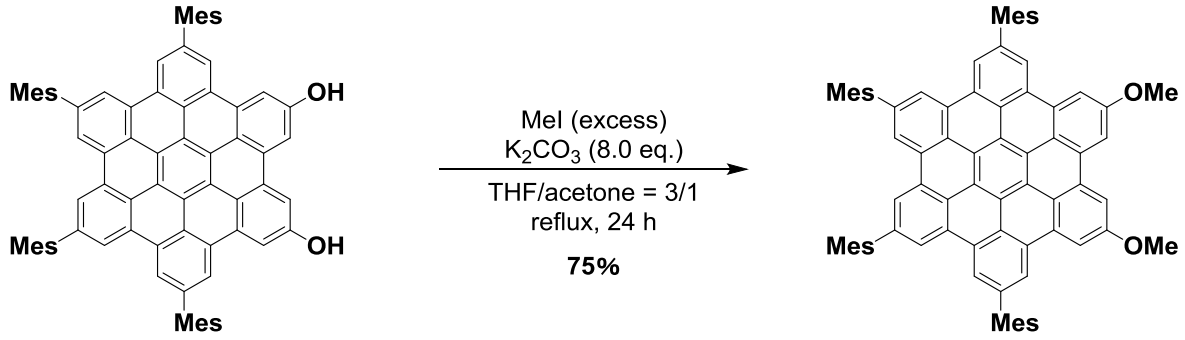

A flask containing **3b** (103 mg, 0.1 mmol) and potassium carbonate (83 mg, 6.0 equiv) was purged with N_2, and then charged with anhydrous and degassed THF/acetone = 3/1 (4 mL). To this mixture was added dropwise iodomethane (0.3 ml, excess) at room temperature. The mixture was then stirred at 60 °C for 24 h, quenched with aqueous HCl (1 M), extracted with CH_2Cl_2, and then dried over Na_2SO_4. The solvents were removed under vacuum, and the crude product was purified by silica gel column chromatography (CH_2Cl_2/hexane = 1/2) and recrystallization from CH_2Cl_2/MeOH to afford **4b** (79.5 mg, 0.075 mmol) in 75% yield as a yellow solid. ^{1}H NMR ($CDCl_3$): δ 9.00 (s, 6H), 8.94 (s, 2H), 8.55 (s, 2H), 8.39 (s, 2H), 7.14 (s, 4H), 7.09 (s, 4H), 4.13 (s, 6H), 2.47 (s, 6H), 2.42 (s, 6H), 2.25 (s, 12H), 2.24 (s, 12H) ppm; ^{13}C NMR ($CDCl_3$): δ 158.5, 139.7, 139.6, 139.3, 139.1, 137.2, 137.1, 136.4, 136.1, 132.3, 131.9, 131.0, 130.81, 130.77, 130.6, 128.4, 124.7, 124.6, 123.5, 123.4, 123.2, 120.7, 120.5, 120.3, 108.6, 107.3, 55.8, 21.3, 21.2 ppm; HR-MS (ESI-MS): *m/z* = 1055.4817, calcd for $(C_{80}H_{62}O_2)^+$ = 1055.4823 [$(M + H)^+$]; UV/vis (CH_2Cl_2): λ_{max} (ε [M^{-1} cm^{-1}]) = 349 (91000), 366 (220000), 396 (64000) nm.

8,11,14,17-Tetramesitylhexabenzo[*bc,ef,hi,kl,no,qr*]coronene-2,5-diyl bis(trifluoromethanesulfonate) (5b)

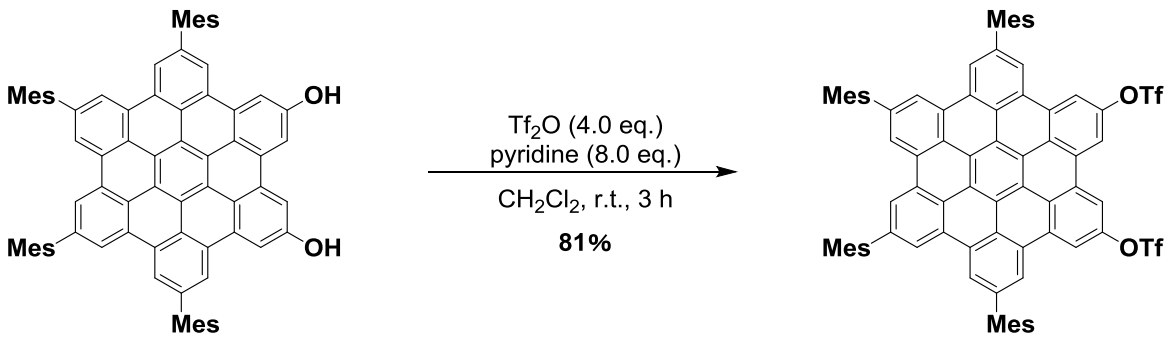

A flask containing **3b** (103 mg, 0.1 mmol) was purged with N_2, and then charged with anhydrous and degassed CH_2Cl_2 (5 mL) and pyridine (0.062 ml, 8.0 equiv), then the mixture was stirred for 1 min. To this mixture was added trifluoromethanesulfonic anhydride (0.017 mL, 4.0 equiv) dropwise at room temperature. The mixture was then stirred at room temperature for 3 h, quenched with aqueous HCl (1 M), extracted with CH_2Cl_2, and then dried over Na_2SO_4. The solvents were removed under vacuum, and the crude product was purified by silica gel column chromatography (CH_2Cl_2/hexane = 1/2) and recrystallization from CH_2Cl_2/MeOH to afford **5b** (105 mg, 0.081 mmol) in 81% yield as a yellow solid. ^{1}H NMR ($CDCl_3$): δ 9.12 (s, 2H), 9.08 (s, 2H), 9.07 (s, 2H), 8.99 (s, 2H), 8.96 (s, 2H), 8.78 (s, 2H), 7.17 (s, 4H), 7.11 (s, 4H), 2.49 (s, 6H), 2.44 (s, 6H), 2.26 (s, 12H), 2.25 (s, 12H) ppm; ^{13}C NMR ($CDCl_3$): δ 148.5, 140.9, 140.7, 138.7, 138.4, 137.6, 137.4, 136.2, 136.0, 133.4, 131.6, 131.2, 131.1, 130.8, 129.4, 128.6, 128.5, 125.2, 125.1, 124.4, 124.1, 123.9, 123.8, 122.1, 121.4, 120.3, 120.0, 117.7, 115.4, 114.5, 21.30, 21.28, 21.17 ppm; HR-MS (ESI-MS): *m/z* = 1291.3526, calcd for $(C_{80}H_{56}F_6O_6S_2)^+$ = 1291.3495 [$(M + H)^+$]; UV/vis (CH_2Cl_2): λ_{max} (ε [M^{-1} cm^{-1}]) = 344 (110000), 360 (280000), 381 (87000) nm.

***N*2,*N*5,8,11,14,17-Hexamesitylhexabenzo[*bc,ef,hi,kl,no,qr*]coronene-2,5-diamine (6b)**

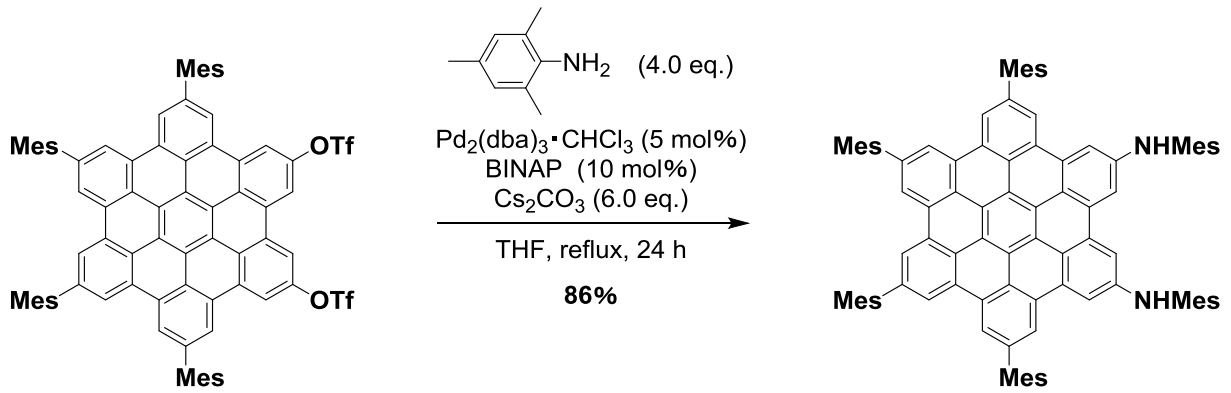

A flask containing **5b** (129 mg, 0.1 mmol), $Pd_2(dba)_3$•$CHCl_3$ (3.1 mg, 3 mol%), 2,2'-bis(diphenylphosphino)-1,1'-binaphthyl (3.7 mg, 6 mol%), cesium carbonate (195 mg, 6.0 equiv) was purged with N_2, and then charged with anhydrous and degassed Toluene (12 mL). To this mixture was added dropwise 2,4,6-trimethylaniline (108 mg, 8.0 equiv) at room temperature. The mixture was then stirred under reflux for 24 h, quenched with CH_2Cl_2, and then the solvents were removed under vacuum. The crude product was purified by silica gel column chromatography

($CHCl_3$/hexane = 1/3) and recrystallization from CH_2Cl_2/MeOH to afford **6b** (108 mg, 0.086 mmol) in 86% yield as a yellow solid. ^{1}H NMR ($CDCl_3$): δ 8.978 (s, 2H), 8.974 (s, 2H), 8.965 (s, 2H), 8.89 (s, 2H), 8.39 (s, 2H), 7.88 (s, 2H), 7.12 (s, 4H), 7.09 (s, 4H), 7.01 (s, 4H), 5.69 (s, 2H, NH), 2.46 (s, 6H), 2.43 (s, 12H), 2.30 (s, 12H), 2.25 (s, 12H), 2.24 (s, 12H) ppm; ^{13}C NMR ($CDCl_3$): δ 145.5, 139.4, 139.30, 139.27, 139.20, 137.05, 136.95, 136.4, 136.1, 135.6, 135.4, 135.1, 132.2, 132.0, 130.9, 130.7, 130.6, 129.5, 128.35, 128.33, 124.83, 124.75, 123.4, 123.29, 123.27, 123.18, 120.5, 120.1, 119.9, 119.3, 108.1, 106.8, 21.31, 21.29, 21.1, 18.5 ppm; HR-MS (ESI-MS): *m/z* = 1260.6293, calcd for $(C_{96}H_{80}N_2)^+$ = 1260.6316 [$(M + H)^+$]; UV/vis (CH_2Cl_2): λ_{max} (ε[M^{-1} cm^{-1}]) = 330 (47000), 382 (140000), 455 (8700), 486 (7900) nm.

8,11,14,17-Tetramesitylhexabenzo[*bc,ef,hi,kl,no,qr*]coronene-2,5-dicarbonitrile (7b)

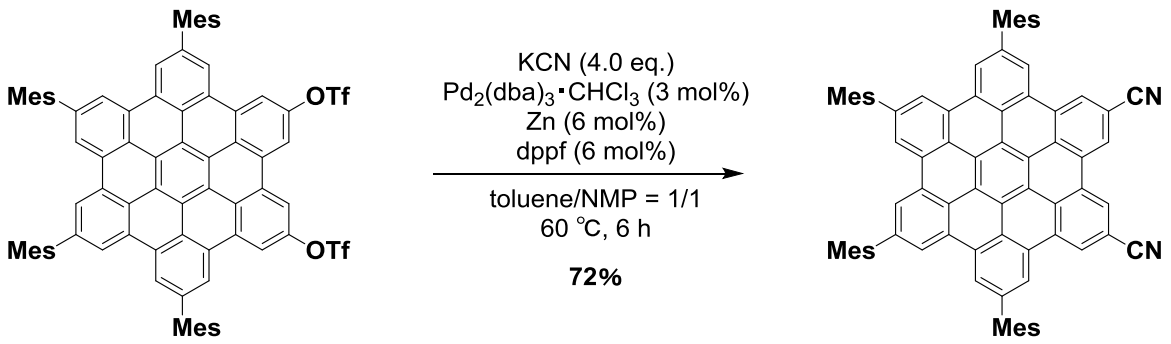

A flask containing **5b** (129 mg, 0.1 mmol), $Pd_2(dba)_3$•$CHCl_3$ (3.1 mg, 3 mol%), 1,1'-bis(diphenylphosphino)ferrocene (3.3 mg, 6 mol%), KCN (52.0 mg, 8.0 equiv) and zinc powder (0.39 mg, 6 mol%) was purged with N_2, and then charged with anhydrous and degassed toluene/NMP = 1/1 (5 mL). The mixture was then stirred at 100 °C for 24 h, quenched with aqueous HCl (1 M), extracted with CH_2Cl_2, and then dried over Na_2SO_4. The solvents were removed under vacuum, and the crude product was purified by silica gel column chromatography ($CHCl_3$/hexane = 2/1) and recrystallization from $CHCl_3$/hexane to afford **7b** (75.1 mg, 0.072 mmol) in 72% yield as a yellow solid. ^{1}H NMR ($CDCl_3$): δ 9.17 (s, 2H), 9.13 (s, 4H), 8.73 (s, 2H), 8.69 (s, 2H), 8.22 (s, 2H), 7.12 (s, 8H), 2.50 (s, 6H), 2.45 (s, 6H), 2.31 (s, 12H) , 2.26 (s, 12H) ppm; ^{13}C NMR ($CDCl_3$): δ 141.5, 140.9, 138.6, 138.1, 137.5, 137.4, 136.1, 135.8, 131.0, 130.9, 130.8, 130.5, 128.6, 128.5, 126.8, 125.3, 124.9, 124.40, 124.37, 123.64, 123.57, 123.4, 123.3, 121.4, 119.6, 118.4, 110.1, 21.4, 21.3 ppm; HR-MS (ESI-MS): HR-MS (ESI-MS): *m/z* = 1045.4489, calcd for $(C_{80}H_{56}N_2)^+$ =

1045.4516 [$(M + H)^+$]; UV/vis (CH_2Cl_2): λ_{max} (ε [M^{-1} cm^{-1}]) = 352 (73000), 370 (150000), 410 (40000), 448 (3000) nm.

2,5-Bis(3,3-dimethylbut-1-yn-1-yl)-8,11,14,17-tetramesitylhexabenzo[*bc,ef,hi,kl,no,qr*]coronene (8b)

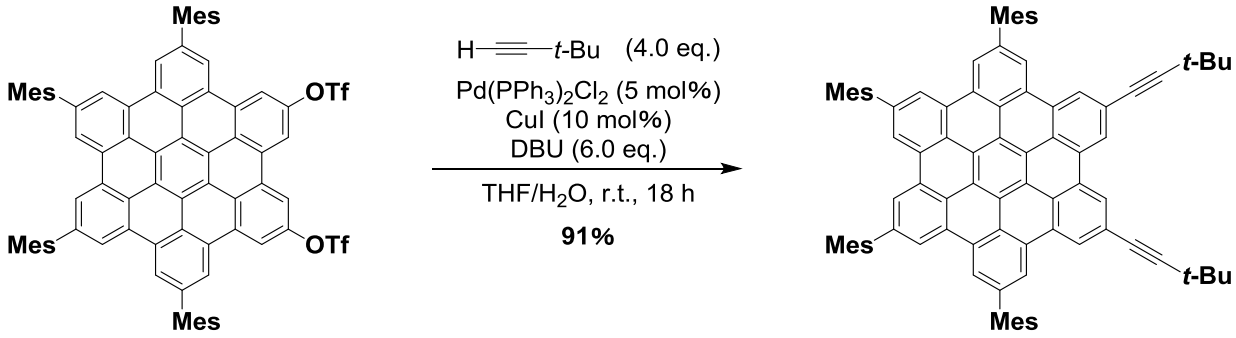

A flask containing **5b** (129 mg, 0.1 mmol), $PdCl_2(PPh)_2$ (2.11 mg, 3 mol%) and copper(I) iodide (1.14 mg, 6 mol%) was purged with N_2, and then charged with anhydrous and degassed THF (5 mL). To this mixture was added 1,8-diazabicyclo[5.4.0]undec-7-ene (91.3 mg, 6.0 equiv) and pure water (3 drops) and 3,3-dimethylbut-1-yne (32.9 mg, 4.0 equiv) at room temperature. The mixture was then stirred under room temperature for 18 h, quenched with aqueous HCl (1 M), extracted with CH_2Cl_2, and then dried over Na_2SO_4. The solvents were removed under vacuum, and the crude product was purified by silica gel column chromatography (CH_2Cl_2/hexane = 1/2) and recrystallization from CH_2Cl_2/MeOH to afford **8b** (106 mg, 0.091 mmol) in 91% yield as a yellow solid. ^{1}H NMR ($CDCl_3$): δ 9.27 (s, 2H), 9.23 (s, 2H), 9.05 (s, 2H), 8.99 (s, 6H), 7.13 (s, 4H), 7.05 (s, 4H), 2.46 (s, 6H), 2.42 (s, 6H), 2.23 (s, 12H), 2.21 (s, 12H), 1.52 (s, 18H) ppm; ^{13}C NMR ($CDCl_3$): δ 140.7, 140.6, 140.3, 139.2, 139.0, 137.8, 136.14, 136.11, 135.7, 131.72, 131.68, 127.75, 127.66, 127.5, 126.5, 124.9, 21.0, 20.33, 20.27 ppm.; HR-MS (ESI-MS): *m/z* = 1155.5813, calcd for $(C_{90}H_{74})^+$ = 1155.5863 [$(M + H)^+$]; UV/vis (toluene): λ_{max} (ε [M^{-1} cm^{-1}]) = 336 (40000), 352 (120000), 370 (290000), 399 (120000) nm.

5,11,17-Trimesitylhexabenzo[*bc,ef,hi,kl,no,qr*]coronene-2,8,14-triyl tris(trifluoromethanesulfonate) (5c)

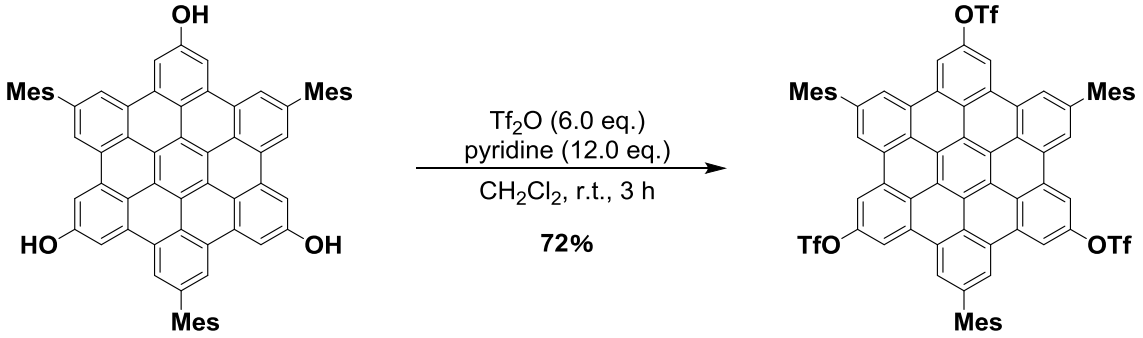

A flask containing **3c** (92.5 mg, 0.1 mmol) was purged with N_2, and then charged with anhydrous and degassed CH_2Cl_2 (5 mL) and pyridine (0.064 ml, 8.0 equiv). To this mixture was added trifluoromethanesulfonic anhydride (0.11 ml, 6.0 equiv) dropwise at room temperature. The mixture was then stirred at room temperature for 16 h, quenched with aqueous HCl (1 M), extracted with CH_2Cl_2, and then dried over Na_2SO_4. The solvents were removed under vacuum, and the crude product was purified by silica gel column chromatography (CH_2Cl_2/hexane = 1/2) and recrystallization from CH_2Cl_2/MeOH to afford **5c** (94.5 mg, 0.072 mmol) in 72% yield as a yellow solid. ^{1}H NMR ($CDCl_3$): δ 9.08 (s, 6H), 9.06 (s, 6H), 7.24 (s, 6H), 2.53 (s, 9H), 2.29 (s, 18H) ppm; ^{13}C NMR ($CDCl_3$): δ 148.9, 141.2, 138.2, 138.1, 136.4, 133.1, 130.0, 128.7, 125.1, 125.0, 124.6, 121.9, 120.8, 120.3, 117.7, 115.0, 21.3, 21.2 ppm; HR-MS (ESI-MS): *m/z* = 1321.2186, calcd for $(C_{72}H_{45}F_9O_9S_3)^+$ = 1321.2155 [$(M + H)^+$]; UV/vis (CH_2Cl_2): λ_{max} (ε [M^{-1} cm^{-1}]) = 329 (30000), 344 (80000), 361 (190000), 391 (64000) nm.

5,11,17-Trimesitylhexabenzo[*bc,ef,hi,kl,no,qr*]coronene-2,8,14-tricarbonitrile (7c)

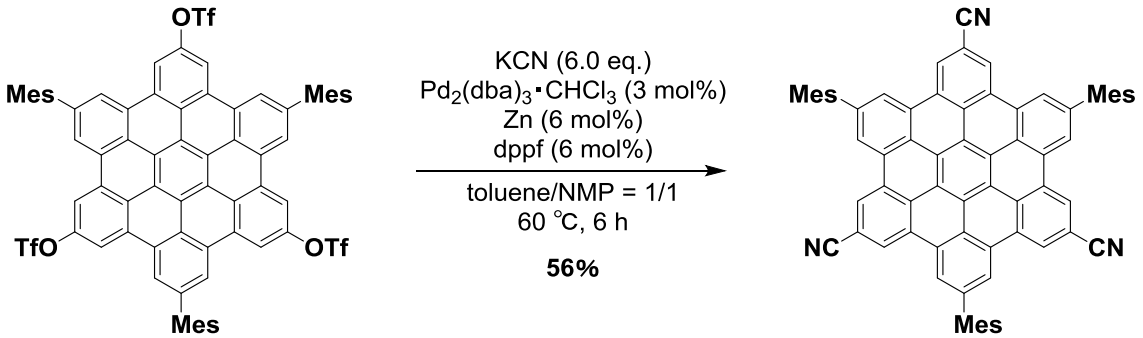

A flask containing **5c** (26.4 mg, 0.02 mmol), $Pd_2(dba)_3$•$CHCl_3$ (1.04 mg, 5 mol%), 1,1'-bis(diphenylphosphino)ferrocene (1.11 mg, 10 mol%), KCN (15.6 mg, 12.0 equiv), and zinc powder (0.078 mg, 6 mol%) were purged with N_2, and then charged with anhydrous and degassed toluene/NMP = 1/1 (2 mL). The mixture was then stirred at 60 °C for 24 h, quenched with aqueous HCl (1 M), extracted with CH_2Cl_2, and then dried over Na_2SO_4. The solvents were removed under vacuum, and the crude product was purified by silica gel column chromatography (CH_2Cl_2/hexane = 1/1) recrystallization from CH_2Cl_2/MeOH to afford **7c** (10.6 mg, 0.011 mmol) in 56% yield as a yellow solid. ^{1}H NMR ($CDCl_3$): δ 9.46 (s, 6H), 9.15 (s, 6H), 7.19 (s, 6H), 2.49 (s, 9H), 2.26 (s, 18H) ppm; ^{13}C NMR ($CDCl_3$, 126 MHz): δ 142.0, 138.0, 137.9, 136.0, 131.3, 129.8, 128.7, 127.6, 125.5, 125.0, 124.3, 123.8, 120.4, 119.2, 111.5, 21.3, 21.2 ppm; HR-MS (ESI-MS): *m/z* = 952.3667, calcd for $(C_{72}H_{45}N_3)^+$ = 952.3686 [$(M + H)^+$]; UV/vis (CH_2Cl_2): λ_{max} (ε [M^{-1} cm^{-1}]) = 329 (30000), 344 (80000), 368 (190000), 391 (64000) nm.

2,8,14-Tris(3,3-dimethylbut-1-yn-1-yl)-5,11,17-trimesitylhexabenzo[*bc,ef,hi,kl,no,qr*]coronene (8c)

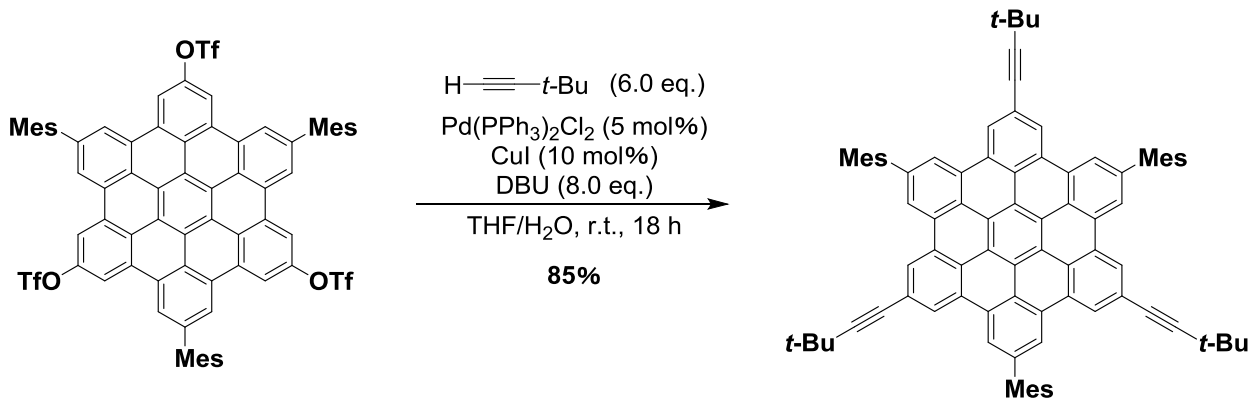

A flask containing **5c** (132 mg, 0.1 mmol), $PdCl_2(PPh)_2$ (3.5 mg, 5 mol%), and copper(I) iodide (1.9 mg, 10 mol%) was purged with N_2, and then charged with anhydrous and degassed THF (10 mL). To this mixture was added 1,8-diazabicyclo[5.4.0]undec-7-ene (91.3 mg, 6.0 equiv) and pure water (2 drops) and 3,3-dimethylbut-1-yne (49.3 mg, 6.0 equiv) at room temperature. The mixture was then stirred under room temperature for 24 h, quenched with aqueous HCl (1 M), extracted with CH_2Cl_2, and then dried over Na_2SO_4. The solvents were removed under vacuum, and the crude product was purified by silica gel column chromatography (toluene/hexane = 1/8) and recrystalliza-

tion from CH_2Cl_2/MeOH to afford **8c** (95.0 mg, 0.085 mmol) in 85% yield as a yellow solid. ^{1}H NMR ($CDCl_3$): δ 9.19 (s, 6H), 9.05 (s, 6H), 7.18 (s, 6H), 2.49 (s, 9H), 2.26 (s, 18H), 1.47 (s, 27H) ppm; ^{13}C NMR ($CDCl_3$): δ 140.7, 140.6, 140.3, 139.2, 139.0, 137.8, 136.14, 136.11, 135.7, 131.72, 131.68, 127.75, 127.66, 127.5, 126.5, 124.9, 21.0, 20.33, 20.27 ppm; HR-MS (ESI-MS): *m/z* = 1117.5751, calcd for $(C_{87}H_{72})^+$ = 1117.5707 [$(M + H)^+$]; UV/vis (CH_2Cl_2); λ_{max} (ε [M^{-1} cm^{-1}]) = 354 (100000), 372 (270000), 401 (120000) nm.

Chapter 4

3,10-dichloro-5,8,14,17-tetramesitylhexabenzo[*bc,ef,hi,kl,no,qr*]coronene-1,2,11,12-tetraol (12a)

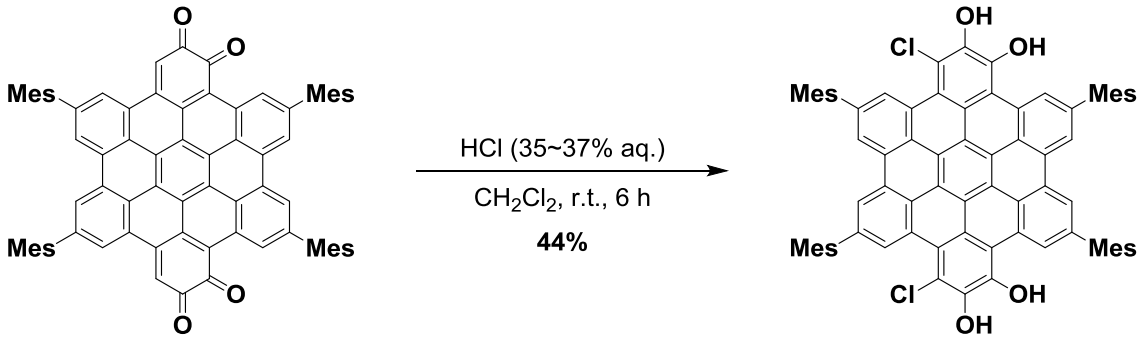

A flask containing 5,8,14,17-tetramesitylhexabenzo[*bc,ef,hi,kl,no,qr*]coronene-1,2,11,12-tetraone **9** (63.6 mg, 0.06 mmol) was purged with N_2, and then charged with anhydrous degassed CH_2Cl_2 (2 mL) and HCl (2 mL, 35~37% aq.). The reaction mixture was stirred at room temperature under light shielding for 6 h. The reaction mixture was diluted with water, and then extracted with CH_2Cl_2, dried over Na_2SO_4, and then concentrated with rotary evaporator at 30 °C under light shielding. The crude reaction mixture was purified by silica gel column chromatography (CH_2Cl_2/hexane = 2/1, neutral silica) and recrystallization from CH_2Cl_2/hexane to afford **12a** (30.1 mg, 0.027 mmol) in 44% yield as a yellow solid. ^{1}H NMR ($CDCl_3$): δ 9.90 (s, 2H), 9.47 (s, 2H), 9.01 (s, 2H), 8.93 (s, 2H), 7.11 (s, 4H), 7.09 (s, 4H), 7.00 (s, 2H, OH), 6.57 (s, 2H, OH), 2.44 (s, 6H), 2.43(s, 6H), 2.25 (s, 12H), 2.22 (s, 12H) ppm; ^{13}C NMR could not be obtained due to the low solubility of the product**;** HR-MS (ESI-MS): *m/z* = 1125.3490, calcd for $(C_{78}H_{56}Cl_2O_4)^-$ = 1125.3472 [$(M - H)^-$]; UV/Vis (CH_2Cl_2): λ_{max} (ε [M^{-1} cm^{-1}]) = 356 (91000), 372 (160000), 405 (63000), 448 (10000) nm.

3,10-Dibromo-5,8,14,17-tetramesitylhexabenzo[*bc,ef,hi,kl,no,qr*]coronene-1,2,11,12-tetraol (12b)

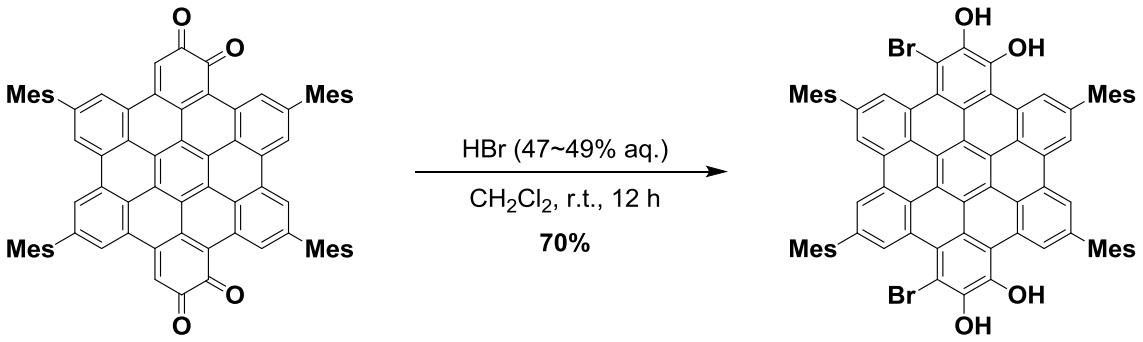

A flask containing 5,8,14,17-tetramesitylhexabenzo[*bc,ef,hi,kl,no,qr*]coronene-1,2,11,12-tetraone **9** (106 mg, 0.1 mmol) was purged with N_2, and then charged with anhydrous degassed CH_2Cl_2 (4 mL) and HBr (0.5 mL, 47~49% aq.). The reaction mixture was stirred at room temperature under light shielding for 12 h. The reaction mixture was diluted with water, and then extracted with CH_2Cl_2, dried over Na_2SO_4, and then concentrated with rotary evaporator at 30 °C under light shielding. The crude reaction mixture was purified by silica gel column chromatography (CH_2Cl_2/hexane = 2/1, neutral silica) and recrystallization from CH_2Cl_2/hexane to afford **12b** (85.0 mg, 0.085 mmol) in 70% yield as a yellow solid. ^{1}H NMR ($CDCl_3$): δ 9.89 (s, 2H), 9.44 (s, 2H), 9.01 (s, 2H), 8.90 (s, 2H), 7.10 (s, 4H), 7.08 (s, 4H), 7.02 (s, 2H, OH), 6.63 (s, 2H, OH), 2.44 (s, 6H), 2.43(s, 6H), 2.25 (s, 12H), 2.20 (s, 12H) ppm; ^{13}C NMR could not be obtained due to the low solubility of the product; HR-MS (ESI-MS): *m/z* = 1217.2641, calcd for $(C_{78}H_{56}Br_2O_4)^+$ = 1217.2612 [$(M + H)^+$]; UV/Vis (CH_2Cl_2): λ_{max} (ε [M^{-1} cm^{-1}]) = 357 (85000), 374 (160000), 406 (62000), 451 (3200) nm.

5,8,14,17-Tetramesityl-3,10-bis(phenylthio)hexabenzo[*bc,ef,hi,kl,no,qr*]coronene-1,2,11,12-tetraol (12c)

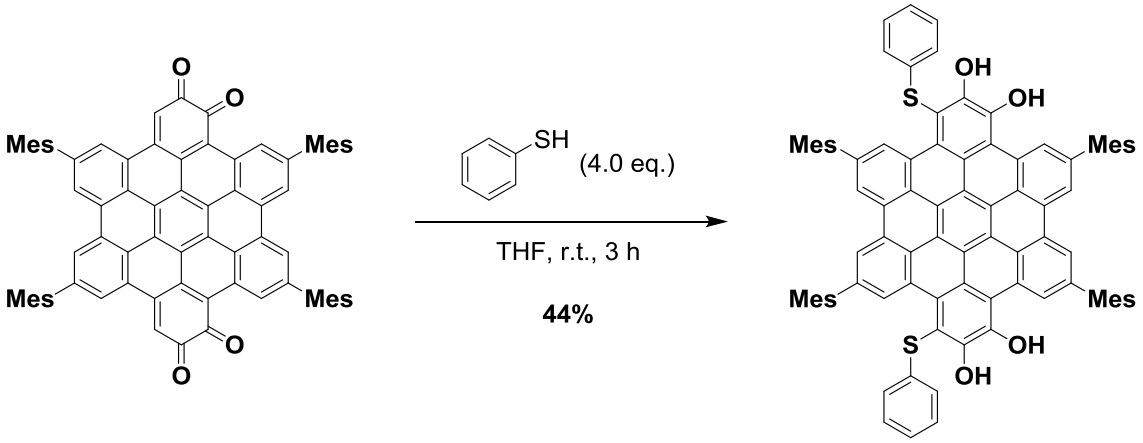

A flask containing 5,8,14,17-tetramesitylhexabenzo[*bc,ef,hi,kl,no,qr*]coronene-1,2,11,12-tetraone **9** (106 mg, 0.06 mmol) was purged with N_2, and then charged with anhydrous degassed THF (8 mL) and Thiophenol (40.8 μl, 4.0 equiv). The reaction mixture was stirred at room temperature for 3 h, and then concentrated with rotary evaporator. The crude reaction mixture was purified by silica gel column chromatography (CH_2Cl_2/hexane = 1/1, neutral silica) and recrystallization from CH_2Cl_2/MeOH to afford **12c** (56.8 mg, 0.045 mmol) in 44% yield as a brown solid. ^{1}H NMR ($CDCl_3$): δ 10.0 (s, 2H), 9.44 (s, 2H), 9.07 (s, 2H), 8.87 (s, 2H), 7.90 (s, 2H, OH), 7.13 (s, 4H), 7.03 (s, 6H, Mes: 4H, OH: 2H), 6.96~7.01 (m, 6H), 6.87~6.92 (m, 4H), 2.46 (s, 6H), 2.42 (s, 6H), 2.29 (s, 12H), 2.08 (s, 12H) ppm; ^{13}C NMR ($CDCl_3$): δ 145.2, 141.8, 139.6, 139.3, 139.2, 138.2, 136.9, 136.7, 136.4, 136.2, 135.0, 129.5, 129.4, 129.3, 129.2, 129.0, 128.8, 128.4, 128.1, 126.35, 126.28, 124.6, 124.2, 123.9, 123.4, 122.7, 121.0, 120.3, 119.9, 118.9, 111.6, 21.3, 21.2, 21.1 ppm; HR-MS (ESI-MS): *m/z* = 1275.4467, calcd for $(C_{90}H_{66}O_4S_2)^+$ = 1275.4475 [$(M + H)^+$]; UV/Vis (CH_2Cl_2): λ_{max} (ε [M^{-1} cm^{-1}]) = 379 (100000), 411 (42000), 456 (5600), 486 (3900) nm.

3,10-Dichloro-5,8,14,17-tetramesitylhexabenzo[*bc,ef,hi,kl,no,qr*]coronene-1,2,11,12-tetraacetate (13a)

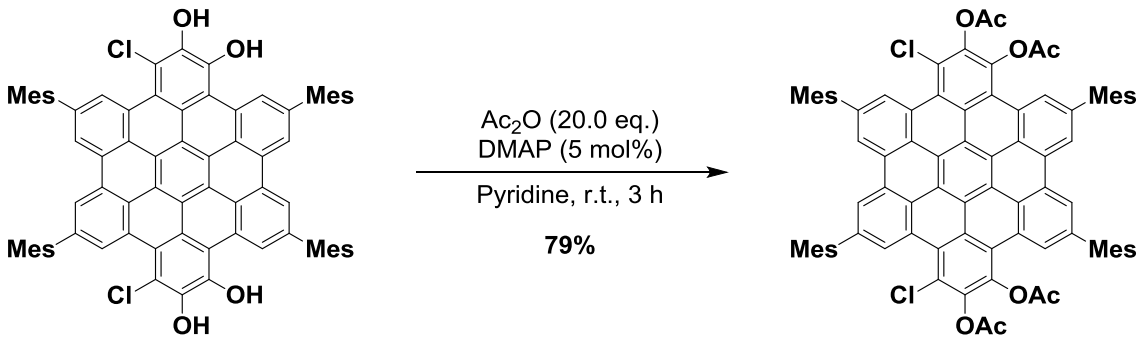

A flask containing 3,10-dichloro-5,8,14,17-tetramesitylhexabenzo[*bc,ef,hi,kl,no,qr*]coronene-1,2,11,12-tetraol **12a** (22.5 mg, 0.02 mmol), acetic anhydride (37.8 μL, 20 equiv), and 4-(*N*,*N*-dimethylamino)pyridine (0.12 mg, 5 mol%) was purged with N_2, and then charged with anhydrous and degassed pyridine (2 mL). The resulting solution was stirred at room temperature for 3 h. The reaction mixture was diluted with CH_2Cl_2 and washed with aqueous HCl (1 M) several times to remove pyridine. The combined organic layers were dried over Na_2SO_4, and concentrated with rotary evaporator. The crude reaction mixture was purified by silica gel column chromatography (CH_2Cl_2/hexane = 4/1) and recrystallization from CH_2Cl_2/MeOH to afford **13a** (20.5 mg, 0.016 mmol) in 79% yield as a yellow solid. ^{1}H NMR ($CDCl_3$): δ 9.65 (s, 2H), 9.25 (s, 2H), 9.04 (s, 2H), 9.00 (s, 2H), 7.09 (s, 4H), 7.07 (s, 4H), 2.560 (s, 3H), 2.556 (s, 3H), 2.43 (s, 12H), 2.420 (s, 3H), 2.416 (s, 3H), 2.21 (s, 12H), 2.14 (s, 12H) ppm; ^{13}C NMR ($CDCl_3$): δ 168.2, 167.7, 140.5, 140.1, 139.8, 138.88, 138.86, 137.19, 137.17, 136.3, 135.8, 129.9, 129.3, 128.8, 128.3, 128.2, 127.8, 127.4, 127.19, 127.17, 124.7, 124.6, 124.4, 124.1, 123.9, 122.9, 120.8, 120.45, 120.35, 21.21, 21.16, 21.10, 20.5 ppm; HR-MS (ESI-MS): *m/z* = 1317.3823, calcd for $(C_{86}H_{64}Cl_2O_8)^+$ = 1317.3870 [$(M + Na)^+$]; UV/Vis (CH_2Cl_2): λ_{max} (ε [M^{-1} cm^{-1}]) = 353 (87000), 370 (190000), 402 (69000) nm.

3,10-Dibromo-5,8,14,17-tetramesitylhexabenzo[*bc,ef,hi,kl,no,qr*]coronene-1,2,11,12-tetraacetate (13b)

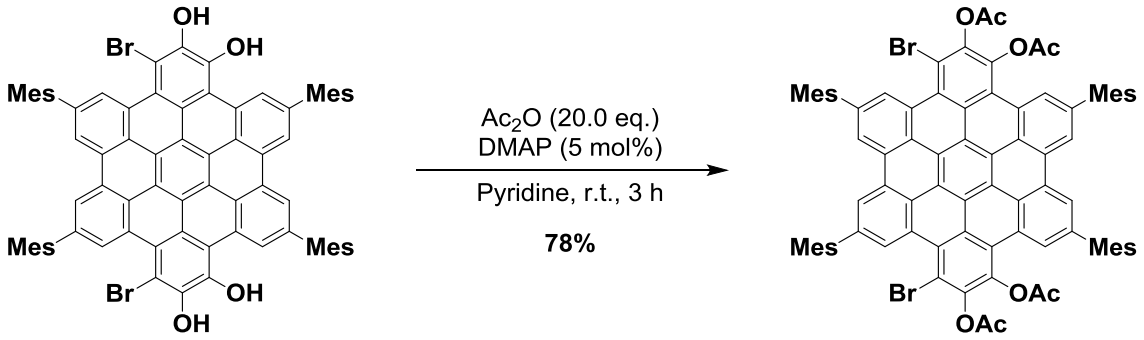

A flask containing 3,10-dibromo-5,8,14,17-tetramesitylhexabenzo[*bc,ef,hi,kl,no,qr*]coronene-1,2,11,12-tetraol **12b** (24.3 mg, 0.02 mmol), acetic anhydride (37.8 μL, 20 equiv), and 4-(*N*,*N*-dimethylamino)pyridine (0.12 mg, 5 mol%) was purged with N_2, and then charged with anhydrous and degassed pyridine (2 mL). The resulting solution was stirred at room temperature for 3 h. The reaction mixture was diluted with CH_2Cl_2 and washed with aqueous HCl (1 M) several times to remove pyridine. The combined organic layers were dried over Na_2SO_4, and concentrated with rotary evaporator. The crude reaction mixture was purified by silica gel column chromatography (CH_2Cl_2/hexane = 4/1) and recrystallization from CH_2Cl_2/MeOH to afford **13b** (21.5 mg, 0.016 mmol) in 78% yield as a yellow solid. ^{1}H NMR ($CDCl_3$): δ 9.650 (s, 1H), 9.647 (s, 1H), 9.24 (s, 2H), 9.011 (s, 1H), 9.009 (s, 1H), 8.998 (s, 1H), 8.996 (s, 1H), 7.076 (s, 4H), 7.068 (s, 4H), 2.56 (s, 6H), 2.43 (s, 12H), 2.41 (s, 6H), 2.0~2.3 (m, 24H) ppm; ^{13}C NMR ($CDCl_3$): δ 168.3, 167.7, 141.7, 140.2, 139.6, 138.9, 138.8, 138.7, 137.2, 136.3, 135.8, 129.9, 129.2, 129.0, 128.9, 128.31, 128.25, 127.8, 127.6, 127.3, 124.6, 124.4, 124.1, 124.0, 123.5, 120.7, 120.4, 120.2, 114.7, 21.24, 21.15, 21.10, 20.72 ppm; HR-MS (ESI-MS): *m/z* = 1407.2848, calcd for $(C_{86}H_{64}Br_2O_8)^+$ = 1407.2856 [$(M + Na)^+$]; UV/Vis (CH_2Cl_2): λ_{max} (ε [M^{-1} cm^{-1}]) = 355 (90000), 371 (200000), 403 (69000), 449 (2000) nm. $C_{92}H_{76}Br_2Cl_6O_{8.38}$, M_w = 1688.20, Triclinic, space group $P1$ $2_1/c1$, a = 28.870(10) Å, b = 8.343(3) Å, c = 34.573(12) Å, β = 101.845(5)º, V = 8150(5) Å^3, Z = 4, D_{calc} = 1.376 g/cm^3, R_1 = 0.0885 ($I > 2.0\sigma(I)$), wR_2 = 0.2808 (all data), GOF = 1.058 ($I > 2.0\sigma(I)$).

5,8,14,17-Tetramesityl-3,10-bis(phenylthio)hexabenzo[*bc,ef,hi,kl,no,qr*]coronene-1,2,11,12-tetraacetate (13c)

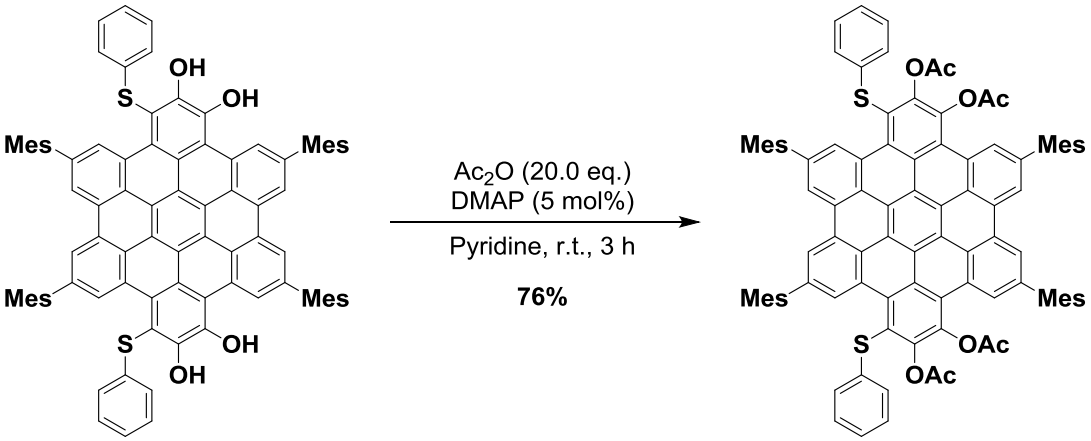

A flask containing 5,8,14,17-tetramesityl-3,10-bis(phenylthio)hexabenzo[*bc,ef,hi,kl,no,qr*]coronene-1,2,11,12-tetraol **12c** (25.5 mg, 0.02 mmol), acetic anhydride (37.8 μL, 20 equiv), and 4-(*N*,*N*-dimethylamino)pyridine (0.12 mg, 5 mol%) was purged with N_2, and then charged with anhydrous and degassed pyridine (2 mL). The resulting solution was stirred at room temperature for 3 h. The reaction mixture was diluted with CH_2Cl_2 and washed with aqueous HCl (1 M) several times to remove pyridine. The combined organic layers were dried over Na_2SO_4, and concentrated with rotary evaporator. The crude reaction mixture was purified by silica gel column chromatography (CH_2Cl_2/hexane = 4/1) and recrystallization from CH_2Cl_2/MeOH to afford **13c** (21.9 mg, 0.015 mmol) in 76% yield as a yellow-orange solid. ^{1}H NMR ($CDCl_3$): δ 9.349 (s, 1H), 9.347 (s, 1H), 9.29 (s, 2H), 9.027 (s, 1H), 9.024 (s, 1H), 8.973 (s, 1H), 8.971 (s, 1H), 7.07 (s, 4H), 7.05 (s, 4H), 6.92-7.02 (m, 6H), 6.84~6.88 (m, 4H), 2.424 (s, 6H), 2.421 (s, 6H), 2.36 (s, 6H), 2.33 (s, 6H), 2.00~2.24 (s, 24H) ppm; ^{13}C NMR ($CDCl_3$): δ 168.7, 167.7, 145.0, 140.0, 139.9, 139.0, 138.74, 138.70, 137.2, 137.1, 137.0, 136.3, 135.8, 133.2, 131.0, 130.0, 128.9, 128.83, 128.76, 128.3, 128.2, 127.9, 127.5, 127.1, 126.9, 125.8, 124.7, 124.6, 124.4, 124.2, 124.1, 120.8, 120.5, 120.4, 21.1, 20.6 ppm; HR-MS (ESI-MS): *m/z* = 1466.4718, calcd for $(C_{98}H_{74}S_2O_8)^+$ = 1466.4751 [$(M + Na)^+$]; UV/Vis (CH_2Cl_2): λ_{max} (ε [M^{-1} cm^{-1}]) = 377 (170000), 410 (68000), 454 (3000), 483 (1300) nm. $C_{103.82}H_{86}Cl_{5.64}O_{8.18}S_2$, M_w = 1728.55, Triclinic, space group *P*-1, *a* = 15.804(8) Å, *b* = 18.294(6) Å,

c = 19.049(9) Å, α = 66.00(4)º, β = 101.845(5)º, γ = 64.00(4)º, V = 4481(3) Å^3, Z = 2, D_{calc} = 1.281 g/cm^3, R_1 = 0.0868 ($I > 2.0\sigma(I)$), wR_2 = 0.2741 (all data), GOF = 0.981 ($I > 2.0\sigma(I)$).

Crystallographic Data

Compound	**3a**	**3b**	**3c**
Formula	$C_{82.45}H_{64.20}Cl_{7.74}O_{6.26}$	$C_{80}H_{60}Cl_6O_2$	$C_{71.63}H_{53.50}C_{l1.25}O_{4.38}$
Formula weight	1429.56	1265.98	1028.46
Crystal system	Monoclinic	Monoclinic	Rhombohedral
Space group	$P2_1/n$	$P2_1/n$	Pa-3
a	15.513(3) Å	8.099(4) Å	21.814(2) Å
b	13.049(2) Å	22.002(11) Å	21.814(2) Å
c	18.801(3) Å	35.641(18) Å	21.814(2) Å
α	90.00°	90.00°	90.00°
β	105.283(4)°	92.477(10)°	90.00°
γ	90.00°	90.00°	90.00°
Volume	3671.4(11) $Å^3$	6346(6) $Å^3$	10380.2(16) $Å^3$
Z	2	4	8
Density (calcd.)	1.293 g/cm^3	1.325 g/cm^3	1.316 g/cm^3
Goodness of fit	1.037	1.050	0.894
R_1 [$I > 2\sigma(I)$]	0.0884	0.0704	0.0590
wR_2 [$I > 2\sigma(I)$]	0.2604	0.1840	0.1575
R_1 (all data)	0.1123	0.1605	0.1431
wR_2 (all data)	0.2916	0.2471	0.1987

Compound	**11**	**13b**	**13c**
Formula	$C_{94}H_{65}Cl_{16}O_8$	$C_{92}H_{76}Br_2Cl_6O_{8.38}$	$C_{103.82}H_{86}Cl_{5.64}O_{8.18}S_2$
Formula weight	1889.66	1688.20	1728.55
Crystal system	Triclinic	Monoclinic	Triclinic
Space group	*P*-1	$P1\ 2_1/c1$	*P*-1
a	14.851(5) Å	28.870(10) Å	15.804(8) Å
b	16.799(6) Å	8.343(3) Å	18.294(6) Å
c	17.678(6) Å	34.573(12) Å	19.049(9) Å
α	68.827(7)°	90.00°	66.00(4)°
β	84.940(8)°	101.845(5)°	73.22(4)°
γ	80.653(7)°	90.00°	64.00(4)°
Volume	4056(2) $Å^3$	8150(5) $Å^3$	4481(3) $Å^3$
Z	2	4	2
Density (calcd.)	1.547 g/cm^3	1.376 g/cm^3	1.281 g/cm^3
Goodness of fit	0.966	1.058	0.981
R_1 [$I > 2\sigma(I)$]	0.1005	0.0885	0.0868
wR_2 [$I > 2\sigma(I)$]	0.2798	0.2572	0.2228
R_1 (all data)	0.1448	0.1056	0.1279
wR_2 (all data)	0.3037	0.2808	0.2741

Appendix

BINAP: 2,2'-bis(diphenylphosphino)-1,1'-binaphthyl (racemic mixture)

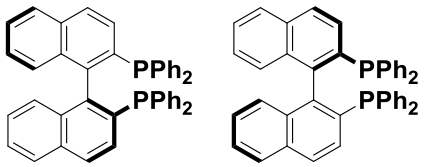

(S)-BINAP (R)-BINAP

DBU: 1,8-diazabicyclo[5.4.0]undec-7-ene

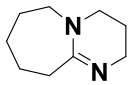

DMAP: N,N-dimethyl-4-aminopyridine

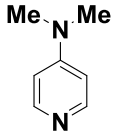

dppf: 1,1'-Bis(diphenylphosphino)ferrocene

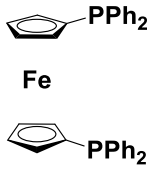

dtbpy: 4,4-di-*tert*-butylbipyridine

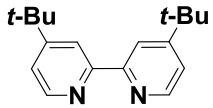

NMP: N-methylpyrrolidone

PIFA: [Bis(trifluoroacetoxy)iodo]benzene

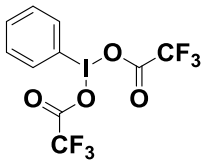

List of Publications

1.

Synthesis of Oxygen-Substituted Hexa-peri-hexabenzocoronenes through Ir-Catalyzed Direct Borylation

R. Yamaguchi, S. Hiroto, and H. Shinokubo,

Org. Lett. **2012**, *14*, 2472.

2.

Intermolecular Oxidative Annulation of 2-Aminoanthracenes to Diazaacenes and Aza[7]helicenes

K. Goto, R. Yamaguchi, S. Hiroto, H. Ueno, T. Kawai, and H. Shinokubo,

Angew. Chem. Int. Ed. **2012**, *51*, 10333.

3.

Functionalization of Hexa-*peri*-hexabenzocoronenes:
Investigation of the Substituent Effects on a Superbenzene

R. Yamaguchi, S. Ito, B. S. Lee, S. Hiroto, D. Kim, and H. Shinokubo,

Chem. Asian. J. **2013**, *8*, 178.

4.

Synthesis of Curved Hexa-*peri*-hexabenzocoronenes

R. Yamaguchi, S. Hiroto, and H. Shinokubo,

Chem. Lett. **2014**, ASAP. [DOI: 10.1246/cl.140577]

Acknowledgements

The author would like to express his gratitude for Prof. Dr. Hiroshi Shinokubo at department of Applied Chemistry graduate school of engineering Nagoya University, for precious advices, and encouragement throughout his study. The author is deeply grateful to Dr. Satoru Hiroto at department of Applied Chemistry graduate school of engineering Nagoya University, for his suggestions and encouragement from the beginning of the research. The author wishes to show acknowledgement to Prof. Dr. Yoshihiro Miyake at department of Applied Chemistry graduate school of engineering Nagoya University, for precise advice, and effective suggestion of the study. The author also desires to express his appreciation to Prof. Dr. Ji-Young Shin at department of Applied Chemistry graduate school of engineering Nagoya University, for X-ray crystal structure analysis, and valuable advices.

The author would like to show my greatest appreciation to Prof. Dr. Takashi Ooi and Prof. Dr. Shigehiro Yamaguchi for their helpful suggestions and discussion on his dissertation committee. It is his great honor to have had his thesis reviewed by two of the leading researchers in the area of organic chemistry.

The author also gratefully acknowledges fruitful collaborations with Prof. Dr. Dongho Kim and his group members, especially Mr. Byung Sun Lee at Department of Chemistry, Yonsei University, Korea, for measurement of TPA cross-section values.

The author thanks to Mr. Satoru Ito for his cooperation for X-ray diffraction analysis and valuable discussion.

The author would like to express the deepest appreciation to all members of the structural organic chemistry. Without their encouragement, this paper would not have materialized.

Dr. Shigeru Yamaguchi	Mr. Takafumi Sakida	Mr. Takuro Teraoka
Mr. Katsuya Suzuki	Mr. Keita Yoshida	Mr. Masanari Akita
Mr. Shoichi Nakamura	Mr. Yosuke Hayashi	Mr. Hiroki Kamiya
Mr. Takumi Nakashima	Mr. Satoru Ito	Mr. Yutaro Koyama
Mr. Takeshi Kondo	Ms. Miki Horie	Mr. Masatomo Tamaru
Mr. Kazuma Oda	Ms. Ayaka Yamaji	Ms. Ami Shigeno
Mr. Takaki Fukuoka	Mr. Kiyohiko Goto	Mr. Tomohiro Ito
Mr. Hiromitsu Kido	Mr. Naruhiko Wachi	Mr. Hiroki Yokoi
Mr. Yuma Serizawa	Ms. Hiroko Tanaka	Mr. Hiroto Omori
Mr. Keitaro Yamamoto	Mr. Shohei Kato	Mr. Takuto Kamatsuka
Mr. Takashi Matsuno	Mr. Ryo Nozawa	Mr. Yuki Ando
Ms. Ayako Ushiyama	Mr. Kawashima Hiroyuki	Mr. Yusuke Morita
Ms. Juri Nagasaki	Mr. Yuya Nagata	

Last but not least, the author deeply indebted to his family, Mr. Akira Yamaguchi, Mrs. Mayumi Yamaguchi, Mr. Hiroshi Yamaguchi, Mr. Takafumi Yamaguchi for their understanding and encouragement.

Ryuichi Yamaguchi

Department of Applied Chemistry
Graduate School of Engineering
Nagoya University
September 2014